Solutions for Innovation

JMS-S3000 SpiralTOF™ series

Imaging
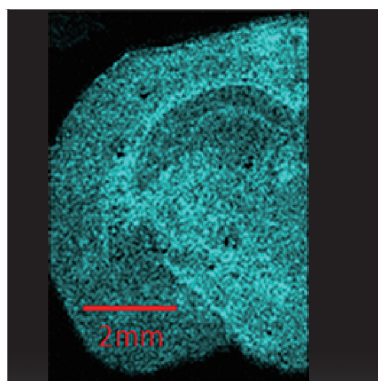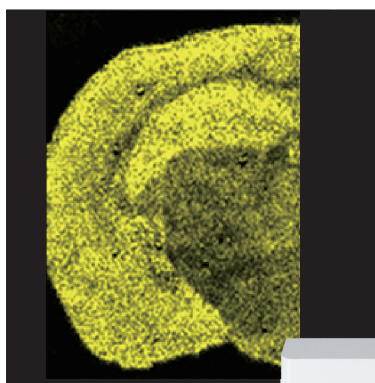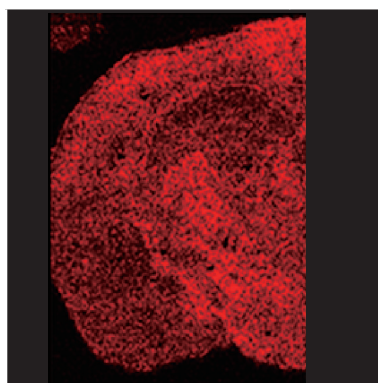# Applications Notebook

Edition June 2020

JEOL Ltd.

JMS-S3000 SpiralTOF™ series
Imaging Applications Notebook

Table of Contents

● For any question or inquiry regarding this Applications Notebook, please contact your local JEOL representative, or use the Product Information Request form on our Global Web Site:
https://www.jeol.co.jp/en/support/support_system/contact_products.html
➢ The contact information on each applications note is that at the time of the initial publication and might not be current.
➢ The contact information and affiliations of the authors on the JEOL News articles are those at the time of the initial publication and might not be current.
● Some of the mass spectrometry imaging data in this applications notebook were processed by using BioMap.
● BioMap is a software for processing mass spectrometry imaging data, developed and ©Novartis Institute, and can be obtained from the Mass Spectrometry Imaging Society web site.

Development of JMS-S3000: MALDI-TOF/TOF Utilizing a Spiral Ion Trajectory

Takaya Satoh

MS Business Unit, JEOL Ltd.

We have developed the JMS-S3000, matrix assisted laser/desorption ionization time-of-flight mass spectrometer (MALDI-TOFMS). An innovative ion optical system, which achieved a spiral ion trajectory, surpassed basic specification of the reflectron ion optical system presently used in most commercially available TOFMSs. Furthermore, we have developed the TOF-TOF option for the JMS-S3000. In the case of attaching the TOF-TOF option, a spiral ion optical system is adopted for the first TOFMS, whereas a reflectron ion optical system with offset parabolic reflectron is adopted for the second one. Utilizing the spiral trajectory ion optical system, the JMS-S3000 provides unprecedentedly high mass resolution and high precursor ion selectivity. In this paper, we demonstrate not only the high mass resolution of more than 60,000 (FWHM) at m/z 2093 but also achievement of high mass resolution over a wide mass range. In addition, we present the high selectivity that enables selection of monoisotopic ions of precursor ions. By selecting only monoisotopic ions of precursor ions, one signal peak corresponding to each fragmentation channel is observed on a product ion spectrum. Consequently, the analysis of the product ion spectrum is made clearer.

Introduction

The time-of-flight mass spectrometer (TOFMS) is one of mass spectrometry techniques, which include the quadrupole mass spectrometer, the magnetic sector mass spectrometer, the ion trap mass spectrometer and the Fourier transform ion cyclotron resonance mass spectrometer. In the case of TOFMS, ions of various m/z values, which are generated in the ion source, are accelerated to the detection plane by a pulse voltage applied from a starting time of data acqisition. Since the time-of-flight of ions at the detection plane are proportional to the square root of their m/z values, the ions generated in the ion source can be separated. One of the TOFMS feature is fast measurement, which is due to the unnecesity of scan for any physical parameters such as electric or magnetic fields. Recently, not only a single type mass spectrometer, but also a tandem type mass spectrometer connected with the quadrupole mass spectrometer (Q/TOF) or tandemly connected two TOFMSs (TOF/TOF) are available.

The mass resolution of TOFMS is expressed by $T/2\Delta T$, where ΔT is the time-of-flight distribution of the ion group with the same m/z value(ion packet) at the detection plane (that is, spatial distribution of the ion packet in the flight direction at the detection plane) and, T is centroid of the time-of-flight distribution. Since TOFMS was invented in 1964 [1], its mass resolution has been improved by increasing T and decreasing ΔT. In 1955, a unique acceleration technique was developed, which focuses the initial space and energy distributions at the detector surface in the flight direction. Applying this technique, the mass resolution was increased by decreasing ΔT [2]. Furthermore, in the early 1970s, a new technique was developed. In this technique, the focus position defined by the above-mentioned acceleration technique is chosen as the start point, and an ion optical system that is composed of ion mirror [3] or elerctrostatic sectors [4] is placed at the post stage. This innovation made it possible to increase the time-of-flight T without increasing ΔT, and led to a dramatic improvement of the mass resolution. Recently, most of commercially available TOFMS instruments use ion mirrors, and their flight paths are 1 to 3 m. For further improvement in the mass resolution of TOFMS, another types of ion optical systems have been proposed. They are the multi-reflecting type [5] and the multi-turn type [6-7] ion optical system where ions fly multiple times on the certain trajectory. These two ion optical systems theoretically achieve an infinitely long flight path in a compact space, and impoved the mass resolution. However, they have the limitation of the mass range because ions with large speed (ions with small m/z) lap the ions with small speed (ions with large m/z) when the ions flying on the same trajectory multiple times.

We have developed an original ion optical system that utilizes a spiral ion trajectory. This ion optical system can overcome the "lap" problem present in multi-reflecting and multi-turn type ion optical systems. In addition, it is possible to achieve mass resolution and mass accuracy higher than those of widely used reflectron ion optical systems. In this paper, we describe the design of the spiral trajectory
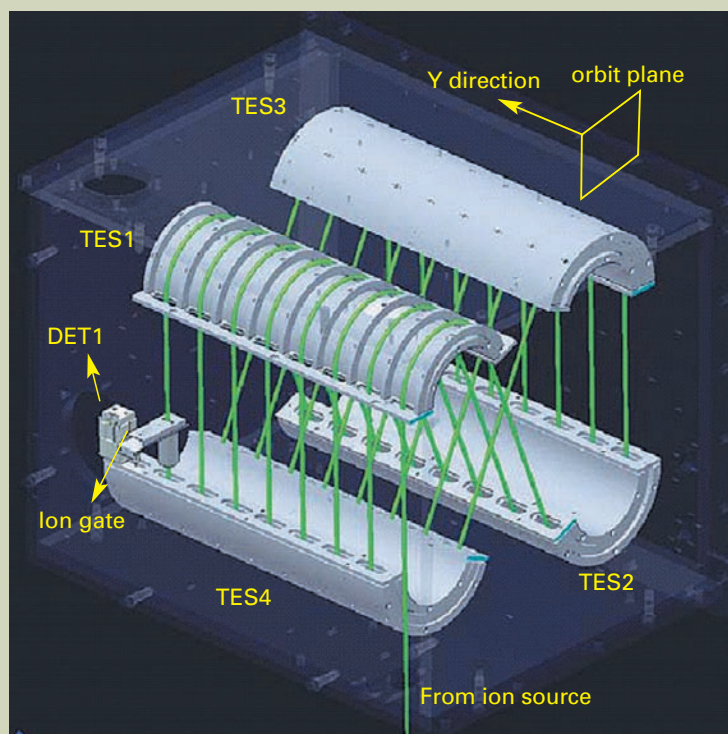
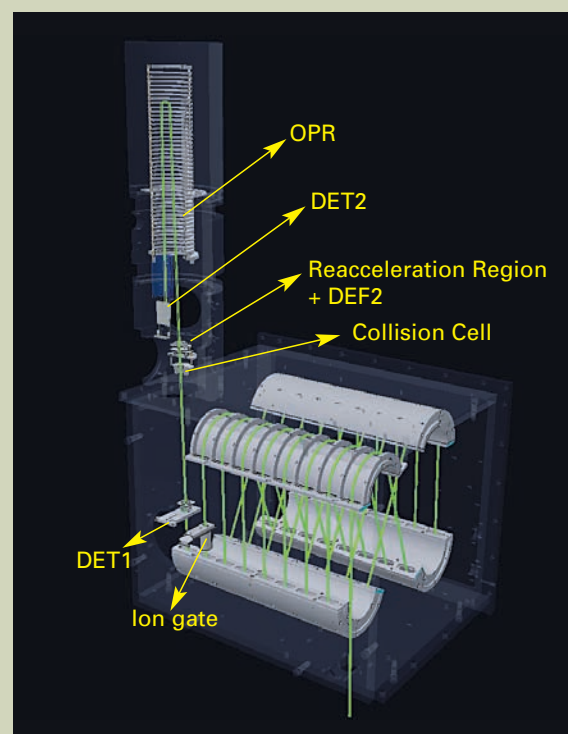Fig. 1 Spiral ion trajectory ion optical system.

Fig. 2 MALDI-TOF/TOF utilizing the spiral ion trajectory ion optical system.

type ion optical system, and basic performance of a MALDI-TOF/TOF system applying it. The system consistsed of the spiral trajectory type ion optical system and reflectron type ion optical system using offset parabolic reflectron for the first and second TOFMSs, respectively. The instrument achieves higher mass resolution, mass accuracy and precursor ion selectivity due to utilizing a spiral ion optical system for the first TOFMS, thus enabling more precise analysis.

Design of the spiral trajectory ion optical system

Multi-turn type ion optical system technique was applied for development of the spiral trajectory ion optical system. Especially, a combination of the "perfect focusing" and "multi-turn" [12] techniques developed at Osaka University, which achieved highest mass resolution in the world, was considered the most suitable for development of the spiral trajectory ion optical system. For conversion of a multi-turn type ion optical system for a spiral trajectory ion optical system, it is necessary to move ion trajectory perpendicular to the orbit plane. In order to achieve this, we have designed the system so that ion injection is slightly tilted to the orbit plane. The advantage of the design is that there is no need for the mechanism to transfer the ions to the next layer. There are concerns about degradation of mass resolution due to the trajectory deviation from a multi-turn type ion optical system. However, the effect should be negligible by keeping the injection angle to several degrees.

Practically, we have designed the spiral trajectory ion optical system based on MULTUM II [7] construction, which consists of four toriodal electrostatic sectors (cylindrical

electrodes with two Matsuda plates). The schematic of the ion optical system is shown in **Fig. 1**. To achieve a spiral trajectory, we have constructed a layered toriodal electric field (TES) by placing (number of cycles +1) Matsuda plates into the cylindrical electrostatic sectors. The Matsuda plates are arranged within certain equal distances L_y in the space L_x between the external and internal electrodes. The three types of voltages applied on TESs 1 to 4 is that of the internal electrode, external electrodes and Matsuda plates. Corresponding voltages are supplied to every Matsuda plates, internal and external electrodes of TESs 1 to 4.

Also, four TESs were placed so that they correspond to MULTUM II when looked from the orbit plane. Y direction was set perpendicular to the periodic orbit plane. In development of the MALDI-TOF/TOF, we have made Y direction to horizontal. The TES1 in the Fig. 1 shows the external electrode is removed so that it can be seen the Matsuda plates are equally spaced. Ions fly through the center of the space, formed by L_x and L_y. Ion passes the same layer of TESs 1 to 4, and after passing the TES 4, it enters to the next layer of TES 1. The process is repeated for several cycles; the ion thus draws a spiral trajectory and reaches the detector (DET1) (Green line in the Figure 1 represents the ion trajectory). The injection angle θ into the layered toriodal electric field can be expressed as follows,

$$\tan \theta = (L_y + L_m) / L_c \quad \cdots \cdots \cdots (1)$$

where, L_m is the thickness of a Matsuda plate and L_c is the one cycle length.

As mentioned above, owing to the usage of four TESs of the same structure in it's construction, the ion optical system can achieve a com-

plicated trajectory within a simple structure.

Production of MALDI-TOF/TOF utilizing spiral trajectory ion optical system

We have developed MALDI-TOF/TOF utilizing the spiral trajectory ion optical system. It consisted of the first TOFMS using the spiral trajectory ion optical system and the second TOFMS using the reflectron ion optical system. The mass spectrum measurement in the first TOFMS is referred as spiral mode, and the product ion spectrum measurement in the second TOFMS as TOF/TOF mode.

An schematic of the system is shown in **Fig. 2** (ion source and the detector DET1 of the first TOFMS are omitted). Spiral trajectory is set to eight cycles of 2.093 m per each. A distance between central trajectories of the adjacent layers is 58 mm, an injection angle is 1.6 degree according to equation (1). Y direction is set as horizontal, so the injection angle is achieved by tilting the extraction direction of the ion source 1.6 degrees from a horizontal plase.

In the spiral mode, ions fly a spiral trajectory and are detected with the spiral mode detector (though not specified in Fig. 2, it is located similarly to DET1 in Fig. 1). Ion gate is placed in the 7th cycle. It allows eliminating high-intensity matrix ions, which are outside of the data acquisition m/z range.

In TOF/TOF mode, selection width of the ion gate is made narrower and monoisotopic ions of precursor ions are selected out of all isotpic ions of them. It is possible to mechanically move the spiral mode detector out of the trajectory so that precursor ions can be introduced into the collision cell. Ions, that entered a collision cell, collide with rare gas inside of the cell with a kinetic energy of approximately

20 keV, and generate fragment ions. Precursor ions and fragment ions are mass-separated in a reflectron ion optical system that combines an offset parabolic reflectron (OPR) [13] and a reacceleration mechanism. OPR is a reflectron connecting a linear and parabolic electric fields. It allows simultaneous observation of ions, from low m/z fragment ions up to precursor ions. In addition, in order to increase transmission of ions, fine adjustment of the ion trajectory is enabled by installing two deflectors (DEF1 and DEF2) on both sides of the collision cell.

Evaluation of MALDI-TOF/TOF with spiral trajectory ion optical system utilized

Figure 3 shows mass spectrum of six types of peptide mixtures (in order of m/z increase: Bradykinin fragment 1-7, Angiotensin II, Angiotensin I, P14R, ACTH fragment 1-17, ACTH fragment 18-39). The mass spectrum of Angiotensin II and ACTH fragment 1-17 are also displayed as an enlarged image. Mass resolution is 58000 (FWHM) and 73000 (FWHM) respectively. The mass error of ACTH fragment 1-17 is 0.16 ppm, when internal calibration is performed among five peptides except ACTH fragment 1-17. It became clear from the above mentioned facts that distance of flight for spiral trajectory ion optical system is 17 m, which is 5 times longer than that of the conventional reflectron type ion optical systems. This allows enhance-

ment of mass resolution and mass accuracy.

Figure 4 shows the relation between m/z value and mass resolution when mass resolution is adjusted with ACTH fragment 1-17. Figure 4 shows that it is possible to achieve high mass resolution simultaneously in a wide m/z range. This overcomes the problem of MALDI-TOFMS utilizing conventional reflectron type ion optical system that could achieve high mass resolution only in a narrow m/z range.

Figure 5.a shows a product ion spectrum diagram of Poly (oxypropylene), acquired in TOF/TOF mode. Selected precursor ions are monoisotopic ions from $[M+Na]^+$ series with m/z 1027. A numbers of fragmentation channels from sodium ions as fragment ion to precursor ion ion are observed. The enlarged spectrum around m/z 780 is shown in Fig. 5.b. The system is able to select only monoisotopic ions of precursor ions, therefore each fragment channels can be observed as one peak without any isotopic peaks. Two peaks in Fig. 5.b indicate different fragmentation channels. It indicates that 2u different fragmentation channels can be clearly separated. Figure 5.c displays an image of the same m/z range as in Fig. 5.b when measured with conventional MALDI-TOF/TOF. Pecursor ion selectivity of traditional TOF/TOF is insufficient so that the fragment ions from all isotopic ions of precursor ions are analyzed in the second TOFMS. Thus every fragmentation channels of product ion spectrum include isotopic peaks. As a result, when m/z values of monoisitopc ions of two fragment channels are close, such as 2 u, their isotopic peaks are overlapped and are

impossible to be clearly identified. The high precursor ion selectivity originated from the spiral trajectory ion optical system used in this system makes the structual analysis of chemical compounds much easier.

Conclusion

This paper reports on the development of the spiral trajectory ion optical system. Also, the paper describes the development of MALDI-TOF/TOF, which combines a spiral trajectory ion optical system and reflectron type ion optical system utilizing offset parabolic ion mirrors. Innovative ion optical system introduced to the JMS-S3000 has overcome preexisting problems related to conventional MALDI-TOF and MALDI-TOF/TOF. Thus, the JMS-S3000 is expected to play a significant role in various areas.

References

[1] W. E. Stephens. *Phys. Rev.,* **69**, 691 (1946)

[2] W.C.Wiley and I. H. McLaren, *Rev. Sci. Instrum.,* **26**, 1150 (1955).

[3] B. A .Mamyrin, V. I. Karataev, D. V. Shmikk and V. A. Zagulin, *So. Phys. JETP*, 3745(1973).

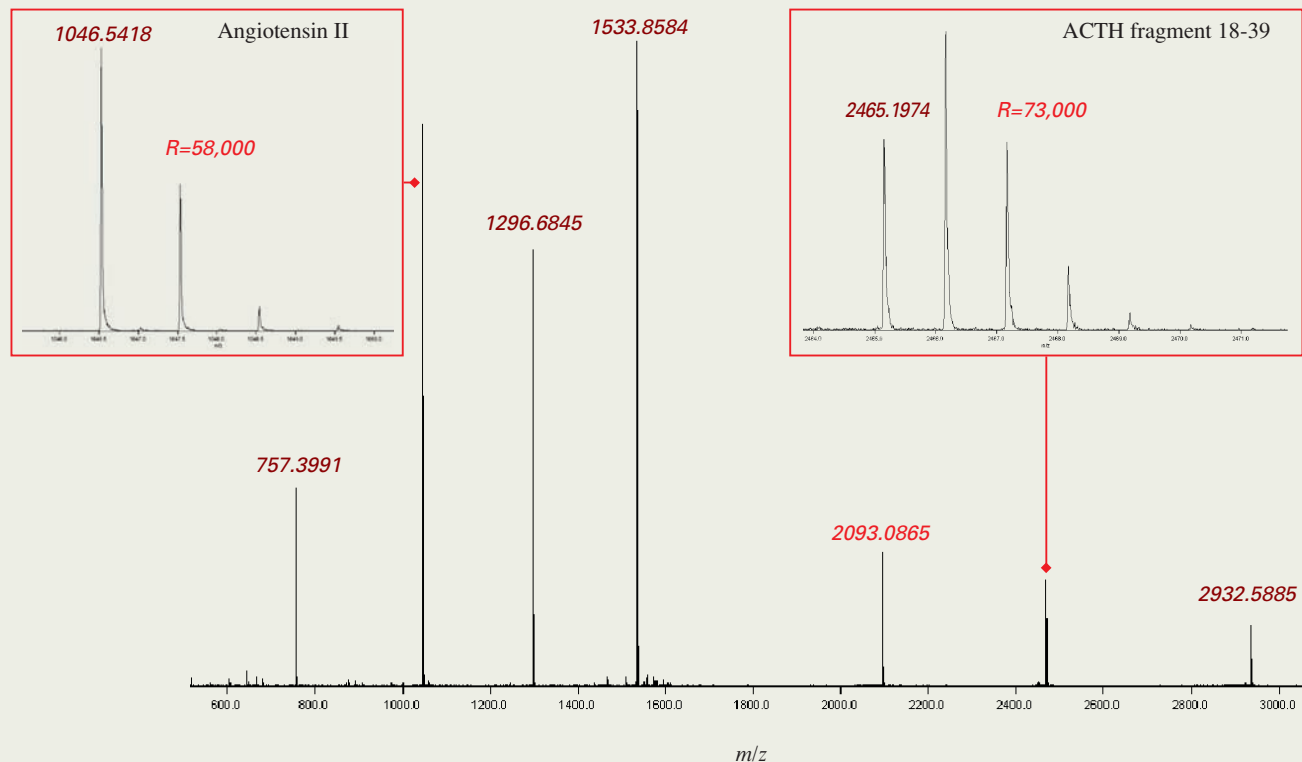[4] W. P. Poschenrieder, *Int. J. Mass Spectrom. Ion. Phys.,* **6**, 357 (1972).
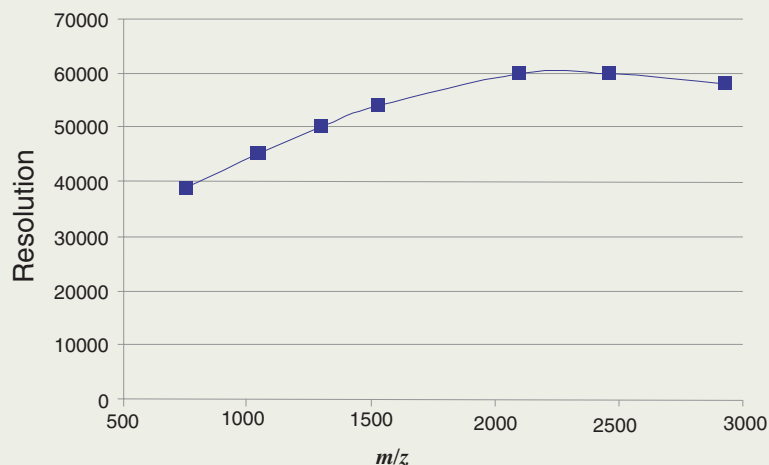
Fig. 3 Mass spectrum of peptide mixtures.

4

Fig. 4 Relation between *m/z* value and mass resolution.

a. Full product ion spectrum.

b. Enlarged spectrum.

2u

Precursor ion: [M+Na]⁺

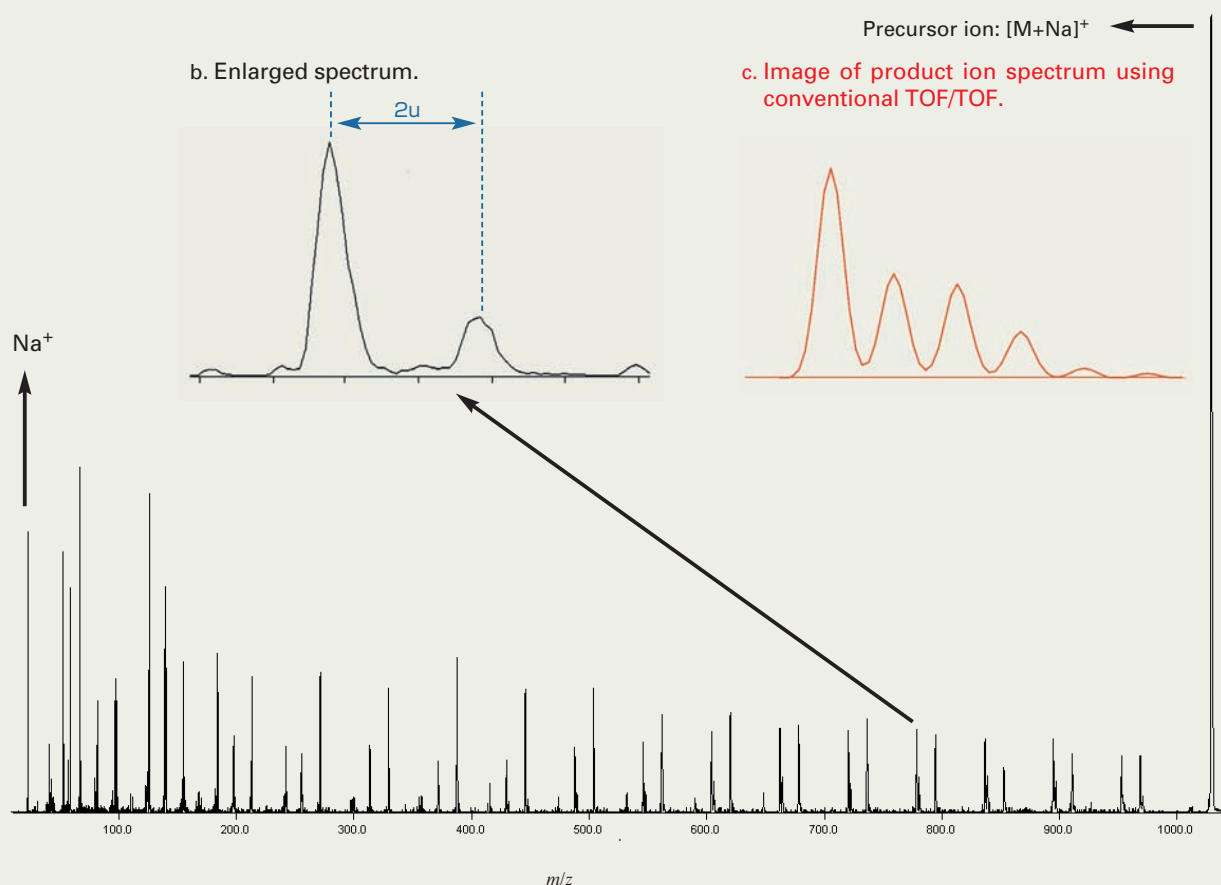c. Image of product ion spectrum using conventional TOF/TOF.

Na⁺

m/z

Fig. 5 Product ion spectrum of Poly(oxypropylene).

[5] H. Wollnik and A. Casares, *Int. J. Mass Spectromety,* **227**, 217 (2003).
[6] M. Toyoda, M. Ishihara, S. Yamaguchi, H. Ito, T. Matsuo, R. Reinhard and H. Rosenbauer, *J. Mass Spectrom.,* **35**, 163 (2000).
[7] D. Okumura, M. Toyoda, M. Ishihara and I. Katakuse, *J. Mass Spectom. Soc. Jpn.,* **51**, 349 (2003).
[8] M. Yavor, A. Verentchikov, J. Hasin, B. Kozlov, M. Gavrik and A. Trufanov, Physics Procedia 1 391 (2008)
[9] T. Satoh, H. Tsuno, M. Iwanaga, Y. Kammei, *J. Am. Soc. Mass Spectrom.,* **16**, 1969 (2005).
[10] T. Satoh, H. Tsuno, M. Iwanaga, and Y. Kammei, *J. Mass Spectrom. Soc. Jpn.,* **54**, 11 (2006).
[11] T. Satoh, T. Sato, and J. Tamura, *J. Am. Soc. Mass Spectrom.* **18**, 1318 (2007).
[12] M. Ishihara, M. Toyoda and T. Matsuo, *Int. J. Mass Spectrom.,* **197**, 179 (2000).
[13] E. N. Nikolaev, A. Somogyi, D. L. Smith, C. Gu, V. H. Wysocki, C. D. Martin and G. L. Samuelson, *Int. J. Mass Spectrom.,* **212**, 535 (2001)

Mass Spectrometry Imaging using the JMS-S3000 "SpiralTOF™-plus" Matrix Assisted Laser Desorption Ionization Time-of-Flight Mass Spectrometer

Takaya Satoh   MS Business Unit, JEOL Ltd.

Matrix assisted laser desorption/ionization (MALDI) is one of the soft ionization methods. By selecting a proper compound to enhance the ionization efficiency (called "matrix"), various kinds of organic compounds can be ionized. In 2010, JEOL released the JMS-S3000 "SpiralTOF™", which adopted a spiral ion optics system combined with MALDI ion source. In recent years, MALDI-TOFMS (time-of-flight mass spectrometer) has been widely used for mass spectrometry imaging (MSI) to visualize the localization of target compounds on the sample surface. The SpiralTOF™ is a suitable system for MALDI-MSI because it can achieve high mass-resolution even in low mass region, which was difficult by the conventional reflectron TOFMS. In 2019, JEOL has introduced the new "SpiralTOF™-plus", which has improved the data acquisition speed while keeping the inherent high mass-resolution. This report presents the features of the SpiralTOF™-plus and the advantages in practical applications using this system.

Introduction

In the Matrix Assisted Laser Desorption Ionization (MALDI), co-crystals of the matrix and sample compounds are made by spotting the mixture of their solutions on the target plate and air-dried. The ultraviolet laser is irradiated on the co-crystal to ionize the sample. By selecting the suitable matrix according to the sample, it is possible to ionize variety kinds of organic compounds, including proteins, peptides, nucleic acids, glycans, lipids, drugs and synthetic polymers. Using MALDI, ions with wide-molecular weight can be generated as singly charged ions. Also, the MALDI is a pulsed ionization technique, and it is best match to combined with a time-of-flight mass spectrometer (TOFMS). The MALDI is difficult to online-connect with a chromatography system (gas chromatography, liquid chromatography, etc.), and separation of compounds included in sample depends on the mass resolution of TOFMS. However, mass resolution of conventional reflectron TOFMS is often insufficient, especially for low mass range. It is even said that the reflectron TOFMS cannot be applicable to analyzing the compounds of molecular weight 500 or less. Another reason is that, the Post Source Decay (PSD) ions which originated from spontaneous decay are detected as the noise in the low molecular range, thus making it difficult to detect minor components. In order to solve this issue, JEOL introduced the MALDI-TOFMS system, the JMS-S3000 "SpiralTOF™" in 2010. With its unique spiral ion optics system, the SpiralTOF™ achieved a 17 m-long flight path in a limited space. Thus, the SpiralTOF™ successfully provided ultrahigh mass-resolution and ultrahigh mass accuracy. Another feature of this ion optical system is consisted of four electrostatic sectors,

which enables to eliminate PSD ions and makes easy to detect minor components. Owing to these features and advantages, it became possible to perform analysis for the low molecular range with high mass-resolution and high mass accuracy, which was difficult to do with the reflectron TOFMS. Recently, MSI (mass spectrometry imaging), which can visualize the distribution of organic compounds on the sample surface, is becoming practical. Most of the target compounds for MSI analyses are low molecular compounds so that SpiralTOF™ has an advantage due to its high analytical capability in the low molecular weight range. In the latter half of 2019, the SpiralTOF™ was upgraded to the "SpiralTOF™-plus". This powerful SpiralTOF™-plus inherits the features of high mass-resolution capability of the SpiralTOF™ and has improved capabilities of MSI. In this report, the features and advantages of the SpiralTOF™-plus will be presented, along with its effectiveness in practical analysis applications.

Features of SpiralTOF™-plus

Figure 1 shows the appearance of the SpiralTOF™-plus and the schematic of the spiral ion optics system. The SpiralTOF™-plus adopts a long-life solid-state laser for ionization, accomplishing fast measurement. The sample ionized in the MALDI source is accelerated to mass separation in the 8-shaped spiral ion optics system which is composed of four electrostatic sectors with eight stories. After one cycle, the ion trajectory is shifted perpendicular to the orbit plane, and thus the spiral orbit is formed. The flight path of one cycle is 2.1 m so that the total flight path extends to 17 m. It is five times longer than that of the reflectron TOFMS. This demonstrates that high mass-resolution is achieved over a

≫ 3-1-2, Musashino, Akishima, Tokyo, 196-8558, Japan | E-mail: taksatoh@jeol.co.jp

Fig. 1 Appearance of SpiralTOF™-plus and schematic of a spiral ion optics system.

(a)

(b)

Spiral ion optics system

Detector for Spiral mode (17 m from ion source)

MALDI ion source
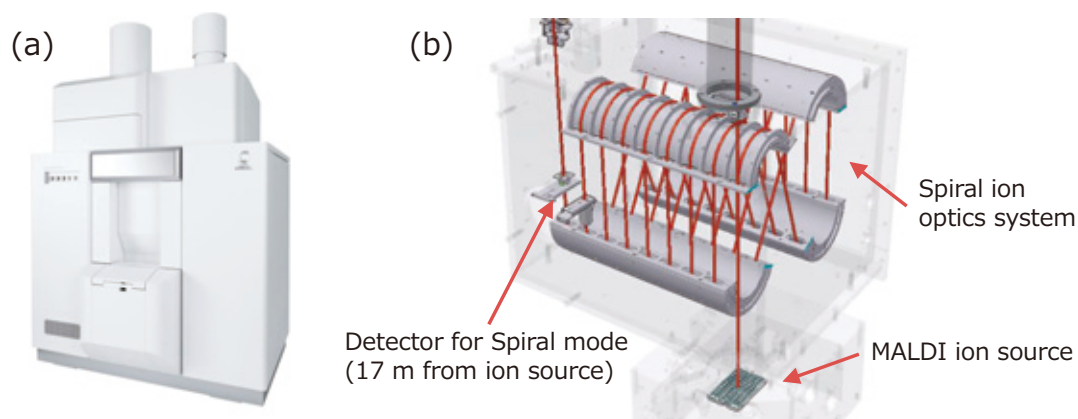
wide mass range. MALDI is one of the major ionization methods, as well as electrospray ionization (ESI). However, MALDI is also known to cause spontaneous fragmentation (called PSD) by excessive internal energy generated at the ionization. The kinetic energy of fragment ions becomes smaller than that of precursor ions. Since the electrostatic sectors have an ability as a kinetic energy filter, the ions derived from PSD with reduced energy cannot pass and these ions are ejected from the ion orbit. As a result, the noise derived from PSD is not detected in a mass spectrum, and thus even trace components can be easily detected.

Mass Imaging (MSI)

In MALDI-MSI, a tissue section (thickness is generally 10 μm or less) is placed on a conductive ITO slide glass, and a matrix solvent is uniformly sprayed using an air-brush, from above the glass. A laser beam is irradiated two dimensionally on the sample surface for acquiring mass spectra from each pixel. After data acquisition, localization of the target compound, which is specified by the peak in mass spectrum, is visualized (see **Fig. 2**). Several MS systems are commercially available for MALDI-MSI. In **Fig. 3**, comparison is made between the mass resolution and data acquisition speed. As described before, the SpiralTOF™-plus provides higher mass-resolution than the reflectron TOFMS and the SpiralTOF™-plus can separate isobaric peaks. In terms of data acquisition speed, the SpiralTOF™-plus is comparable to the reflectron TOFMS. On the other hand, FT-ICR or FT-MS, which has higher mass resolution than TOFMS, is also used for MALDI-MSI. However, an increased data acquisition speed will lead to reduction of mass resolution. Since the mass resolution and data acquisition speed is independent in TOFMS, SpiralTOF™-plus can achieve optimal combination of high mass-resolution and high-speed acquisition.

Improvements and Advantages of SpiralTOF™-plus

The SpiralTOF™-plus has improved the data acquisition speed for MALDI-MSI to 3 times at a maximum, compared to the conventional SpiralTOF™. Furthermore, the SpiralTOF™-plus has increased the maximum number of pixels for measurement from 32,000 points to 200,0000 points. In MALDI-MSI, the sample preparation (making tissue sections and selecting matrix selection) and confirmation of reproducibility take the most

Fig. 2 Conceptual view of MALDI-MSI (mass imaging).

Intensity

m/z
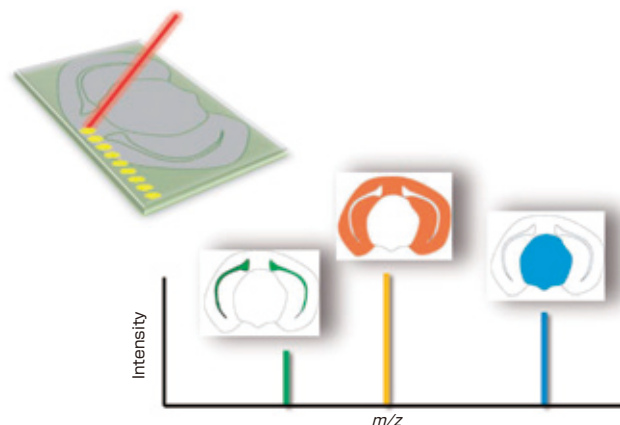
time. The present improvements of the SpiralTOF™-plus has greatly enhanced the efficiency of these processes due to an improved data acquisition speed. In many cases in MALDI-MSI measurement, the size of the pixel is set to 20-50 μm due to enough sensitivity to get. The increase of the maximum number of pixels of SpiralTOF™-plus allows to acquire the data even from a small sample of a few cm squares under the same acquisition conditions. In **Fig. 4**, the mass images of PC (38:4)[M+K]$^+$(m/z 848.557) and Galactosyl ceramide (C24h:1)[M+K]$^+$(m/z 848.638) from a a mouse brain tisseu section are shown. These two lipids have only a mass difference of 0.1 u, which cannot be separated with the reflectron TOFMS. By comparing these two mass iamges made by SpiralTOF™-plus, it is clear that the two lipids have different localization. In the case of using a reflectron TOFMS, which cannot separate two masses, it cannot provide proper information of compounds and their localization. The size of measurement range is 10.46 × 6.06 mm. In the mass images on the top column, the mass-image pixel size is 20 μm, enabling high-resolution mass images to be created. The number of pixels is 158,000 and this indicates that the SpiralTOF™ can only create a mass image of one-fifth area compared to the SpiralTOF™-plus. In the mass images on the middle column and bottom column in Fig. 4, pixel binnings were performed with 3 × 3 and 5 × 5 to make the pseudo 60 μm and 100 μm pixel mass images. The number of pixels were 17,000 and 6,000, respectively (left-side

Fig. 3 Correlation diagram between mass resolution and data acquisition speed for MALDI-MSI.
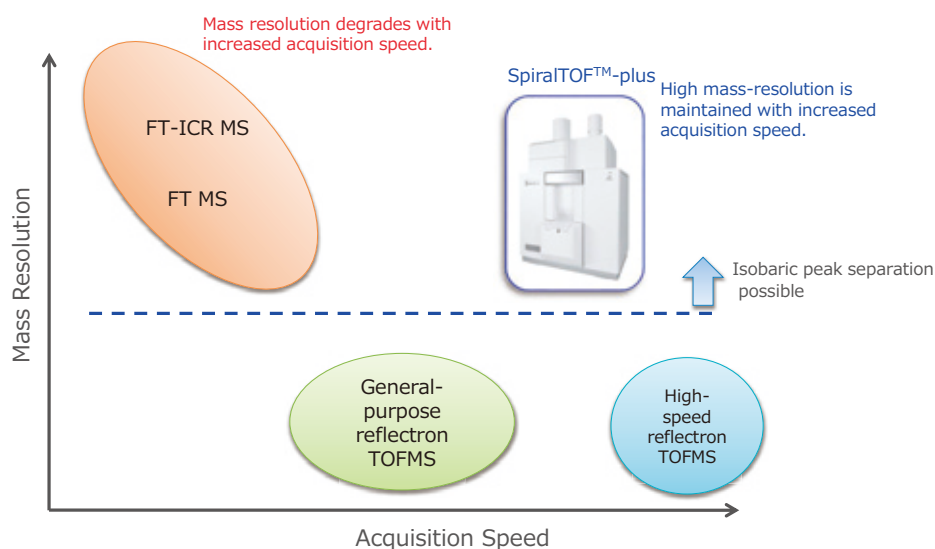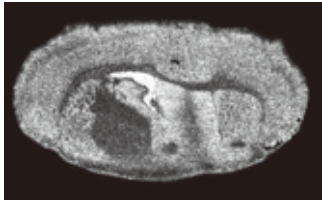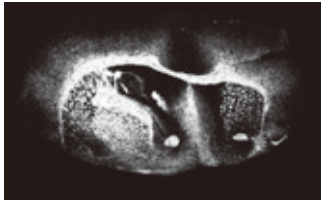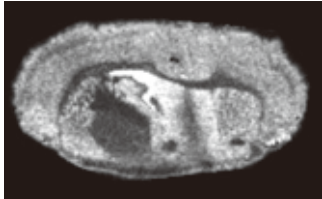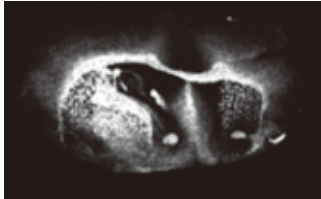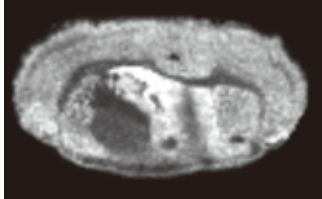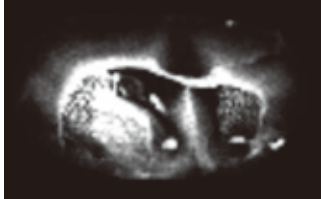

Fig. 4 Mass images acquired with SpiralTOF™-plus: PC(38:4) [M+K]⁺ (*m/z* 848.557), left side and Galactosyl ceramide(C24h:1) [M+K]⁺ (*m/z* 848.638), right side.

	PC (38:4) $[M+K]^+$(*m/z* 848.557)	Galactosyl ceramide (C24:1) $[M+K]^+$(*m/z* 848.638)
20 μm		
60 μm		
100 μm		

and right-side). It is estimated that, the time requried to acquire the data with these numbers of pixels is one hour and 22 minutes, respectively. Although the mass images show a little unclear contrast, it is sufficient to consider the preparation methods and to confirm the data repoducibility. The time for data acquistion, which will be comparable to time for making tissue selction or matrix application, will be shortened enough to eliminate bottle neck through the MSI measurement.

Conclusion

The SpiralTOF™-plus has maintained high mass-resolution provided by the SpiralTOF™ and has improved capabilities of MALDI-MSI. Due to higher data acquisition speed and the increased maximum number of pixels, the SpiralTOF™-plus has achieved more efficient study using MALDI-MSI, thus playing a significant role in various mass spectrometry studies.
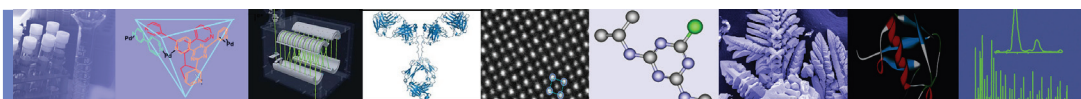
SpiralTOF™

High Mass Resolution MALDI-Imaging MS
High Stability of Peak Position during Imaging MS Measurement

Introduction

Matrix-assisted laser desorption/ionization imaging mass spectrometry (MALDI-Imaging MS) is a powerful tool for the biochemical analyses of surfaces. Previously, this technique has been used to determine the spatial distribution of hundreds of unknown compounds in thinly sliced tissue sections. The mass spectral images are generated by changing the laser irradiation point at regular intervals across the sample surface and collecting a mass spectrum for each point. Time-of-flight mass spectrometers (TOFMS) are widely used as the mass analyzer for MALDI-Imaging MS because they are well matched for the MALDI ionization process. However, the fine structure of the matrix crystals and small irregularities in the tissue surface flatness can cause peak drift in the collected mass spectra that is caused by slight differences in the starting point of the flight path for the ions at each laser irradiation point. As a result, the typical reflectron type TOFMS systems have a difficult time achieving high mass resolution from spot to spot over a thinly sliced biological surface. Conversely, the JEOL JMS-S3000 "SpiralTOF™", which has 5-10 times longer flight path than the reflectron type TOF, is able to reduce the effect of this mass drift to achieve high mass resolution and high mass accuracy.

In this work, we report the advantages of using the SpiralTOF for MALDI-Imaging MS analyses of lipids in a mouse brain tissue section.

Experimental

A mouse brain tissue section was placed on an ITO conductive glass slide plate. The matrix compound DHB was sprayed onto the surface of the tissue and then the sample was introduced into the mass spectrometer. The Imaging MS measurements were performed on the left half of the brain tissue section (5 mm×7 mm) with 40 μm spatial resolution.

Results and Discussion

The averaged mass spectrum of all image pixels is shown in Fig. 1. The base peak ion m/z 798 was estimated as Phosphatidylcholine (PC) (34:1) [M+K]+. The mass image of m/z 798 with ±0.1 u mass window is also shown in Fig.1. This image shows that the PC (34:1) is distributed uniformly throughout the brain tissue section. The four regions-of-interest (ROI) 1 – 4 were selected from the top, right, bottom and left in the measured area, respectively. The peaks for the PC (34:1) [M+K]+ from the accumulated mass spectra for ROI 1 – 4 are shown in Fig. 2. These results show that the mass drift was reasonably small dur-
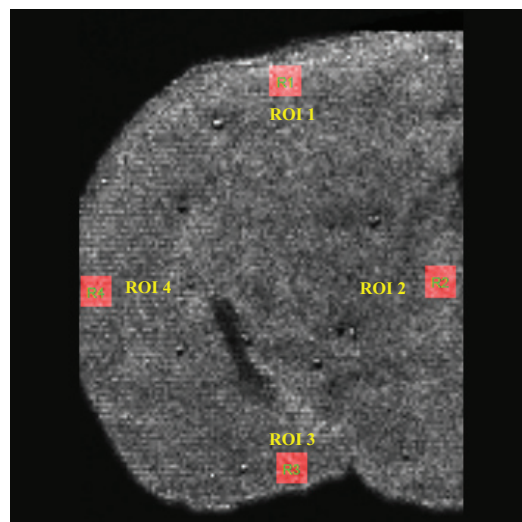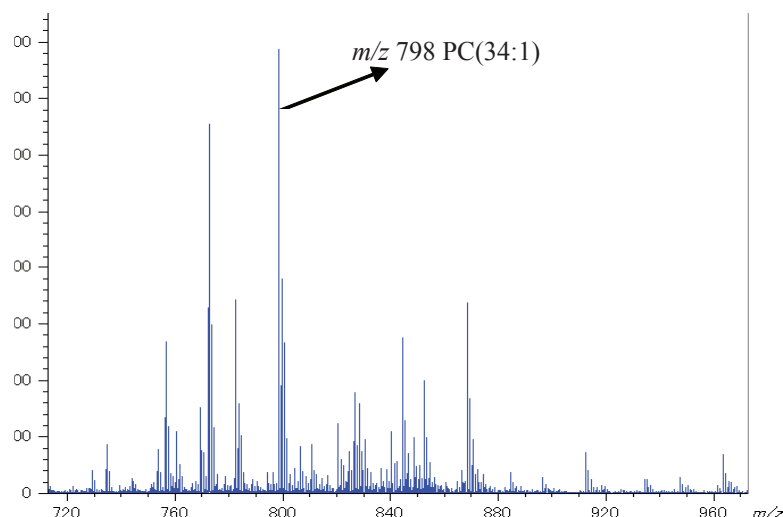

Figure 1. Averaged mass spectrum and mass image of m/z 798

ing their measurements.

It is important to note that for the mass analysis of lipids in mouse brain tissue, various types of lipid ions are observed as doublet or triplet peaks in the mass spectrum. For example, the mass spectra of ROI 1 – 4 at *m/z* 822 - 823 are shown in Fig. 3. The mass differences for these peaks were only 0.1 u. As it turns out, commercially available TOF/TOF instruments have insufficient precursor ion selectivity so it is difficult to determine their structures through MS/MS. Therefore, high mass resolution and high mass accuracy, which result when the measured peak positions are stable during Imaging MS measurements, are necessary for elemental composition estimations. As these results show, the JEOL SpiralTOF provides very good mass stability during MALDI Imaging of tissue. Therefore, the average mass

spectrum for the whole image (Fig. 1) can be used to calculate the elemental composition of an unknown compound in the mouse brain tissue surface using a single point calibration [1].

Acknowledgment
This data was acquired in a joint research project with the Graduate School of Science, Osaka University. We thank Mr. N. Moriguchi, Assistant Professor Dr. H. Hazama and Professor Dr. K. Awazu for providing the mouse brain tissue specimens.

Reference
(1) Takaya Satoh et al., *Mass Spectrometry,* Vol. 1 (2012), A0013
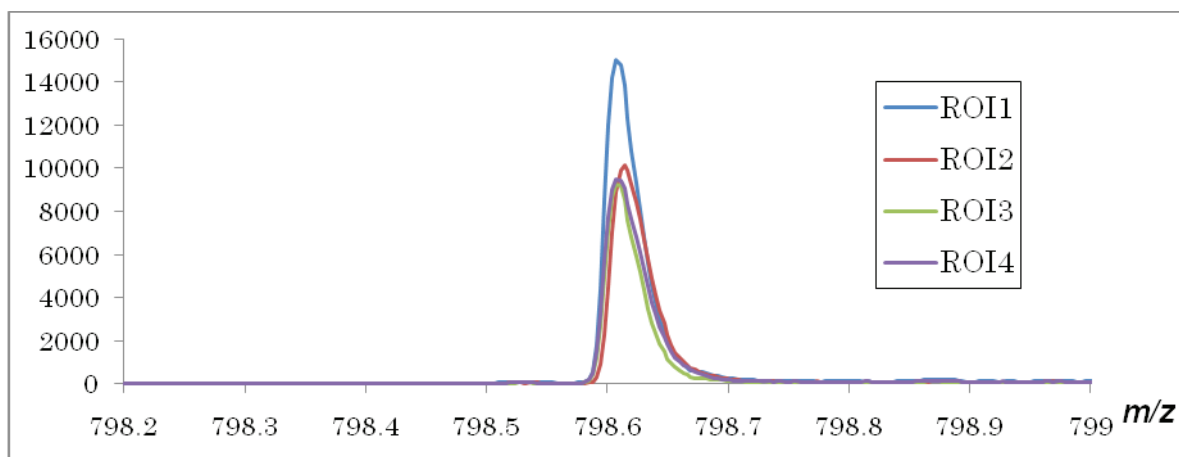

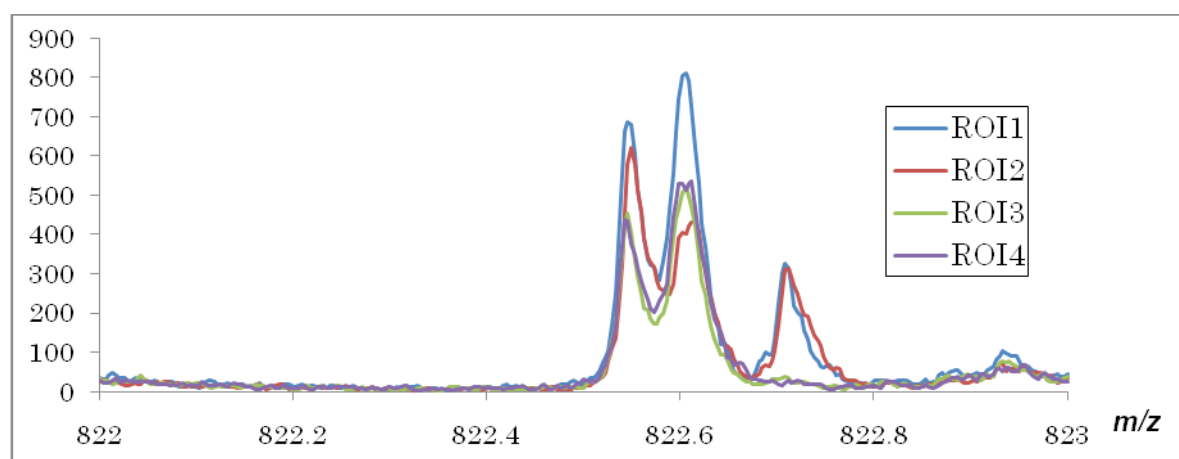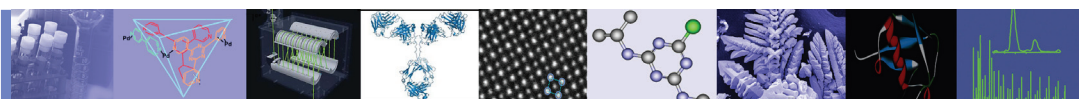Figure 2. Mass spectra of ROI 1 – 4 at m/z 798

Figure 3. Mass spectra of ROI 1 – 4 at m/z 822

SpiralTOF™

The Relationship between Crystal Condition and Mass Resolving Power, Mass Accuracy

Introduction

The JMS-S3000 SpiralTOF™ has a unique 17 m flight path that offers the highest resolution MALDI-TOF MS system currently available. With an extended flight distance, the SpiralTOF reduces topographic effect of matrix crystal to a minimum and achieves highly reproducible mass resolving power and high mass accuracy with external mass calibration.

In this work, we demonstrate the measurement of a polymer standard with 4 types of matrices that are typically used for MALDI polymer measurement by using the JEOL SpiralTOF system. Additionally, we looked at the crystal condition using the JEOL JSM-7600F thermal field emission scanning electron microscope (FE-SEM).
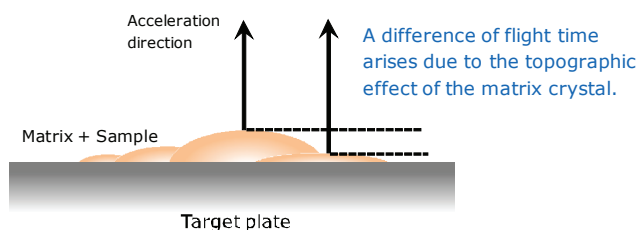

Figure 1. Reduced topographic effect of matrix crystal.

Experimental

Sample information and preparation conditions are shown in Table 1. PEG1500 was dissolved in water at a concentration of 10 mg/mL. Each matrix was dissolved in THF at a concentration of 10 mg/mL. NaI used as the cationization agent was dissolved in THF at a concentration of 1 mg/mL. Next, the PEG1500, NaI and matrix solutions were mixed together 1:1:2 (1:1:4 for DIT) by volume. Afterwards, 0.75 µL of this mixture was placed on the hairline finish stainless steel plate (MTP format, 384 spots for samples and 96 spot for calibrant). Finally, the dried sample was measured using the JMS-S3000 SpiralTOF MS system. We also obtained SEM images for each crystal condition with the JSM-7600F.

Polymer standard	Conc.	Solvent
Polyethylene glycol (PEG) 1500	10 mg/mL	Water
Cationization agent		
NaI	1 mg/mL	Water
Matrix		
α-Cyano-4-hydroxycinnamic acid (CHCA)	10 mg/mL	Tetrahydrofuran (THF)
2,5-Dihydroxybenzoic acid (DHB)	10 mg/mL	THF
Dithranol (DIT)*	10 mg/mL	THF
trans-3-Indoleacrylic acid (IAA)	10 mg/mL	THF
Sample		
PEG1500/NaI/Matrix = 1/1/2 (v/v)		
* PEG1500/NaI/DIT = 1/1/4 (v/v)		
0.75 µL of this sample solution mixture was placed on the MALDI target plate		
JSM-7600F conditions		
Sample preparation	Uncoated	
Acceleration voltage	1 kV	
Magnification	x500 and x2,000	

Table 1. Sample information and preparation conditions.

Figure 3. JMS-3000 SpiralTOF.

Figure 4. JSM-7600F Thermal FE-SEM.

Results & discussion:
The MALDI mass spectra of PEG1500 are shown in Figure 4 for each matrix. We set the delay time to achieve the maximum mass resolving power at *m/z* 1537.9. Therefore, the resolving power was approximately 70,000 for the $[HO(C_2H_4O)_{34}H + Na]^+$ peaks, well in excess of that needed to separate isotope peaks. Additionally, we observed excellent mass distributions.

We determined the average mass resolving power (n=10) and external mass accuracy (n=8) for *m/z* 1097.6, *m/z* 1537.9 and *m/z* 1978.2 for each matrix. The results are shown in Figure 5 and 6, respectively. We achieved high mass resolving power for the three selected ions with each matrix. In addition, we obtained excellent mass error (less than 10 ppm) with external calibration for each matrix.
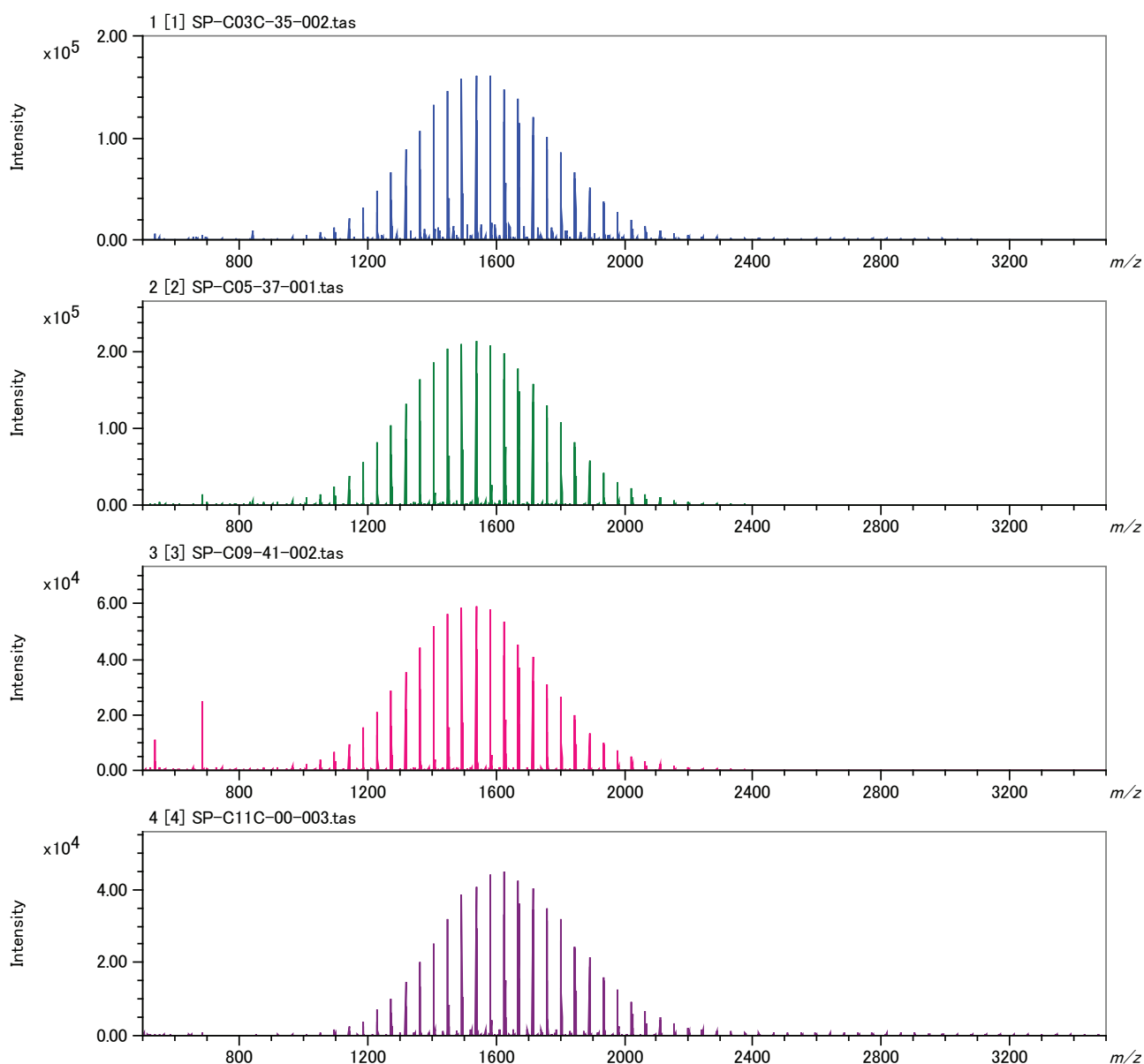

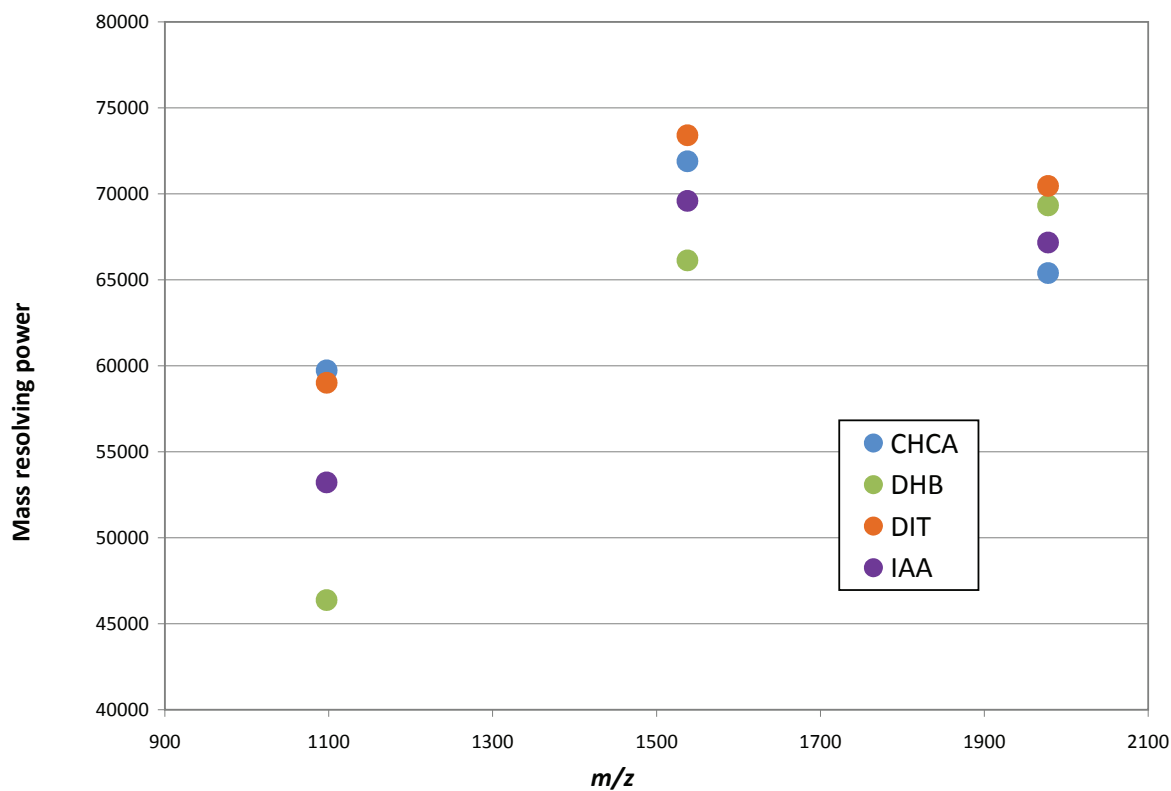Figure 4. MALDI mass spectra of PEG1500.

Figure 5. Averaged mass resolving power (n=10) for *m/z* 1097.6, *m/z* 1537.9 and *m/z* 1978.2.
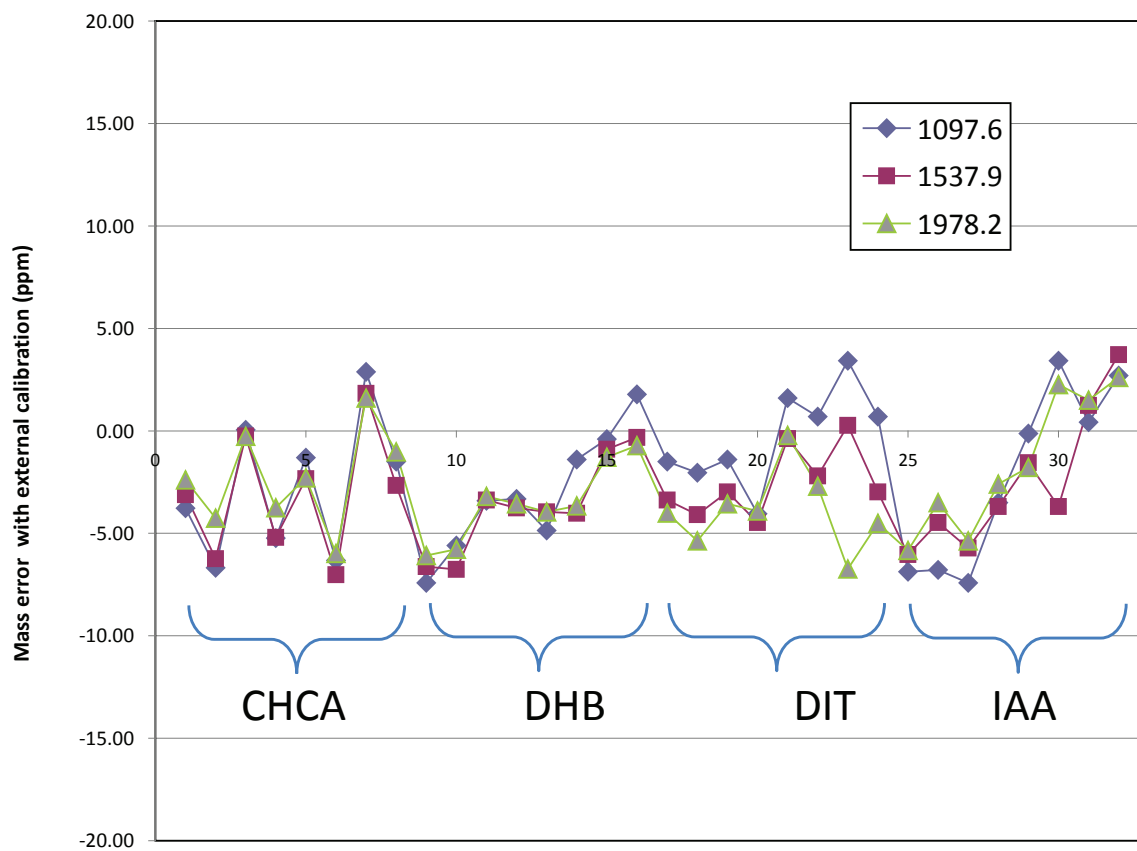

Figure 6. Mass error with external calibration (n=8) for *m/z* 1097.6, *m/z* 1537.9 and *m/z* 1978.2.

We examined the crystal condition with the JEOL JSM-7600F thermal field emission scanning electron microscope. The SEM images are shown Figures 7-10. The crystal shape, size and dispersion were quite different in each matrix crystal. However, SpiralTOF performance was not affected by the topographic effects because these spatial differences were a negligible fraction of the 17 m flight path.

Conclusions

SpiralTOF achieved highly reproducible mass resolving power and high mass accuracy with external mass calibration for all samples. These values were not significantly influenced by the different crystal morphologies for the different matrices. This is attributed to the SpiralTOF's very long (17 meter) flight path.
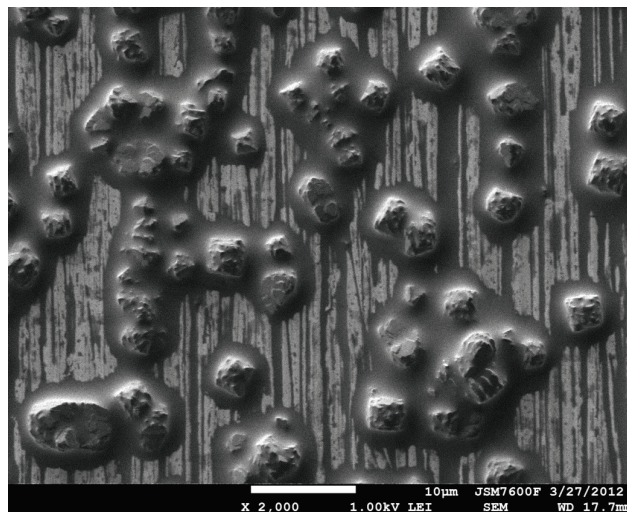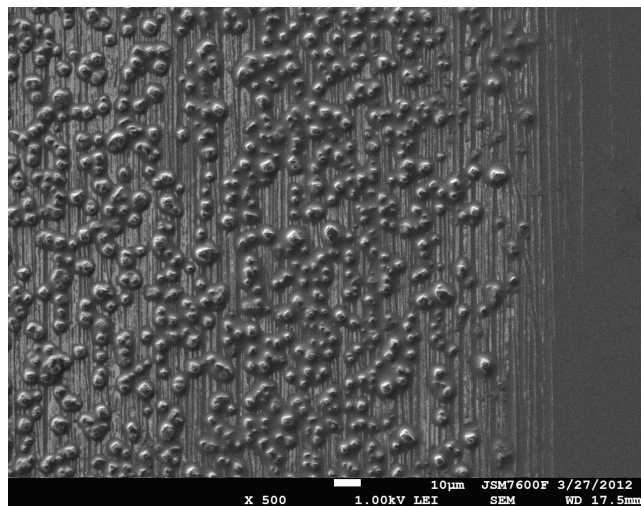

Figure 7. SEM images of CHCA crystal with PEG1500: left: x500, right: x2,000.
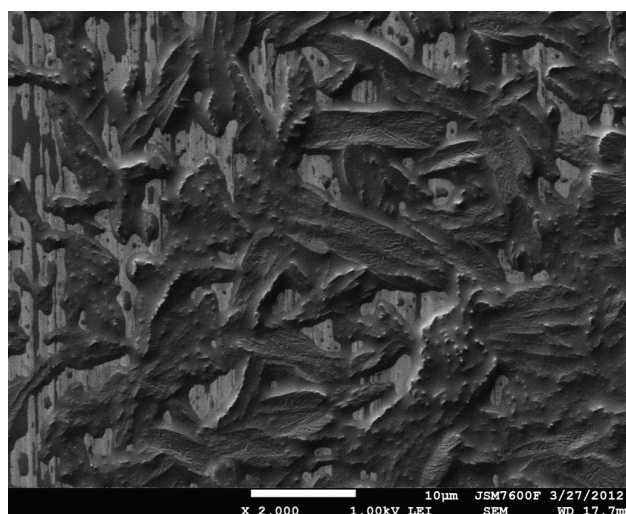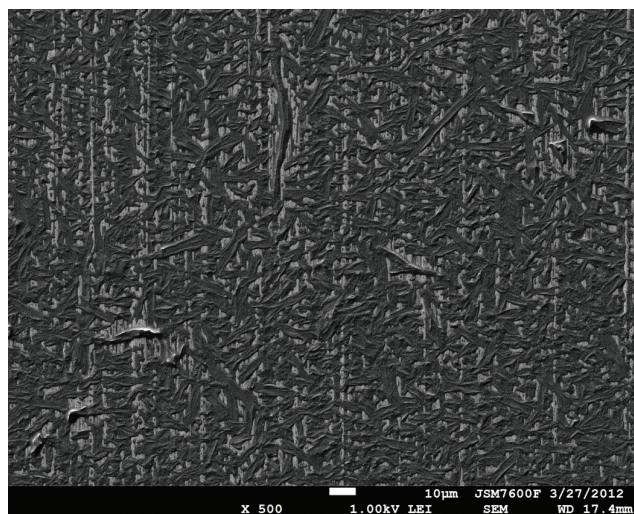

Figure 8. SEM images of DHB crystal with PEG1500: left: x500, right: x2,000.
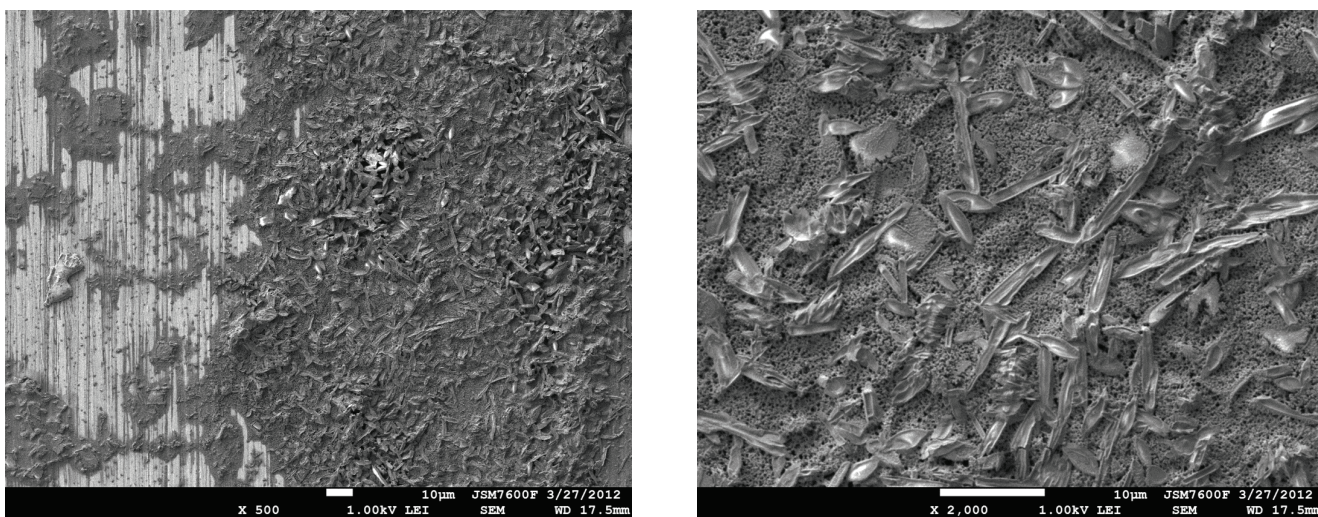
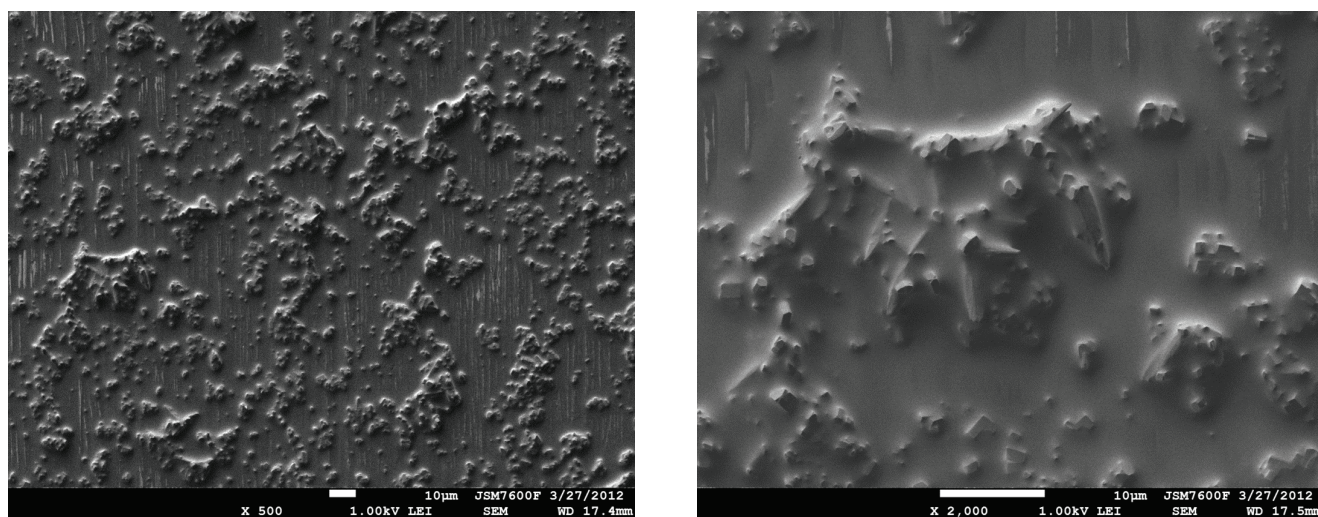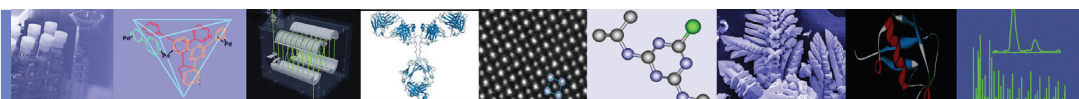Figure 9. SEM images of DIT crystal with PEG1500: left: x500, right: x2,000.

Figure 10. SEM images of IAA crystal with PEG1500: left: x500, right: x2,000.

SpiralTOF™

High Mass-Resolution MALDI-imaging MS for Drug Metabolism in Tissue Using the JMS-S3000

Introduction

Imaging by using matrix-assisted laser desorption/ionization mass spectrometry (MALDI-Imaging) has been expanded during the last decade into biological applications in order to assess the distribution of proteins, peptides, lipids, drugs, and metabolites in tissue specimens. For a drug metabolism analysis, MALDI-Imaging has an advantage in that it can visualize the distributions of drugs and metabolites without using radio isotopes which are used for whole body autoradiography.

In MALDI-Imaging measurements, a laser is used to irradiate each point across a sample surface in order to acquire a mass spectrum for a given location. By combining the mass spectra with their two-dimensional position information, localization of compounds with inherent molecular weights can be visualized or the mass spectra for certain regions of interests (ROIs) can be created.

The JMS-S3000 SpiralTOF is a MALDI-TOFMS, which utilizes the JEOL patented spiral ion optics system. It has a 5-10 times longer flight path than the typical reflectron type MALDI-TOFMS. As a result, it can achieve high mass-resolution to separate peaks that have the same nominal mass but have different exact masses (isobaric separation). This feature is particularly effective for MALDI-Imaging for drug metabolism, which typically consist of relatively low molecular weight compounds which are often interfered with by matrix compounds and/or surface contaminants.

Experiments

Sample and preparation conditions are listed in Table1.

The MS Imaging measurements on the liver tissue section (7.8 mm×9.2 mm) were performed on the SpiralTOF in positive ion mode with a spatial resolution of 50 μm. The MS Imaging data was processed with msMicroImager (JEOL). The MS/MS measurements with TOF-TOF positive ion mode were also performed for structure analysis of the drug and its metabolite.

Results and Discussion

The peak observed at m/z 472.3425 in the averaged mass spectrum was assigned to terfenadine ($C_{32}H_{41}NO_2$) [M+H]$^+$ (m/z 472.3210) and was supported by the MS/MS measurements (described below). The averaged mass spectrum, which was mass corrected using the assigned peak of terfenadine, is shown in Fig. 1. The enlarged mass spectrum at m/z 472 and 502 are also shown. The peak at m/z 502.2944 was assigned to fexofenadine ($C_{32}H_{39}NO_4$) [M+H]$^+$ (m/z 502.2952), a metabolite of terfenadine, by accurate mass and MS/MS measurements (also described below). The isobaric separation capability of 0.2-0.3 u was then used to draw the inherent mass images for each target peak. The optical image of the tissue section and the mass images for m/z 472.3 and m/z 502.3 with 0.1u mass window are shown in Fig.2. Both terfenadine and fexofendine were distributed across the liver tissue sections. The product ion spectrum of a) terfenadine spotted on ITO glass, b) m/z 472.3 and c) m/z 502.2 from the liver tissue section are shown in Fig. 3. The fragmentation channels observed in Fig. 3a and b were nearly identical so that m/z 472.3 was assigned to terfenadine. The estimated fragmentation paths observed at m/z 216, 270 and 288 are shown in the structural formula for terfenadine. Most of the fragments observed in Fig. 3c were similar to Fig 3a, but several of them were observed to have a 30 u difference (red numbers). These differences were likely due to the methyl group in terfenadine changing to a carboxyl group in fexofendine.

Acknowledgment

Drug	Terfenadine
Animal	Male SD rat (7 weeks)
Liver correction	Terfenadine: 1 h after 50 mg/kg po administration
Sample preparation	10-mm-thick sections were prepared from the frozen liver blocks in a cryostat and placed onto ITO glass slides
Matrix application	50 mg/mL DHBA in 50% MeOH/water containing 0.1% TFA was sprayed on the sections with an airbrush

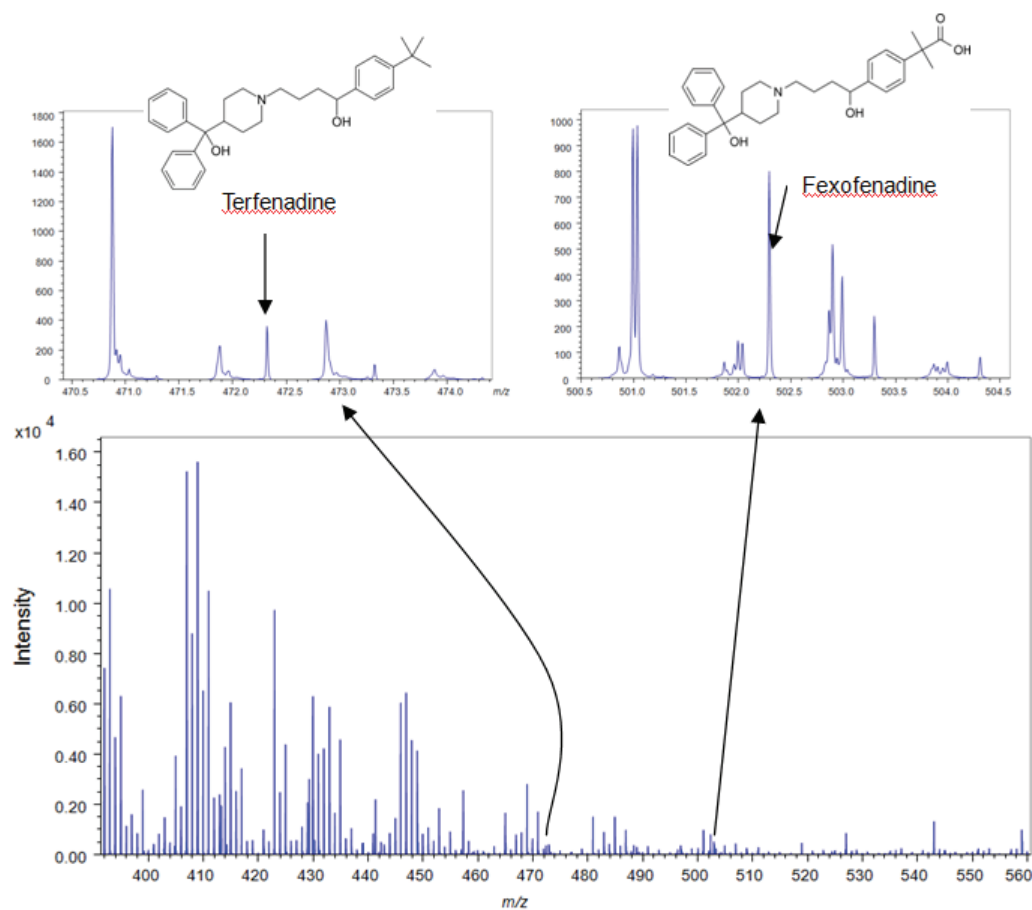Table 1. Sample and sample preparation conditions.

Fig. 1 Averaged mass spectrum of all pixels acquired during the MALDI-Imaging measurement.
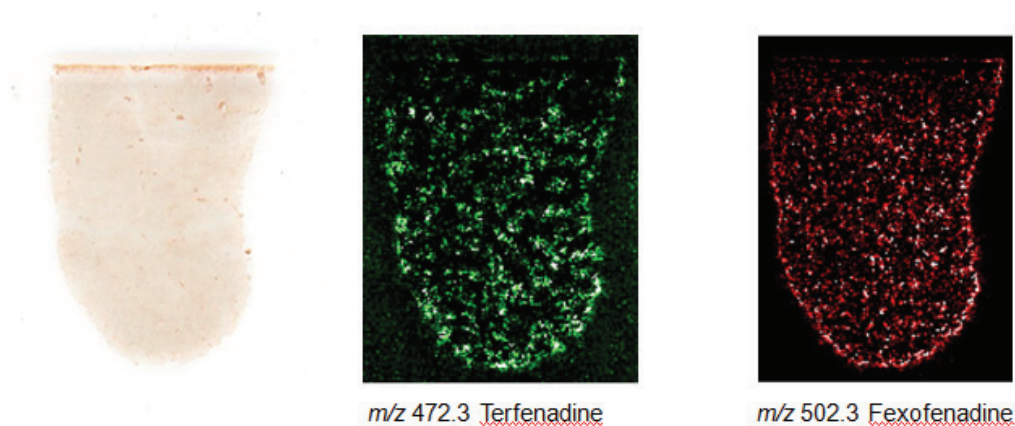

m/z 472.3 Terfenadine

m/z 502.3 Fexofenadine

Fig.2 Picture of the tissue section and the extracted mass image for *m/z* 472.3 and 502.3.
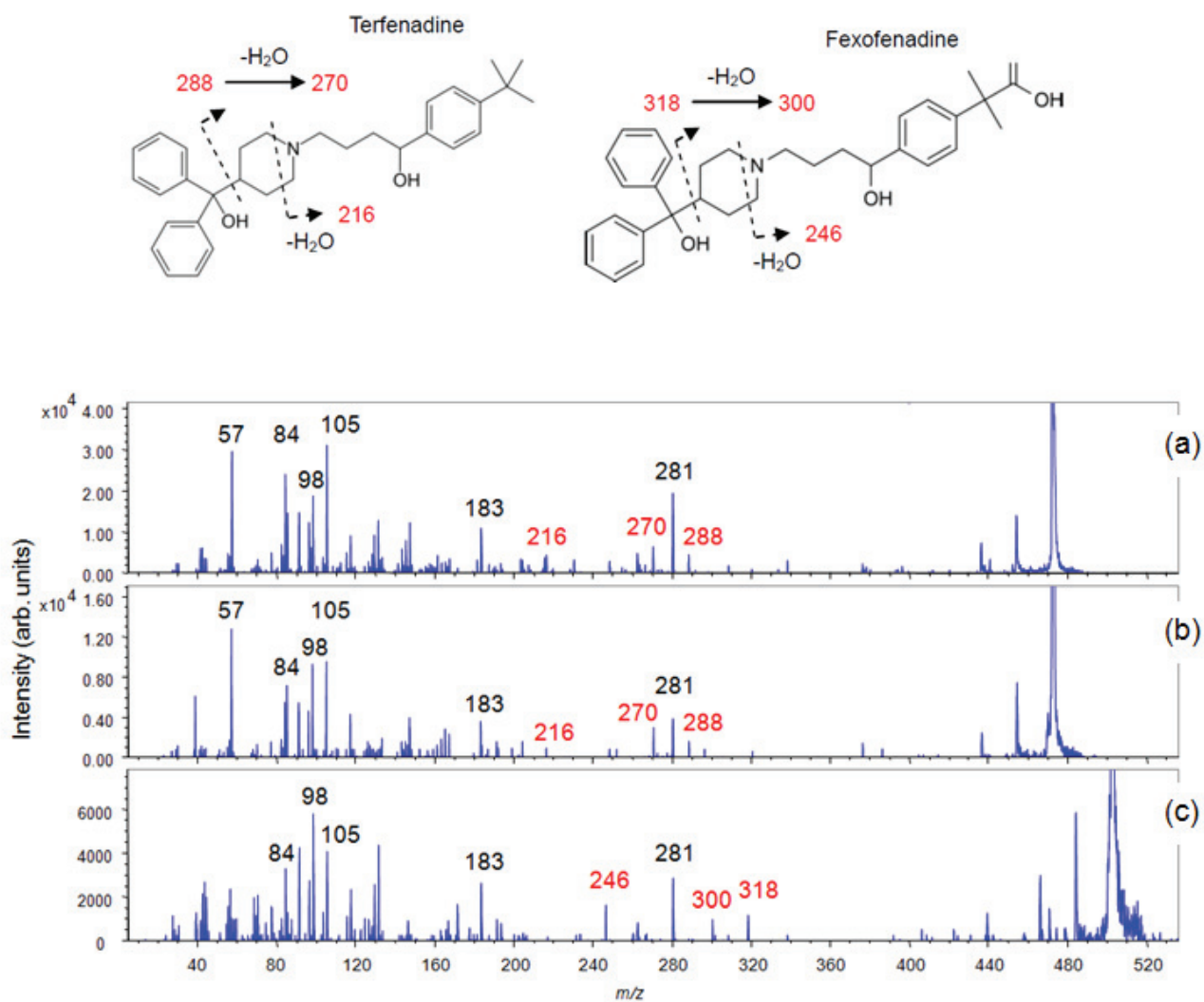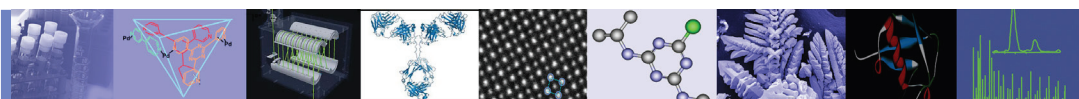
Fig.3 The product ion spectrum of *m/z* 472.3 from standard terfenadine(a). The product ion spectra from the liver tissue section, *m/z* 472.3(b) and *m/z* 502.3 of fexofenadine (c).

SpiralTOF™

High Mass Resolution MALDI-imaging MS Using JMS-S3000 SpiralTOF and msMicroImager

Introduction

Imaging mass spectrometry using matrix-assisted laser desorption/ionization mass spectrometry (MALDI-Imaging) has been expanded during the last decade in biological applications, to assess the distribution of proteins, peptides, lipids, drugs, and metabolites in a tissue specimen. In MALDI-Imaging measurements, a laser irradiation point was scanned on a sample surface to acquire a mass spectrum at each point. Analyzing the mass spectra with two-dimensional position information, localization of compounds with inherent molecular weights can be visualized or the mass spectra for certain regions of interests (ROIs) can be created. The JMS-S3000 SpiralTOF (Fig. 1) is a MALDI-TOFMS, which utilizes the JEOL patented spiral ion optical system. It has a 5-10 times longer flight path than the typical reflectron type MALDI-TOFMS. As a result, it can achieve high mass-resolution to separate peaks that have the same nominal mass but have different exact masses (isobaric separation). On the other hand, there are some issues for analyzing high mass resolution and high lateral resolution MALDI-Imaging raw data with common imaging software options such as Biomap.

1. It is difficult to handle the large size raw data, especially for a large number of mass spectrum points.
2. It is difficult to use the detailed information from high mass resolution MALDI-Imaging by extracting mass images manually. Furthermore, peaks observed in the mass spectra cannot be identified by its origin, such as samples, matrix compounds or surface contaminations, before drawing the mass images.
3. A lack of function to overview a large number of mass images.

The JEOL msMicroImager software for high mass resolution MALDI-Imaging raw data was designed to resolve all of these issues.
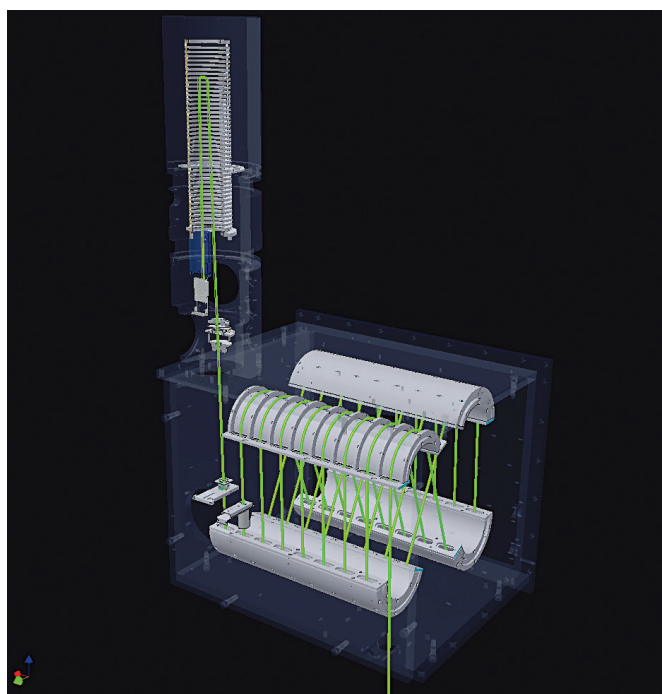
a)

b)

Fig. 1 a) Appearance of JMS-S3000 SpiralTOF and b) its spiral type ion optics

Experimental

A mouse brain tissue section was placed on an ITO conductive glass slide plate. The matrix compound DHB was sprayed onto the surface of the tissue and then the sample was introduced into the mass spectrometer. The MS Imaging measurements were performed on the left half of the brain tissue section (5 mm×7 mm) with 40 μm spatial resolution. The sampling interval of data acquisition system was 0.5 ns, which included 170,000 mass data points in *m/z* 500-1000. The total pixel was 21,125 and raw data size was 14GB.

Results and discussion
Handling large MALDI-Imaging data

The size of high mass resolution and high lateral resolu-
tion mass imaging data can be quite large. The raw data used in this report was 14 GB. Consequently, it often took 10 sec to extract one image by accessing the data on external storage devices. The msMicroImager software has a function that improves the processing speed by storing the compressed data on the RAM. The data compression can be achieved by limiting the mass ranges, mass spectrum binning or pixel binning. Binning is a process to average intensities of several points to one point. For example 3 point mass spectrum binning and 2×2 pixel binning, the 14 GB data was compressed to 1GB. The mass images of *m/z* 868 without binning and 2×2 points pixel binning are shown in Fig. 2. This process has an advantage in extracting hundreds of mass images simultaneously, as described in next section.
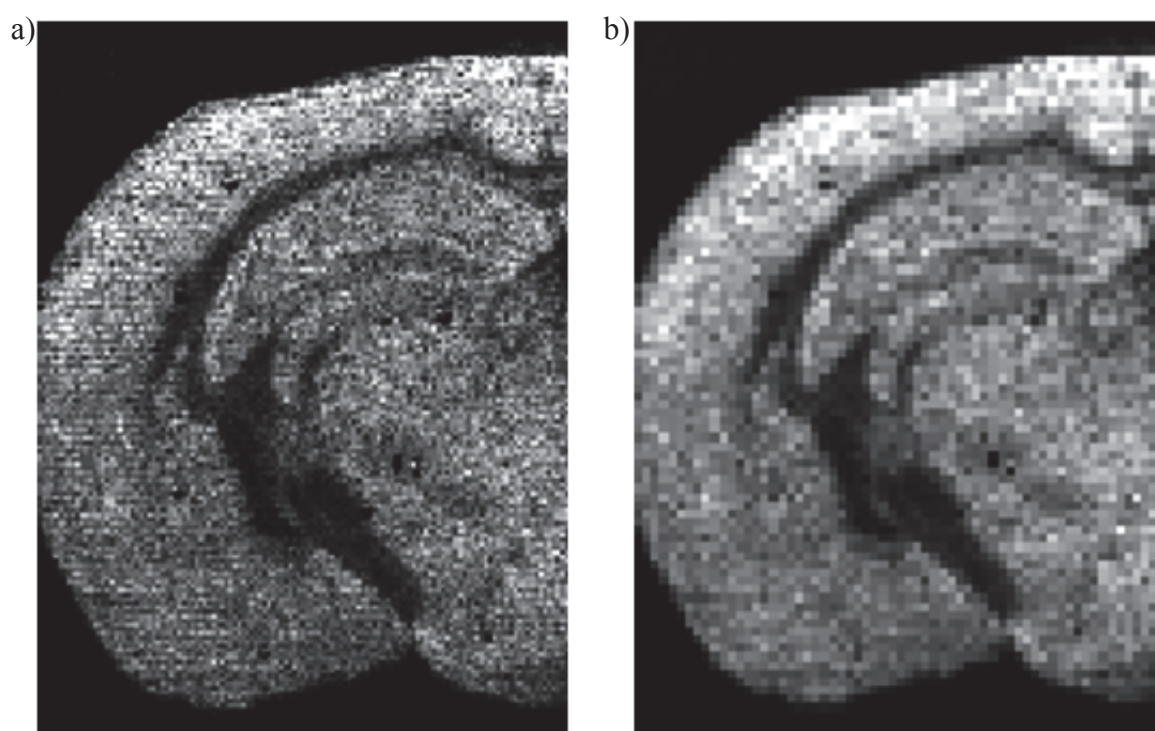

Fig. 2 a) The mass images at *m/z* 866 without binning process and b) after 2×2pixels binning process.

Extracting large number of mass images

An averaged mass spectrum of all pixels is shown in Fig. 3a. The enlarged mass spectrum at *m/z* 820-825 after 2×2 points pixel binning process was shown in Fig. 3b. The high mass resolution capability of the SpiralTOF is able to achieve isobaric peak separation even for minor components in the mass spectrum. In the case of MALDI-Imaging, a matrix compound is sprayed on the sample surface. The peaks observed in the mass spectrum were originated from target compounds, matrix compounds, and surface contamination. It is difficult to extract a number of mass images for the minor components manually by using common imaging MS software, because

a manual extracting process includes several times of mass spectrum expanding. Furthermore, their origin cannot be identified before extracting the mass images. The msMicroimager software has two additional ways for extracting mass images beyond manual peak selection: extract mass images using i) import target peak list and ii) import peak list made by mass spectrum analysis software for SpiralTOF "msTornado Analysis". The green bands shown in Fig. 3b were selected peaks using the peak pick list from the msTronado Analysis software. Over 200 peaks can be selected between *m/z* 700-1000. The extracting time for these 200 mass images was only a few seconds after the binning process, where it took an hour without the binning process.
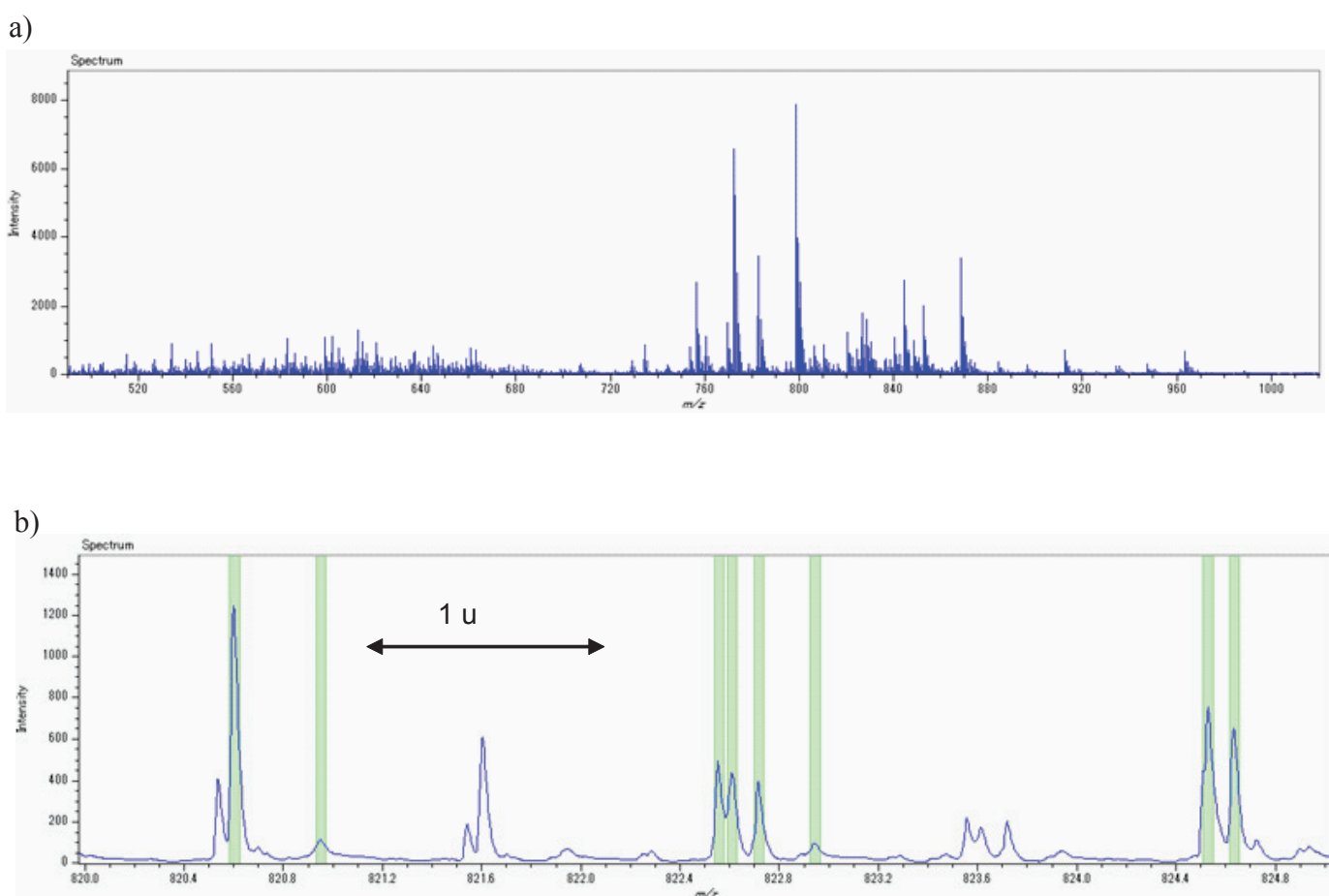
a)

b)

Fig. 3. a) Averaged mass spectrum of all measured pixel and b) an enlarged spectrum at *m/z* 820-825 after binning process.
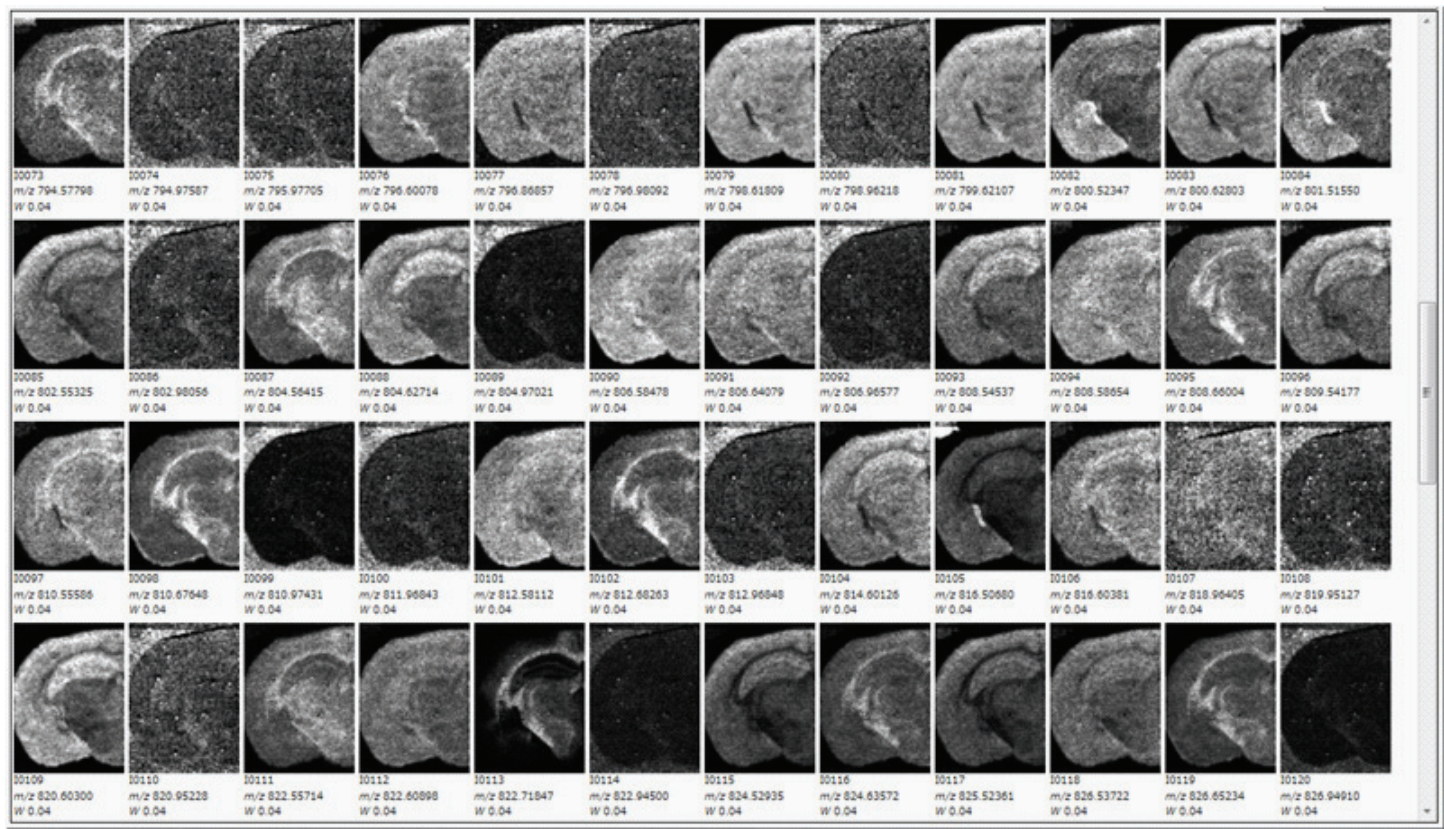
Fig. 4 Display a list of mass images extracted from high mass resolution imaging data.

The overview of extracted mass images

The msMicroImager is able to overview the extracting mass images. Fig. 4 shows a part of the 200 extracted mass images in the last section. The characteristic distribution can be found by looking at the mass images in order to guide a more detailed analysis of the sample.

Conclusion

MALDI-Imaging using SpiralTOF and msMicroImager make it easier to extract a number of mass images from large size raw data. The full use of the detailed information can be obtained from high mass-resolution and high lateral resolution MALDI-Imaging.
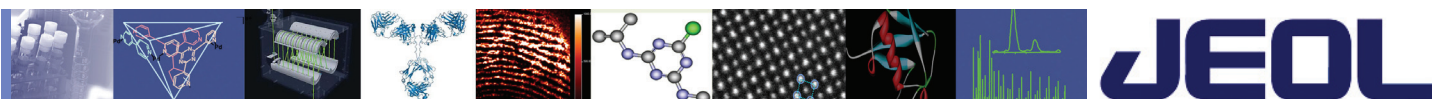
SpiralTOF™

Fingerprint Analyses Using MALDI Imaging and SEM Imaging

Introduction:

MALDI imaging is a state-of-art mass spectrometry technique that allows for the visualization of chemical distributions on the surfaces of biological and material samples. This analytical technique can provide the chemical distribution on the surface as an image that is mapped using the intensity of the observed ions. The image contains individual MALDI mass spectra at each pixel. Therefore, it is possible to simultaneously carry out high-mass-resolution qualitative analysis and chemical distribution analysis.

The JMS-S3000 SpiralTOF (Figure 1) has a unique 17m flight path that offers the highest mass resolution and mass accuracy MALDI-TOF MS system.   In this work, we demonstrated the MALDI imaging measurement for the fingerprints of a smoker and a non-smoker by using the JEOL SpiralTOF system. Additionally, we looked at the smoker's fingerprint using the JEOL JSM-7800F thermal field emission scanning electron microscope (FE-SEM) shown in Figure 2.

Experimental:

Sample information and preparation conditions are described below.

Samples
- A non-smoker's fingerprint
- A smoker's fingerprint

MALDI Imaging measurement
- Measurement mode: SpiralTOF positive mode
- Matrix: 2,5-Dihydroxybenzoic Acid (DHB), 2mL spray @ 30mg/mL
- Measurement region: Width 7.0 mm x Length 10.0 mm
- Analytics Software: Biomap 3.8 - Raw data was converted to imzML files

SEM Imaging measurement
- Sample preparation: Uncoated
- Acceleration voltage: 1 kV
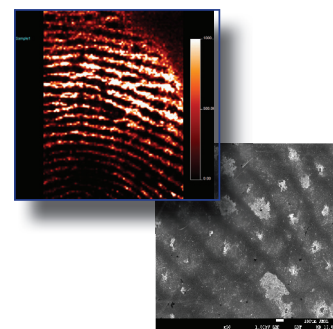- Magnification: 50x and 5,000x

Figure 1. JMS-S3000 SpiralTOF.

Figure 2. JSM-7800F Thermal FE SEM.

Sample Preparation and Measurement:

The fingerprint samples (Figure 3) were created by pressing the right index finger onto an electrically conductive ITO glass slide (HST inc., 0.7 mm thickness, Type II). The DHB MALDI matrix was dissolved in 70%-MeOH at a concentration of 30 mg/mL. Two milliliters of this DHB matrix solution was sprayed onto the fingerprint using an airbrush. PPG was used for the external calibration standard. After the samples were dried, they were measured using the JMS-S3000 SpiralTOF MS system. We also obtained SEM images for the smoker's fingerprints with the JSM-7800F.
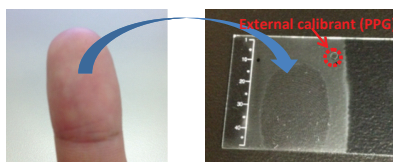

Figure 3. Fingerprint sample.

Results & Discussion:

Lipids analysis on the fingerprint

As a starting point, the MALDI images for three lipids (*m/z* 717.7, 827.8, 907.8) and a full-range mass spectrum averaged over a section of the fingerprint are shown in Figure 4. All MALDI images are set to the same intensity scale. The scale bar is displayed on the right side of each image with the white color indicating the highest intensities, the dark green color indicating the lower intensities, and the black color indicating the background (absence of ions). Figure 4a-c show the lipid distribution along the fingerprint. For these samples, the lipids appear to be most strongly present at the edge of the finger.

Nicotine analysis on the fingerprint

Next, we examined the nicotine distribution on both a smoker's and non-smoker's fingerprints. The MALDI mass spectra of nicotine and related chemicals are shown in Figure 5.

As might be expected, the smoker's fingerprint had several chemicals present around the expected mass for nicotine as shown in the top spectrum in Figure 5. First, we focused on determining the chemical composition of observed *m/z* 163 on the fingerprint by using the accurate mass values with internal calibration method. DHB matrix ions were used as internal calibrant for this accurate mass measurement. The mass error of the *m/z* 163 was just -0.6 mDa when compared to the protonated molecule of nicotine standard using internal calibration. However, the isotopic pattern was slightly different from the theoretical isotopic pattern of nicotine because more than one compound was present. On this fingerprint, both $C_{10}H_{15}N_2$ (Nicotine) and $C_{10}H_{17}N_2$ appear to be present.
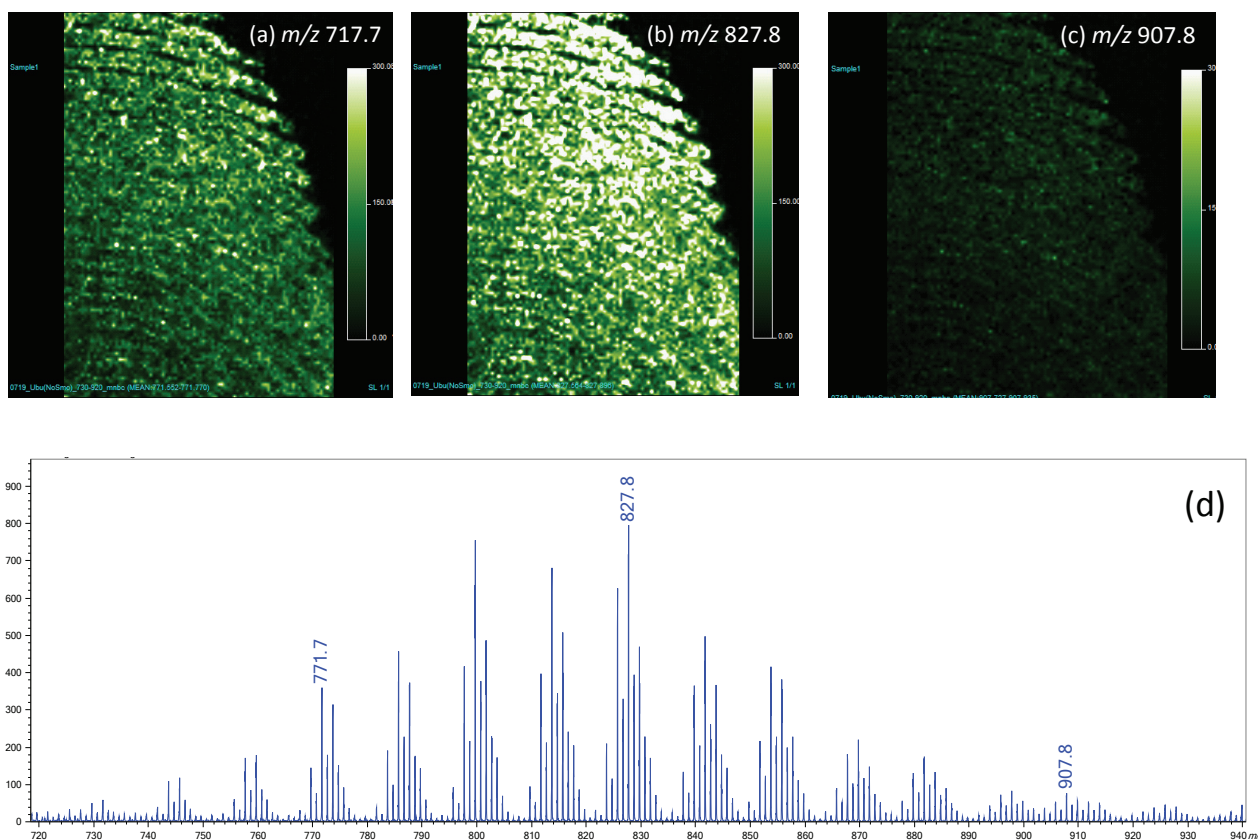

Figure 4. MALDI images: (a) *m/z* 717.7, (b) *m/z* 827.8, (c) *m/z* 907.7, and (d) full range mass spectrum.
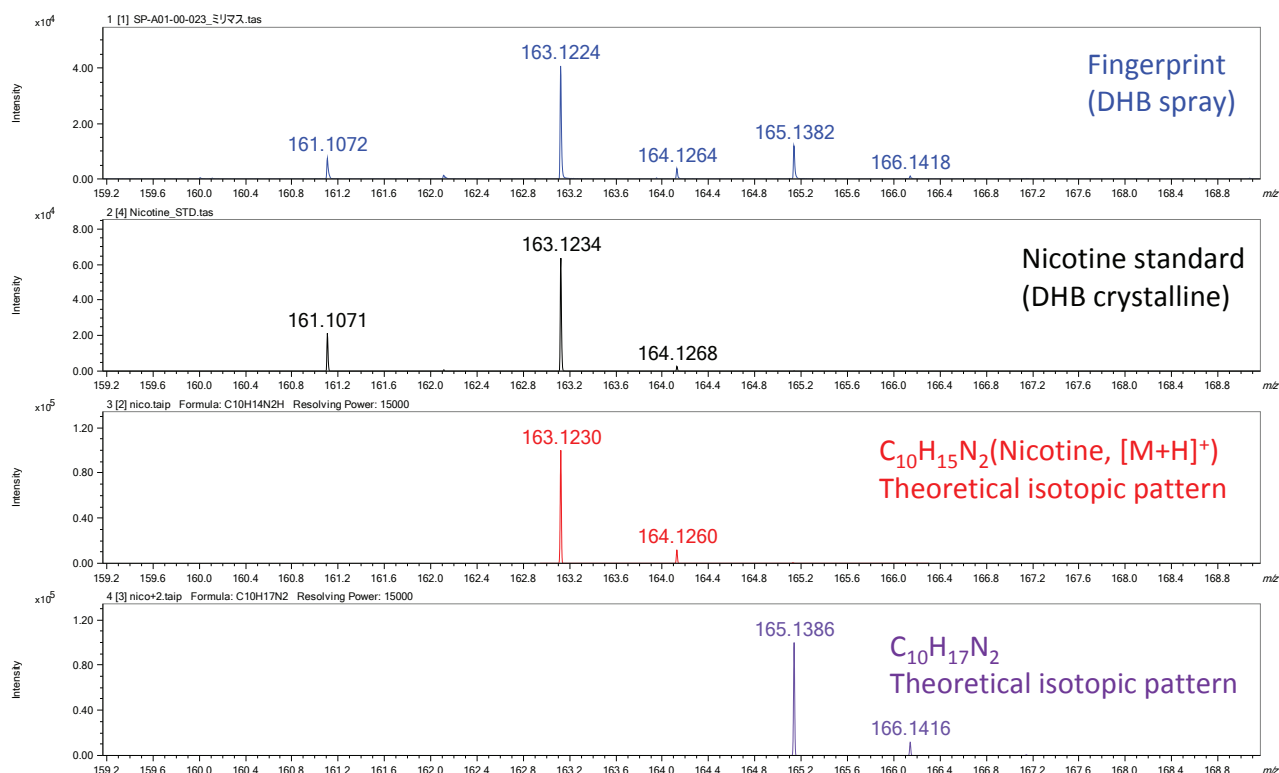
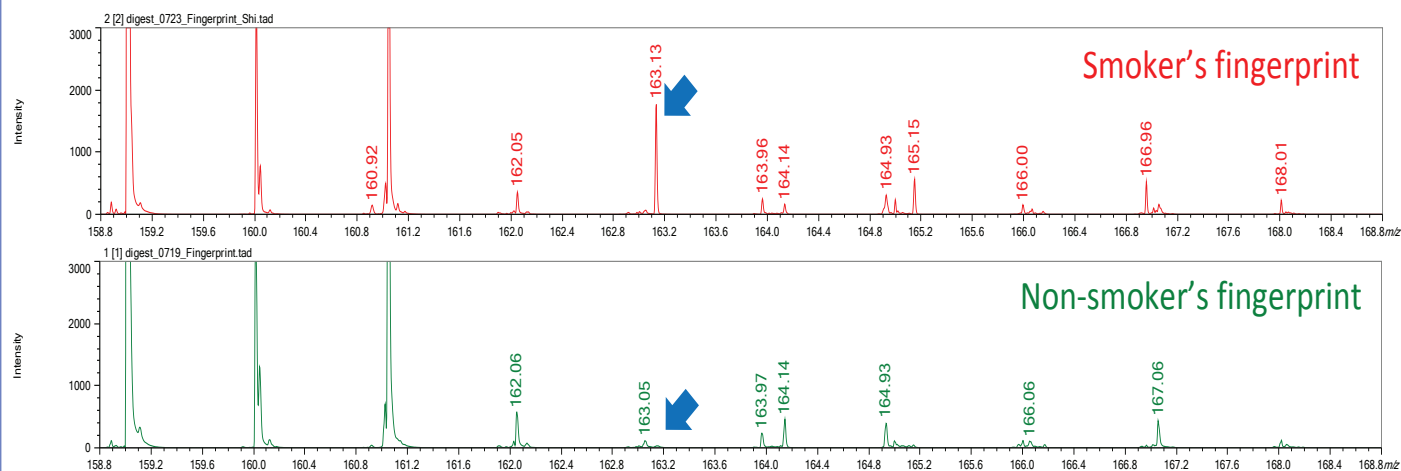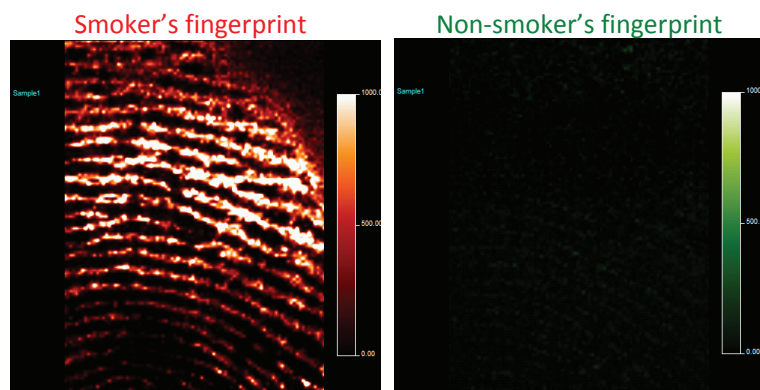Figure 5. MALDI mass spectra of nicotine and other chemical.

Figure 6. MALDI images: (left) smoker's, (right) non-smoker's, and enlarged digest mass spectrum.

Applications Note

MS-0918A

The MALDI images for nicotine and a full range mass spectrum around *m/z* 163 are shown in Figure 6. Both MALDI images are normalized to the same intensity scale. The scale bar is displayed on the right side of each image with white indicating a higher intensity of protonated Nicotine molecule ion, dark red (green in nonsmoker fingerprint) indicating lower intensities, and black indicating background (absence of ions).

There was a strong nicotine distribution on the smoker's fingerprint that was not detected on the non-smoker's fingerprint. This is a very reasonable result considering the smoker is exposed to nicotine when smoking. The results show that SpiralTOF MALDI imaging can be a very useful analytical tool for visualizing the distribution of small molecules on surfaces.

SEM analysis of the fingerprint

Next, we examined a smoker's fingerprint with the JEOL JSM-7800F thermal field emission scanning electron microscope. The SEM images are shown Figures 7. There were a lot of sebum, particles and other contaminations observed in the fingerprint. The JSM-7800F provided clear imaging data for the organic matter by using a lower acceleration voltage.

Conclusions:

We were able to show MALDI images for Lipids and Nicotine on the fingerprint. The SpiralTOF MALDI imaging capabilities were shown to be:

1. High mass resolving power
2. Good for small molecule analysis
3. Good spatial resolution

Additionally, the JEOL JSM-7800F SEM provided clear images of the organic material present in the fingerprint.
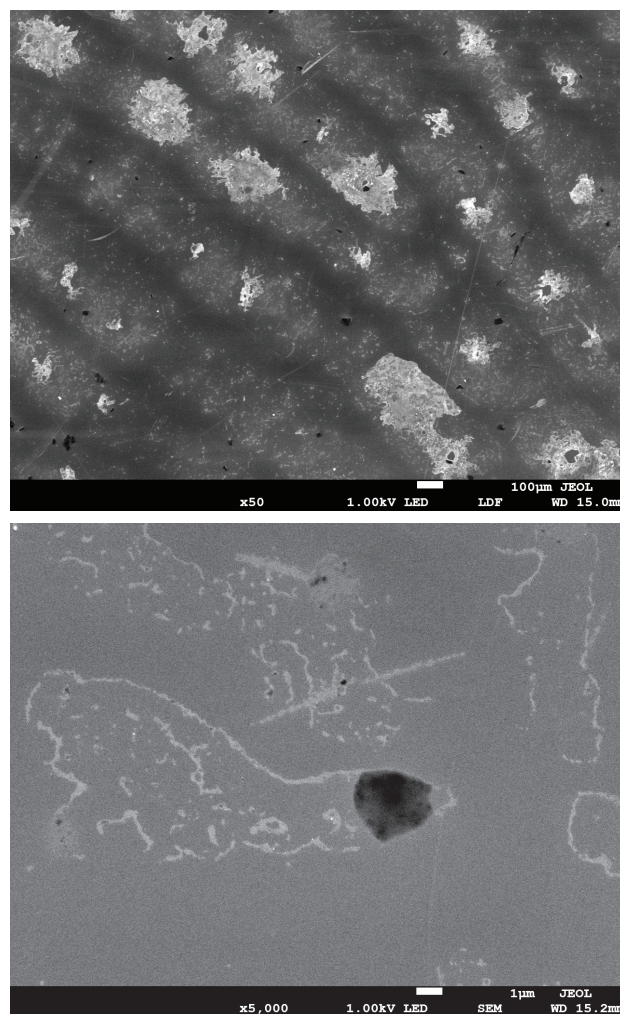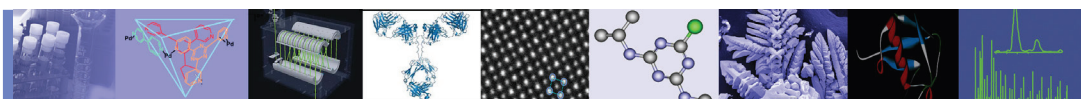
Figure 7. SEM images of a smoker's fingerprint: (top) 50X, (bottom) 5,000X.

SpiralTOF™

MALDI-Imaging MS of Lipids on Mouse Brain Tissue Sections Using Negative Ion Mode

Introduction

The main biological functions of lipids include energy storage, signaling, and acting as structural components of cell membranes. Not only their chemical composition and structures but also the distributions in biological body are important for biochemistry. Matrix-assisted laser desorption/ionization imaging mass spectrometry (MALDI-Imaging MS) is a powerful tool for the biochemical analyses of surfaces. Different lipid types are observed in positive or negative-ion MALDI mass spectra, depending on the presence of polar functional groups. Phosphatidyl cholines and galactosyl ceramides were mainly observed in the MALDI-Imaging MS of positive ion mode using JMS-S3000 SpiralTOF[1].

In this work, we report the use of the SpiralTOF for negative-ion MALDI-Imaging MS of sulfatides. High-resolution, accurate mass data and MS/MS data obtained under high-energy CID conditions provide information about structures, elemental compositions, and localization of many types of sulfatides.

Experimental

A mouse brain tissue section was placed on an ITO conductive glass slide plate (Fig. 1). The matrix compound 9-aminoacridine was sprayed on the surface of the tissue and then the sample was introduced to the mass spectrometer. The imaging MS measurements were performed in negative-ion mode on the whole brain tissue section (6.3 mm × 9.24 mm) with 60 μm spatial resolution. The images consisted of 16170 mass spectra equivalent to the accumulation of 500 laser shots for each mass spectrum.

Results and Discussion

The averaged mass spectrum of all pixels is shown in Fig. 2. The base peak ion at nominal m/z 888.6 was assigned as sulfa-
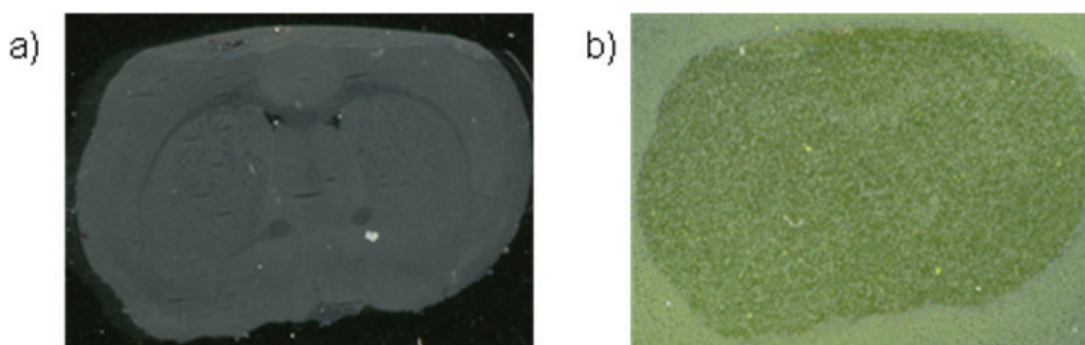

Figure 1. A mouse brain tissue on an ITO coated glass plate.
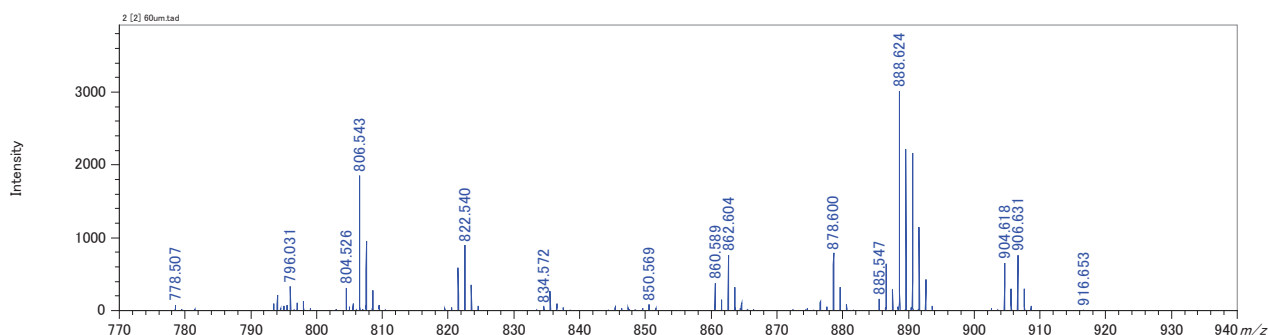a) before matrix coating, b) after matrix coating

Figure 2. Averaged mass spectrum of mouse brain tissue.

tide C24:1[M-H]⁻ . Structural analysis using TOF-TOF mode confirmed the assignment. The product-ion mass spectrum for *m/z* 888.6 is shown in Fig. 3. The structural formula and expected fragmentation channels of sulfatide C24:1 [M-H]⁻ are also shown in Fig. 4. The observed peaks in Fig. 3 are a very good match with the expected fragmentation channels shown in Fig. 4. The clear observation of charge-remote fragmentation in *m/z* > 600 due to high-energy collision induced dissociation is a characteristic feature of the SpiralTOF, which provides high-quality structural information for lipids.

   For the accurate mass analysis, the averaged spectrum was mass corrected by a single point calibration using the calculated *m/z* 888.6240 of confirmed sulfatide C24:1 [M-H]⁻. The results of composition estimation of major peaks observed in the averaged mass spectrum are shown in Table. 1. Nearly all compounds were assigned within 5 ppm mass error. The mass images of all compounds listed in Table.1 are shown in Fig. 5. The phosphatidylinositol (PI) (38:4) (Fig.5 Image #8) is

uniformly distributed on mouse brain tissue section. On the other hand, all sulfatides are localized in the same characteristic region. Because the different types of lipids are observed by MALDI-Imaging measurement both in positive[1] and negative ion mode, measurements made using both polarities provide complementary information about the nature and distribution of lipids in tissue sections.

Acknowledgment

Reference

[1] Takaya Satoh et al., *Mass Spectrometry*, Vol. 1 (2012), A0013
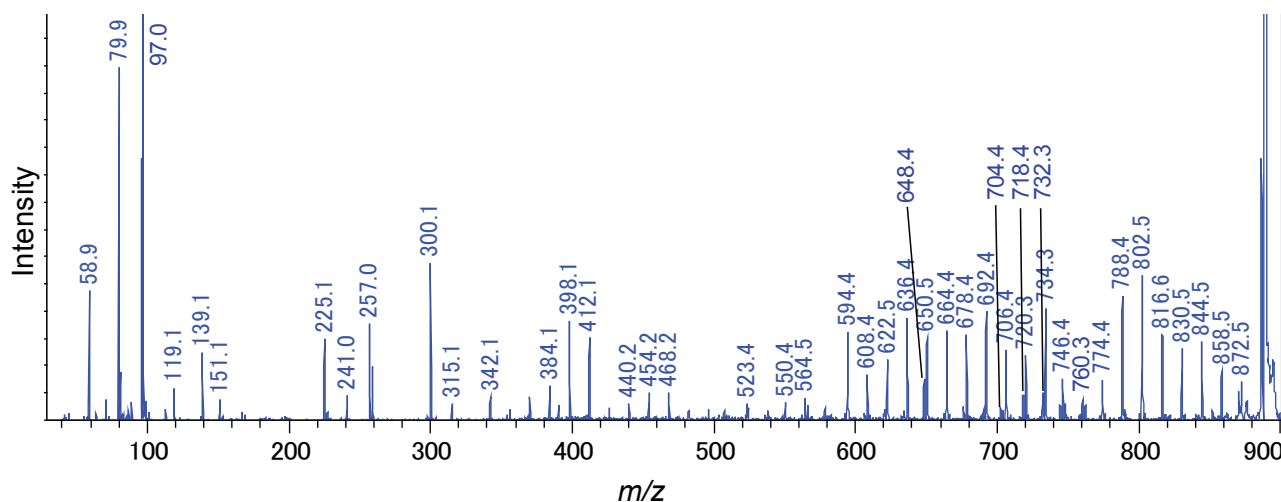

Figure 3. Product-ion mass spectrum of the ions corresponding to the peak at *m/z* 888.6.
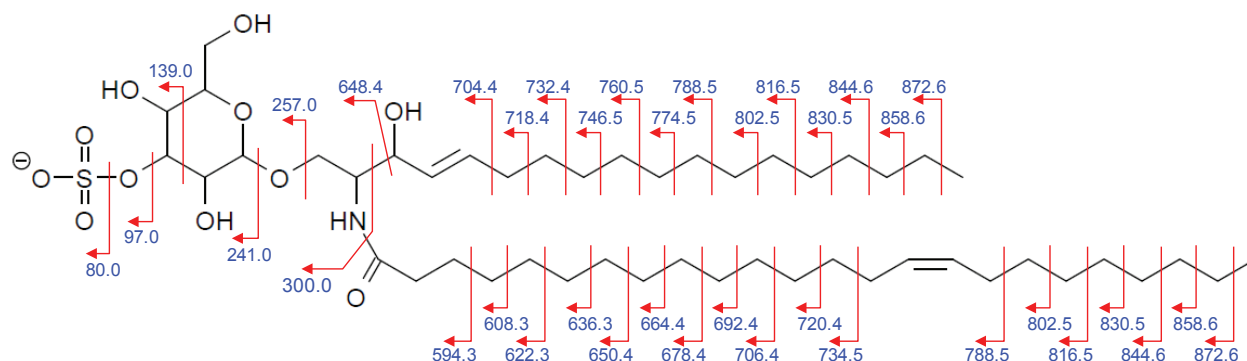

Figure 4. Structure and peak assignments of Sulfatide C24:1.

Number	Compound	Formula	m/z value (Observed)	m/z value (Calculated)	Error [mu]	Error [ppm]
1	C16 Sulfatide	$C_{40}H_{76}NO_{11}S$	778.5070	778.5145	-7.5	-9.6
2	C18 Sulfatide	$C_{42}H_{80}NO_{11}S$	806.5426	806.5458	-3.2	-3.9
3	C18-OH Sulfatide	$C_{42}H_{80}NO_{12}S$	822.5398	822.5407	-0.9	-1.1
4	C20 Sulfatide	$C_{44}H_{84}NO_{11}S$	834.5718	834.5771	-5.3	-6.3
5	C20-OH Sulfatide	$C_{44}H_{84}NO_{12}S$	850.5694	850.5720	-2.6	-3.0
6	C22 Sulfatide	$C_{46}H_{88}NO_{11}S$	862.6037	862.6084	-4.7	-5.4
7	C22-OH Sulfatide	$C_{46}H_{88}NO_{12}S$	878.6003	878.6033	-3.0	-3.4
8	PI(38:4)	$C_{47}H_{82}O_{13}P$	885.5466	885.5499	-3.2	-3.7
9	C24:1 Sulfatide	$C_{48}H_{90}NO_{11}S$	888.6240	888.6240	—	—
10	C24:1-OH Sulfatide	$C_{48}H_{90}NO_{12}S$	904.6179	904.6189	-1.0	-1.1
11	C24-OH Sulfatide	$C_{48}H_{92}NO_{12}S$	906.6308	906.6346	-3.8	-4.2
12	C26:1 Sufatide	$C_{50}H_{94}NO_{11}S$	916.6529	916.6553	-2.4	-2.6

Table 1. Differences between calculated and observed m/z values for peaks observed in the averaged mass spectra after mass-correction using confirmed Sulfatide C24:1.
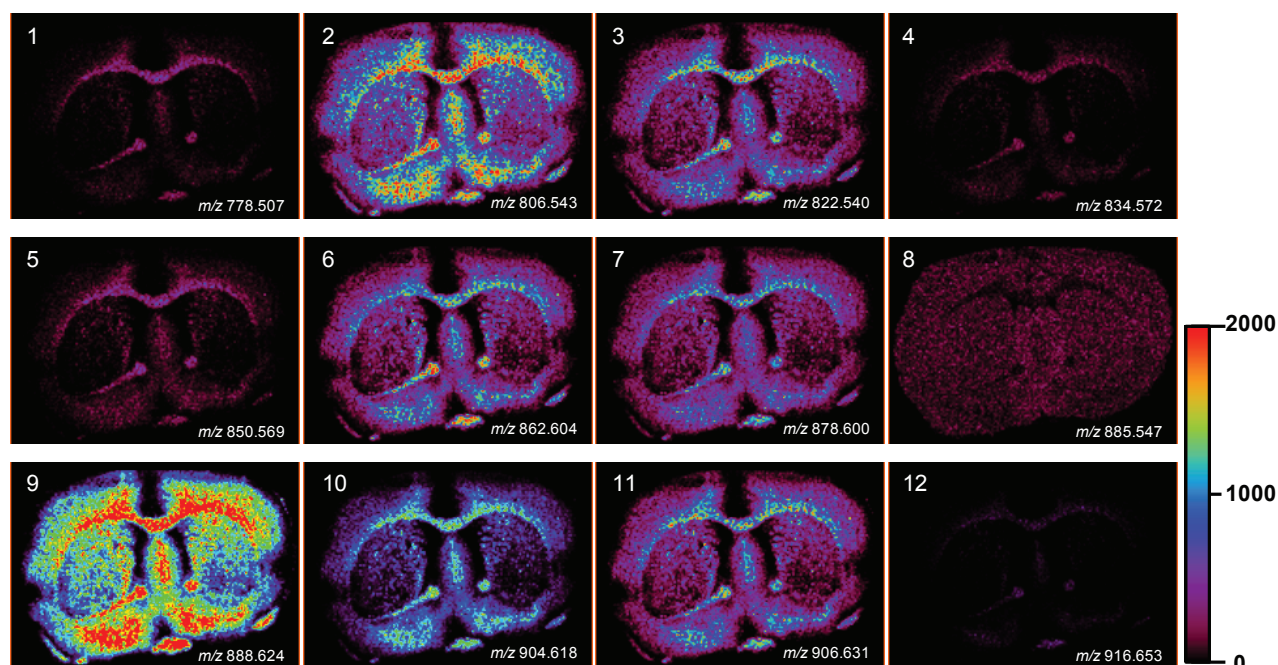

Figure 5. Mass images of compounds from mouse brain tissue.

Applications note   **HS05**

Degradation analysis of polyethylene terephthalate film by UV irradiation using imaging mass spectrometry and scanning electron microscopy

Product：Scanning Electron Microscope(SM), Mass spectrometry(MS)

Introduction

Surface analysis equipment is commonly used to evaluate industrial material for information such as elements, bonding states, and functional groups on the sample surface. However, commonly used tools like scanning electron microscopes (SEM) are not able to provide the elemental composition or structural information about the organic compounds present in/on the sample. Conversely, organic mass spectrometry (MS) can provide this information for organic molecules on surfaces and in the bulk material. Among the MS techniques available, matrix assisted laser desorption/ionization (MALDI) mass spectrometry is a powerful tool for the analysis of synthetic polymers. By using MALDI with a high-resolution time-of-flight mass spectrometer and Kendrick mass defect (KMD) analysis, polymer materials can be quickly analyzed to identify differences in monomer, polymer end groups, and their molecular weight distributions. More recently, MALDI mass spectrometry imaging (MALDI-MSI) has been used to visualize the locations of compounds on sample surfaces, thus suggesting that it is possible to obtain polymer molecular information present on sample surfaces, which is not possible by conventional surface analysis methods like SEM. In a previous report [1], we showed the effects of ultraviolet (UV) irradiation degradation for polyethylene terephthalate (PET) spots. In this report, we have expanded MALDI-MSI to analyzing a PET film that was exposed to UV radiation. Additionally, a SEM was used to look at the morphological differences in the PET film before and after UV irradiation.

Experiment

A 30 μm-thick PET film was used for the sample. First, the right-half of the PET film was masked with aluminum foil, and then UV irradiated for 30 minutes using Handicure 100 (manufactured by Mizuka Planning Co., Ltd.). 2,4,6-Trihydroxyacetophenone (THAP) was used as the matrix, and sodium trifluoroacetate (NaTFA) was used as the cationizing agent. THAP and NaTFA were dissolved in tetrahydrofuran (THF) at concentrations of 10 mg/mL and 1 mg/mL, respectively. A THAP and NaTFA mixture (10:1 v/v) solution was sprayed on the PET film with an airbrush. The MALDI-MSI measurements were done by using the JMS-S3000 in SpiralTOF positive ion mode. The pixel size for the MSI images was 50 μm. The msMicroImager™ software was used for MSI analysis, and msRepeatFinder was used for KMD analysis. The scanning electron microscope measurement conditions are described in the text above Figure 2.

UV Irradiation Time

30 min	0 min

Figure 1. Schematic of the irradiation region of PET film using ultraviolet ray.

Results

Figure 2 shows the secondary electron images for the PET film surface before (A, B) and after (C, D) UV irradiation. These results were obtained by SEM without coating the sample for analysis. In particular, secondary electrons emitted from the sample surface are sensitive to irregularities which makes it suitable for looking at changes in sample surfaces. Figures 2A and B show the secondary electron images before UV irradiation (magnifications of 50,000 and 100,000, respectively), in which the PET surface is smooth. On the other hand, Figure 2C and D show the secondary electron images after UV irradiation (magnifications of 50,000 and 100,000, respectively), in which surface irregularities of approximately 100nm were observed. These results show that SEMs are effective for observing changes in morphology and nanostructures on sample surfaces.

【SEM observation condition】
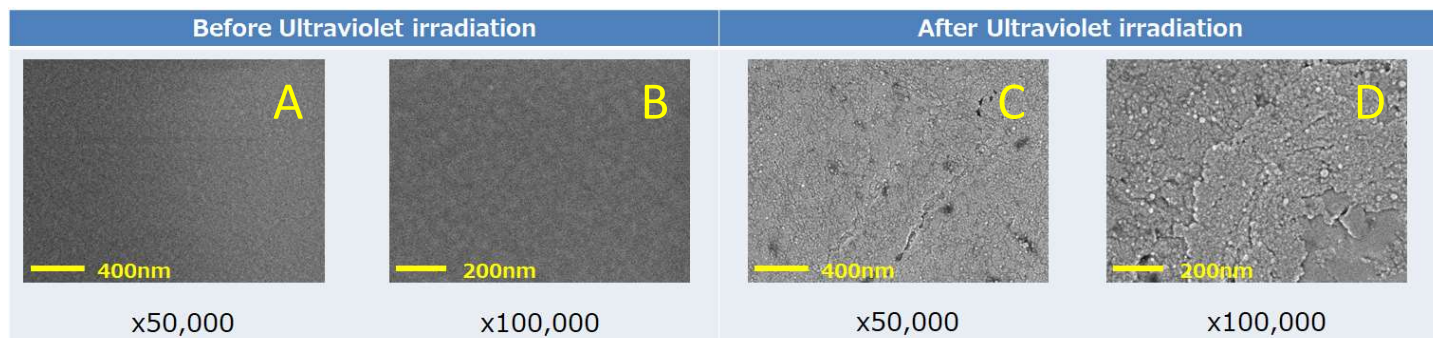Acceleration voltage：0.8 kV, Signal：Secondary electron image, Pretreatment：without coating

Before Ultraviolet irradiation		After Ultraviolet irradiation	
A — 400nm	B — 200nm	C — 400nm	D — 200nm
x50,000	x100,000	x50,000	x100,000

Figure 2. Secondary electron image of PET film surface before (A,B) and after (C,D) ultraviolet irradiation.

JEOL Ltd.

Figure 3A shows the averaged mass spectrum for the entire measurement area. Figure 3B shows the $C_{10}H_8O_4$ KMD plot for the average mass spectrum in which eight different PET series (192u intervals) were identified. Series I thru IV are exactly the same series observed previously in MSTips 307. These series were identified as sodium adduct ions for (I) cyclic oligomer, (II) COOH/COOH end groups, (III) cyclic oligomer + C_2H_4O, and (IV) COOH/OH end groups, respectively. Series I and III are components that were present before ultraviolet irradiation, and Series II and IV are the components that appear after ultraviolet irradiation. The Series I and II images (Figure 4A and 4B) were generated by summing the mass image intensities included in the KMD plot blue and red groups, respectively. The Series I ion intensities are relatively low in the irradiated side (left) so this means that UV irradiation reduces the presence of this series (Figure 4A). On the other hand, the Series II ion intensities are relatively high in the irradiated side (left) so this means that UV irradiation increases the presence of this series (Figure 4B). To show this degradation more clearly, Figure 4C normalizes Series II to Series I by ratioing their ion intensities (Series II/I) in each pixel. Figure 5 shows the Series II to VIII images using Series I for normalization (2×2 pixel binning). Figure 5 clearly shows that the Series III, V, and VIII, which have the same color tone for both the irradiated and unirradiated sections, are present in the sample regardless of UV irradiation. However, Series II, IV, VI, and VII show brighter color areas for the irradiated section of the sample, thus indicating that these PET series are generated by irradiating the surface with UV light.

Conclusion

In this report, we compared UV irradiated and non-irradiated PET thin films by using SEM to observe morphology changes on the surface and MALDI-MSI to detect changes in molecular information on the film surface. Each technique provided complementary information about the UV degradation of a PET thin film.

Reference

[1] MSTips 307 "Mass spectrometry imaging for degradation of polyethylene terephthalate by UV irradiation using JMS-S3000 "SpiralTOF™-plus""
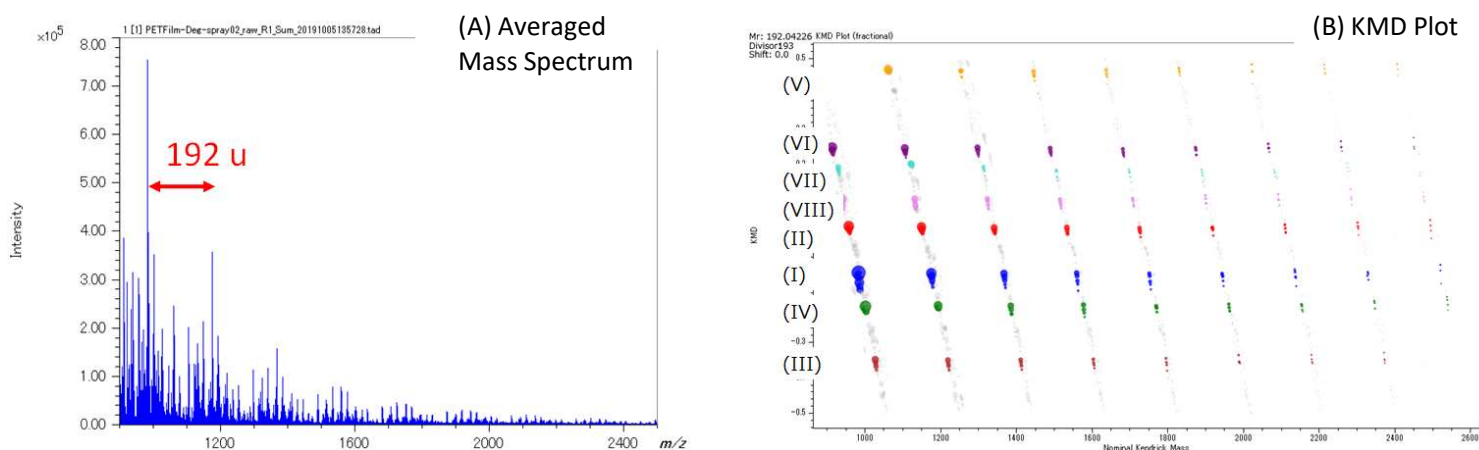

Figure 3. (A) Averaged mass spectrum for the MSI measurement region and (B) KMD plot (base unit $C_{10}H_8O_4$, X=192). The KMD plot easily showed the presence of eight PET series (I) – (VIII).
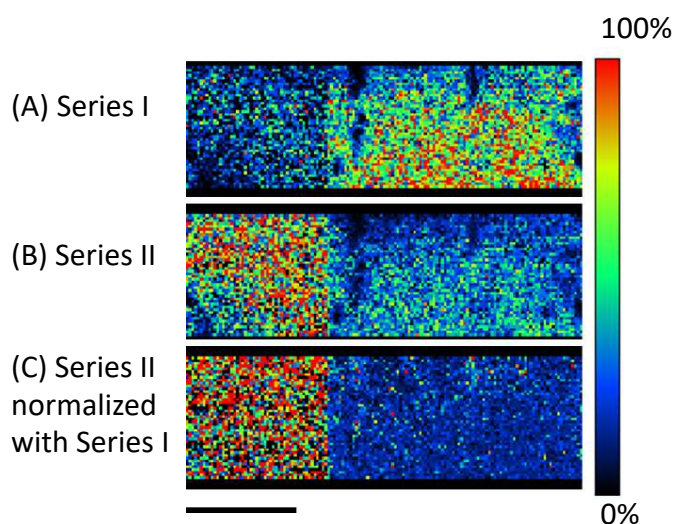

Figure 4. Images of (A) the cyclic oligomer of PET series (Series I), (B) the ultraviolet degraded PET polymer series (Series II), and (C) Series II normalized to Series I.

Figure 5. Images of PET series II –VIII normalized with image of PET series I.

Mass spectrometry imaging for degradation of polyethylene terephthalate by UV irradiation using JMS-S3000 "SpiralTOF™-plus"

Product : Mass spectrometry(MS)

Introduction

Matrix assisted laser desorption/ionization (MALDI) mass spectrometry is a powerful tool for the analysis of synthetic polymers. This technique, when combined with a high-resolution time-of-flight mass spectrometer, can be used to identify differences in monomer, polymer end groups, and their molecular weight distributions. The molecular weight distribution is often expressed as number average molecular weight (M_n), weight average molecular weight (M_w), and dispersity (D). More recently, MALDI mass spectrometry imaging (MALDI-MSI) has been used to visualize the locations of compounds on sample surfaces. However, this technique has not been widely used for polymer analysis. Previously in MSTips 306, we reported combining M_n, M_w and D visualization methods with Kendrick mass defect (KMD) analysis. In this report, we have applied this combined method to analyze a polyethylene terephthalate (PET) that was degraded by ultraviolet (UV) irradiation.

Experiment

Polyethylene terephthalate (PET) was dissolved in hexafluoroisopropanol (HFIP) at 10 mg/mL. The matrix acetophenone (THAP) was dissolved in tetrahydrofuran (THF) at 10 mg/mL. First, the PET solution was spotted in the upper right section of the measurement area, and UV irradiation was performed using a Handicure 100 lamp (manufactured by Mizuka Planning Co.) for 20 minutes. Afterwards, the UV irradiation was interrupted, and the PET solution was spotted in the upper left section of the measurement area. Next, both sections were exposed to UV irradiation for 10 minutes. Subsequently, the PET solution was spotted onto the lower section of the measurement area. As a result, the UV irradiation time for each spot was 30, 10 and 0 minutes as shown in Figure 1. Afterwards, the THAP matrix solution was airbrushed onto the sample and then the JMS-S3000 positive ion SpiralTOF mode was used to measure MALDI-MSI data. The laser spot size/pixel size was 50 µm. The MSI analysis and visualization was performed by using the JEOL msMicroImager™ software, and the KMD analysis was performed by using the JEOL msRepeatFinder software.
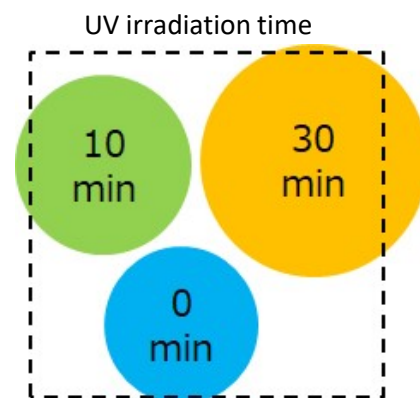
UV irradiation time

Figure 1. Schematic of the model sample.

Results

The average mass spectrum for the entire sample region is shown in Figure 2A. A KMD plot for $C_{10}H_8O_4$ (monomer unit for PET) is shown in Figure 2B and clearly shows two horizontal series with 192u intervals corresponding to the PET polymer. Series I (highlighted in blue) represents the [M+Na]$^+$ for the cyclic PET oligomer that are present in the sample prior to UV irradiation. Series II (highlighted in red) appeared in the samples after UV irradiation and likely originated from photo-oxidative degradation in which the PET has COOH/COOH end groups.
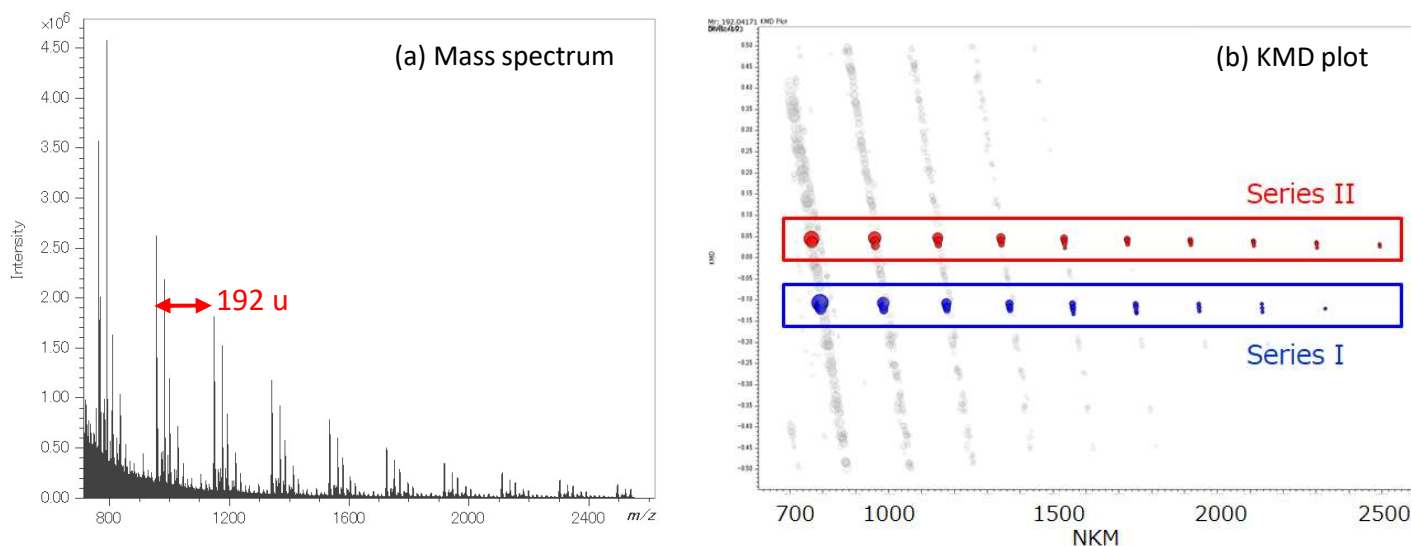

Figure 2 (a) Averaged mass spectrum for the whole measurement region and (b) KMD plot for $C_{10}H_8O_4$. Series I represents the cyclic PET oligomers, and Series II represents the photo-oxidative degradation of PET.

The summed intensity images for series I and II are shown in Figure. 3. These images were made by summing the mass image intensities for the masses included in the groups that were highlighted as red and blue in the KMD plot. Series I had the strongest ion intensity before UV irradiation (0min) and decreased as the UV irradiation time increased. Series II was not observed before UV irradiation (0min), and then the ion intensities increased as the irradiation time increased. Figure 4 shows the ROI (region of interest) mass spectra of UV irradiation time 0, 10, and 30 min. Before UV irradiation (0 min), the [cyclic oligomers+Na]$^+$ (Series I) and the [cyclic oligomers+C$_2$H$_4$O]$^+$ (Series III) were observed in the mass spectrum. However, as the UV irradiation time increased, the ion intensities for these series decreased. On the other hand, Series II with COOH/COOH end groups and Series IV with COOH/OH end group, which were not observed before UV irradiation, showed increased intensities as the UV irradiation increased.

Conclusion

In this work, we have reported a new MSI method for analyzing the degradation of synthetic polymers (in this case UV degradation of PET). As a result, using this technique with the high mass-resolution MALDI-SpiralTOF™ system, we were able to easily observe a decrease in the original series as degradation occurred as well as the appearance and increase of a newly generated series that resulted from the degradation. These results indicate that MALDI-MSI can be an effective for visualizing the degree of degradation and their spatial distributions.
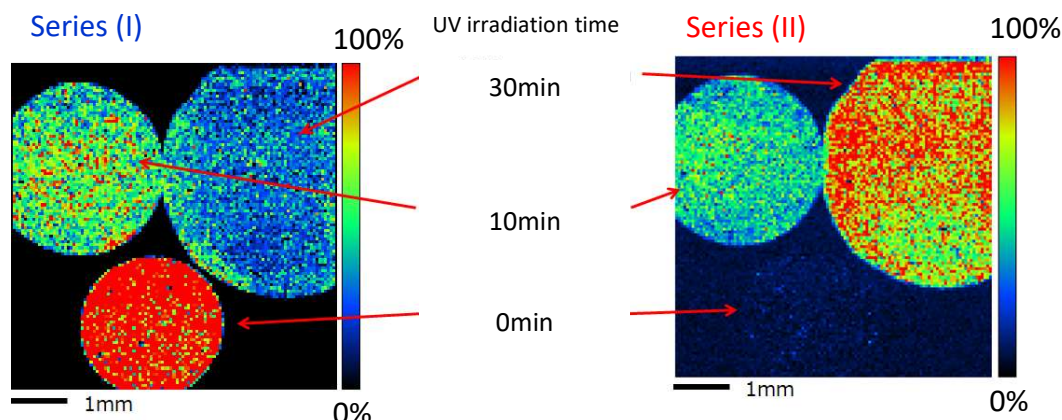

Figure 3 Images for the PET cyclic oligomer series (Series I) and the ultraviolet degraded PET polymer series (Series II).
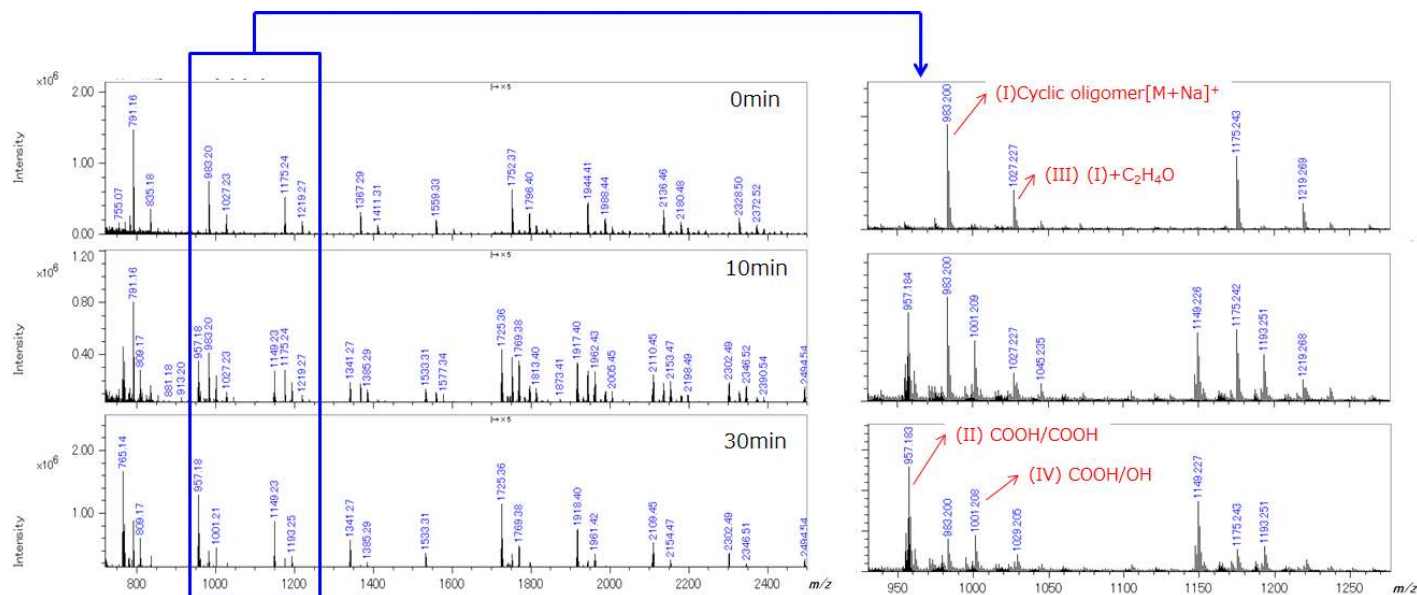

Figure 4 ROI mass spectra of UV irradiation time 0, 10 and 30 minutes. The originally observed polymer series, I and III, had reduced intensities as the irradiation time increased. On the other hand, the polymer series generated by photo-oxidative degradation, II and VI, had increased intensities as the irradiation time increased.

A mass spectrometry imaging method for visualizing synthetic polymers combined with Kendrick mass defect analysis

Product : Mass spectrometry(MS)

Introduction

Matrix assisted laser desorption/ionization (MALDI) mass spectrometry is a powerful tool for the analysis of synthetic polymers. This technique, when combined with a high-resolution time-of-flight mass spectrometer, can be used to identify differences in monomer, polymer end groups, and their molecular weight distributions. The molecular weight distribution is often expressed as number average molecular weight (M_n), weight average molecular weight (M_w), and dispersity (D). More recently, MALDI mass spectrometry imaging (MALDI-MSI) has been used to visualize the locations of compounds on sample surfaces. However, this technique has not been widely used for polymer analysis. One reason for this is that polymers have molecular weight distributions which means that mass images based on specific degrees of polymerization (specific *m/z* value typically used by conventional methods) do not necessarily express a clear picture for the full polymer localization. In the previous MSTips 305 report [1], we proposed a new MALDI-MSI visualization method for synthetic polymers that used the M_n, M_w and D as indices. In this report, we have combined this method with the Kendrick Mass Defect (KMD) method to effectively visualize polymer series mixtures.

Experiment

A model sample was prepared using polyethylene glycol (PEG), polyethylene glycol monododecyl ether (PEG-$C_{12}H_{25}$), and polypropylene glycol (PPG) .The reagents used are shown in Table 1. A mixed solution of PEG, PEG-$C_{12}H_{25}$, α-CHCA, and NaTFA 1/0.1/10/1 (v/v/v/v) was spotted on the left-hand spot, and a mixed solution of PEG, PPG, α-CHCA, and NaTFA 1/0.1/10/1 (v/v/v/v) was spotted on the right-hand spot (Figure 1). The MALDI-MSI data was measured by using the SpiralTOF positive ion mode on the JMS-S3000. The pixel size was 50 μm, and the laser irradiation frequency was 50 times for each pixel. The MSI analysis and visualization was performed by using the JEOL msMicroImager™ software, and the KMD analysis was performed by using the JEOL msRepeatFinder™ software.

Samples	Polyethylene glycol(PEG) M_w2000 Polyethylene glycol monododecyl ether (PEG-$C_{12}H_{25}$) Polypropylene glycol(PPG) M_w 2000 1mg/mL (in MeOH)
Matrix	α-CHCA 10mg/mL (in MeOH)
Cationization	NaTFA 1mg/mL (in MeOH)

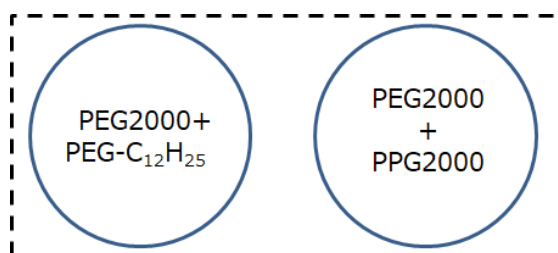**Table 1.** Samples, matrix and cationization agent.

Figure 1. Schematic of the model sample.

Results

The average mass spectrum for the entire sample region (right-hand and left-hand spots) is shown in Figure 2A. Two polymer distributions with repeat units of 44 u (C_2H_4O) were easily observed around m/z 900-1800 and m/z 1500-2800 that corresponded with PEG-$C_{12}H_{25}$ and PEG 2000, respectively. However, the polypropylene series with repeat units 58 u (C_3H_6O) was more difficult to observe in the average mass spectrum. The C_2H_4O KMD plot for the average mass spectrum is shown in Figure 2B. This plot clearly showed the presence of three polymer series as highlighted by the three colors (blue, red, and green). The two major series for PEG2000 (colored with blue) and PEG-$C_{12}H_{25}$ (colored with red), which both have C_2H_4O monomer units, made a horizontal line across the KMD plot. The minor series for PPG2000 (colored with green) showed a sloped line due to the fact that it has a repeat unit of C_3H_6O. These results clearly show the advantage of using a KMD plot to easily visualize polymer series, even with low intensity ions that can be difficult to observe in the mass spectrum. Using the KMD plot, three polymer peak lists were extracted from the average mass spectrum peak list and images for M_n and D were made for each polymer series. The PEG, PEG-$C_{12}H_{25}$ and PPG polymer peak lists contained 216, 84, and 70 peaks, respectively. It would be time consuming to use conventional methods that involve looking at all 370 mass images individually to make any reasonable determinations about the samples. However, the M_n and D were easily calculated using each extracted peak list. The corresponding M_n and D images for each polymer series are shown in Figure 3. From these images, the M_n values of PEG, PEG-$C_{12}H_{25}$ and PPG were approximately 2200, 1350 and 2200, respectively, and the D values of PEG, PEG-$C_{12}H_{25}$ and PPG were approximately 1.01, 1.015 and 1.008, respectively.

Conclusion

In this report, we have introduced the advantages of combining KMD analysis with the visualizing method reported in MSTips 305 to analyze samples containing multiple synthetic polymer series. By using the KMD method, it is easy to visualize each polymer series, even for minor components that are difficult to identify in the mass spectrum.

Reference

[1]MSTips 305 A mass spectrometry imaging method for visualizing synthetic polymers by using average molecular weight and polydispersity as indices.
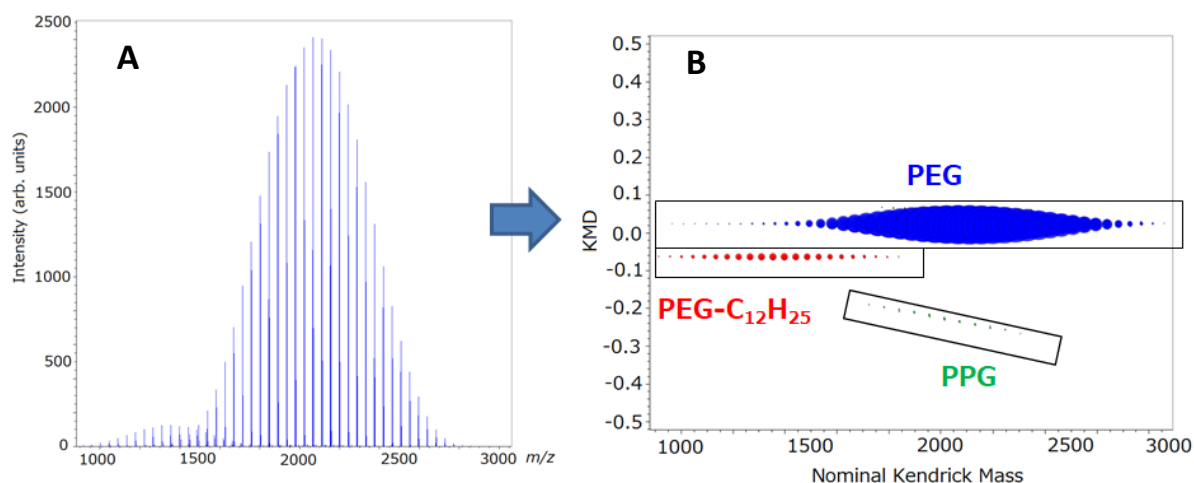

Figure 2. (A) Averaged mass spectrum showing two clearly defined polymer series with a repeat unit of 44 u (C_2H_4O). (B) KMD plot (based on C_2H_4O) for the entire peak list from the averaged mass spectrum. The PEG and PEG-$C_{12}H_{25}$ polymer series were observed as horizontal lines across the plot. Also, the PPG series that was difficult to find in the mass spectrum is clearly observed in the KMD plot.
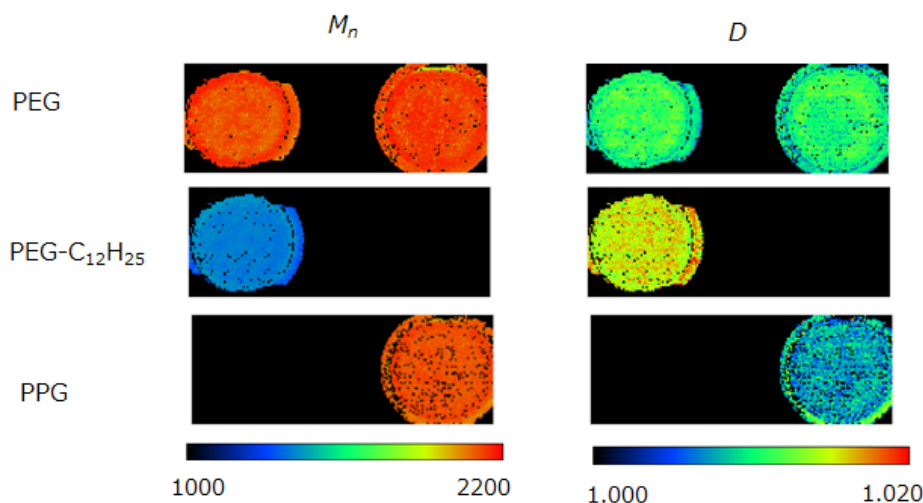

Figure 3. The M_n and D images for PEG, PEG-$C_{12}H_{25}$ and PPG polymer series.

A mass spectrometry imaging method for visualizing synthetic polymers by using average molecular weight and polydispersity as indices.

Product：Mass spectrometry(MS)

Introduction

Matrix assisted laser desorption/ionization (MALDI) mass spectrometry is a powerful tool for the analysis of synthetic polymers. This technique, when combined with a high-resolution time-of-flight mass spectrometer, can be used to identify differences in monomer, polymer end groups, and their molecular weight distributions. The molecular weight distribution is often expressed as number average molecular weight (Mn), weight average molecular weight (Mw), and dispersity (D). More recently, MALDI mass spectrometry imaging (MALDI-MSI) has been used to visualize the locations of compounds on sample surfaces. The MALDI-MSI raw data includes the position information (X and Y) as well as the mass spectral information (m/z and intensity) for each position. A target compound peak can then be specified to calculate the ion intensity for each pixel in order to draw a mass image. MALDI-MSI has been widely used to show the localization of proteins, peptides, lipids, and drugs on frozen tissue sections. However, this technique has not been widely used for polymer analysis. One reason for this is that polymers have molecular weight distributions which means that mass images based on specific degrees of polymerization (specific m/z value typically used by conventional methods) do not necessarily express a clear picture for the full polymer localization. In this report, we investigate a MSI visualization method for synthetic polymers that uses Mn, Mw and D as indices for visualization.

Work flow

The work flow for visualizing polymers is shown in Figure 1. This function is implemented in the JEOL msMicroImager™ V2 software.
1: Acquire the MALDI-MSI data using JMS-S3000.
2: Load raw data into msMicroImager™ and make average mass spectrum or region of interest (ROI) mass spectrum.
3: Make a polymer peak list for the mass spectrum made in Step 2.
   The polymer peak list can also be calculated from the monomer and end group information.
4: All of the mass images corresponding to the peaks in the polymer peak list are extracted.
5: The M_n, M_w, and D are calculated for each pixel using the following equations.

$$M_{n,p} = \sum_{i=1}^{k}(I_{p,i} \times M_i)/\sum_{i=1}^{k}(I_{p,i})$$

$$M_{w,p} = \sum_{i=1}^{k}(I_{p,i} \times M_i^2)/\sum_{i=1}^{k}(I_{p,i} \times M_i)$$

$$D_p = M_{w,p}/M_{n,p}$$

$M_{n,p}$, $M_{w,p}$, and D_p represent the M_n, M_w and D for each pixel, respectively. In the equation, p is the pixel number, i is the mass image number, k is the total number of polymer peaks.
M_i is the mass for mass image number i, $I_{p,i}$ is the intensity for pixel number p in mass image number i.
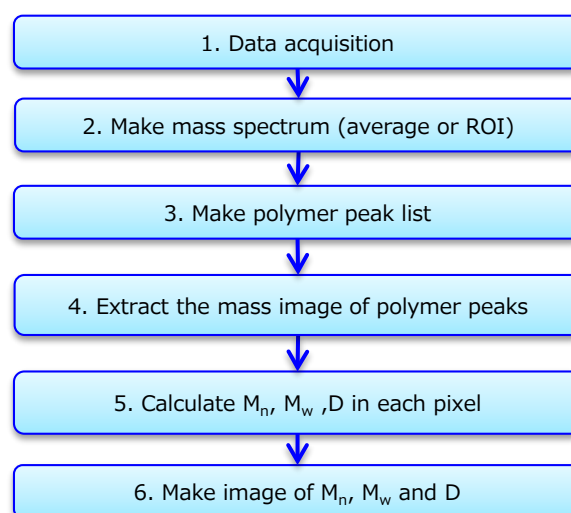
6: Make images for M_n, M_w and D.

1. Data acquisition

⬇

2. Make mass spectrum (average or ROI)

⬇

3. Make polymer peak list

⬇

4. Extract the mass image of polymer peaks

⬇

5. Calculate M_n, M_w ,D in each pixel

⬇

6. Make image of M_n, M_w and D

Figure 1   The procedure for making the images of M_n, M_w, and D.

Experimental

In order to verify the visualization method for synthetic polymers, a model sample was prepared using polyethylene glycol molecular weights of 600 and 1000 (PEG600 and PEG1000, respectively).The reagents used are shown in Table 1. A mixed solution of PEG1000, α-CHCA, and NaTFA 5/10/1 (v/v/v) was spotted on the left-hand spot, and a mixed solution of PEG600, PEG1000, α-CHCA and NaTFA 5/5/10/1 (v/v/v/v) was spotted on the right-hand spot (Figure 2). The MALDI-MSI data was measured by using the SpiralTOF positive ion mode on the JMS-S3000. The pixel size was 50 μm, and the laser irradiation frequency was 50 times for each pixel. The MSI analysis and visualization was performed by using the JEOL msMicroImager™ software.

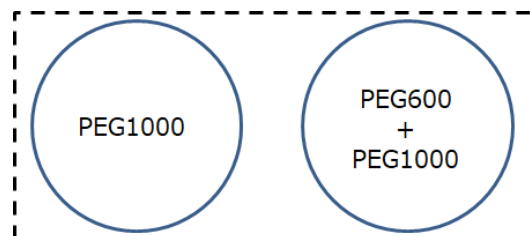| Polymer	PEG600 and PEG1000 1mg/mL (in MeOH)
Matrix	α-CHCA 10mg/mL (in MeOH)
Cationization agent	NaTFA 1mg/mL (in MeOH)

Table 1 Samples, matrix and cationization agent.

Figure 2 Schematic of the model sample.

Results

The average mass spectrum for the entire sample region (right-hand and left-hand spots) is shown in Figure 3. The observed PEG series is $HO(C_2H_4O)nH + Na+$. The mass images for *m/z* 569.3 (n=12), 1009.6 (n=23) and 1361.8 (n=30) are also shown in Figure 3. All three ions were observed in the right-hand spot images (PEG600 and PEG1000 mixture). However, the *m/z* 569.3 mass image did not show any significant signal in the left-hand spot due to the presence of only the higher molecular weight PEG1000. In total there were eighty peaks observed in the averaged PEG series mass spectrum. If one carefully reviewed the eighty mass images associated with these ions, it could be possible to understand that the right-hand spot had a broader polymer distribution than the left-hand spot. However, it is difficult to intuitively and quantitatively determine these results.
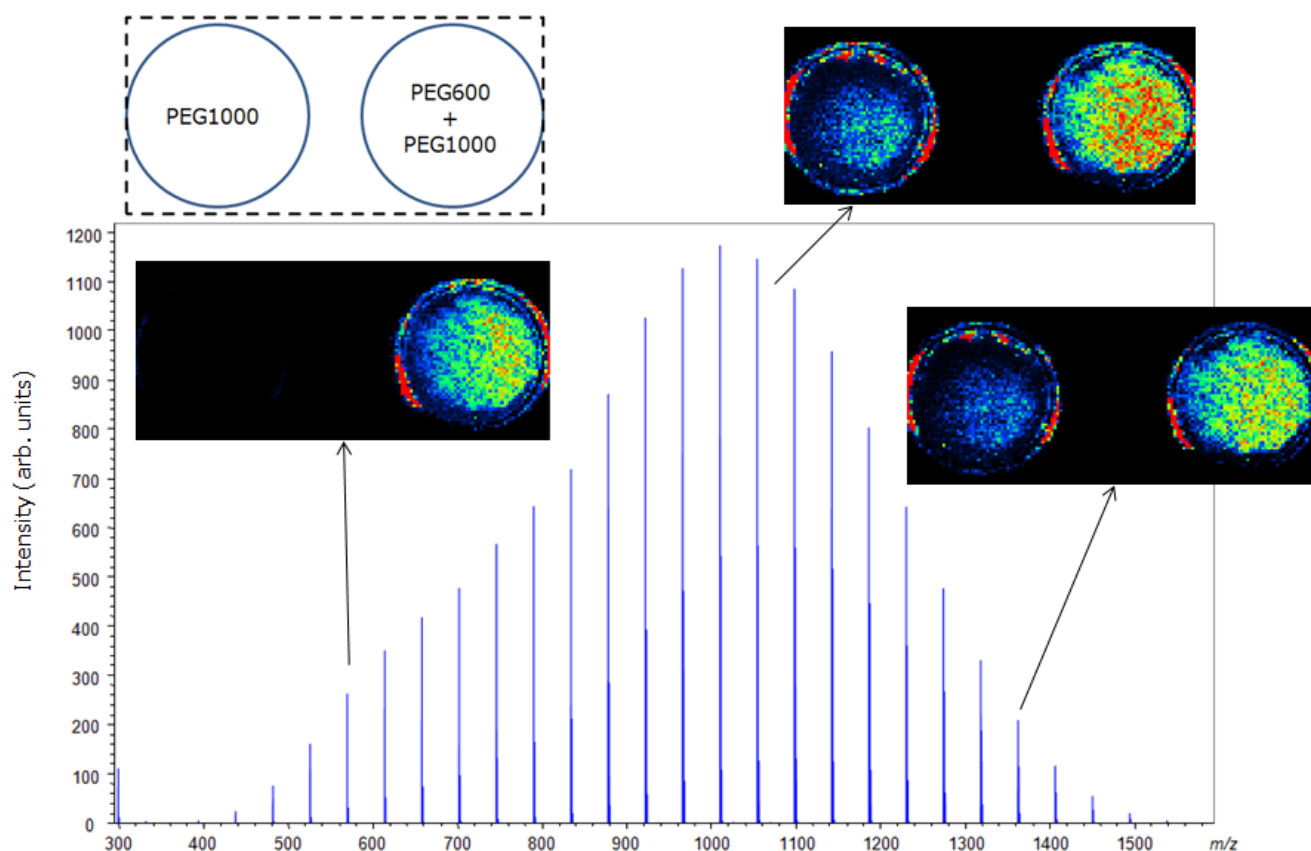

Figure 3 Averaged mass spectrum of entire region of the sample. The polymer series with repeat unit of 44 u (C_2H_4O) was observed. The three mass images of PEG, *m/z* 569.3 (n=12), 1009.6 (n=23) and 1361.8 (n=30), were also shown.

To solve this issue, the M_n, M_w and D images were calculated by the msMicroImager™ software using all eighty PEG series mass images (Figure 4). The M_n, M_w and D values can be easily understood by using the color tone of each pixel. For the image of M_n and M_w the values for the left-hand spot were larger than the values for right-hand spot which is logical because only the larger molecular weight PEG1000 is present in that spot. In contrast, the D image for the right-hand spot was larger than left-hand spot due to the wider molecular weight distribution present in the right-hand spot which contained both PEG600 and PEG1000. Additionally, the right-hand spot images showed 2 regions (A, B) in which the M_n, M_w and D are different. Region A shows a higher M_n and M_w and a lower D, thus indicating the presence of a higher average molecular weight, less disperse polymer in that region. The region of interest (ROI) mass spectra for these two areas (Figure 5) also show higher intensity peaks for *m/z* < 800 for Region B than for Region A. These mass spectra further support the observation that Region B has smaller M_n and M_w as well as a larger D, thus indicating a wider mass distribution in this region. Additionally, these image results indicate that the PEG600 and PEG 1000 were not uniformly deposited in the right-side spot. It is noteworthy that this variation would be extremely difficult (if not impossible) to determine by using the conventional MSI method of creating each ion image separately (Figure 3) and comparing them individually to each other.

Conclusions

In this report, a MALDI-MSI visualization method was introduced for synthetic polymers. Using this method, the mass images for a polymer series (including ~100 mass images) can be summarized into three images – number average molecular weight (M_n), weight average molecular weight (M_w) and polydispersity index (D) – which are all commonly used indices for polymer analysis. Since these three indices represent the synthetic polymer as a whole, the spatial distribution of the synthetic polymers can be understood more intuitively.
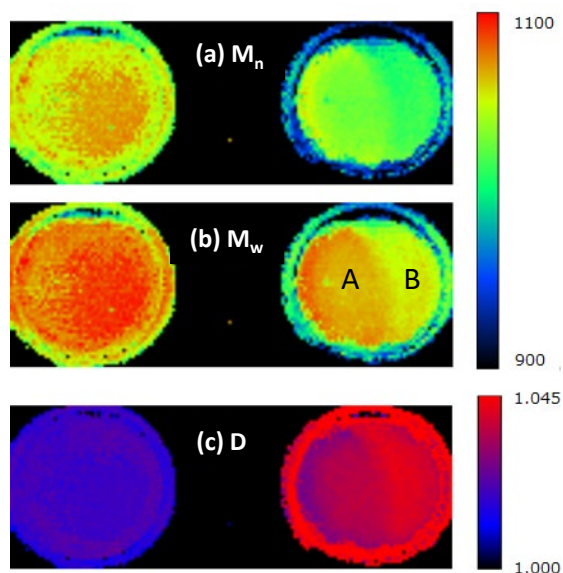

Figure 4 Three images of M_n, M_w and D summarize the eighty mass images included in PEG peak list.
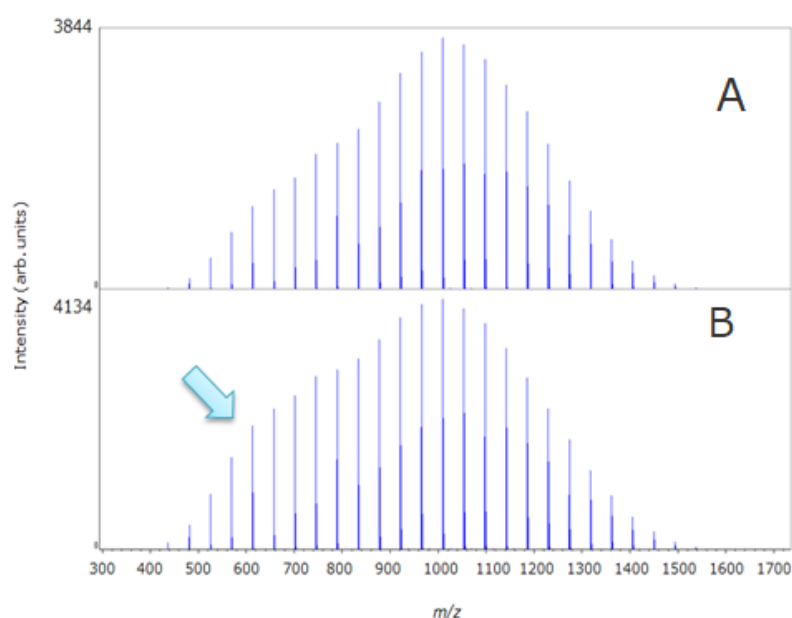

Figure 5 The ROI mass spectra at (A) left and (B) right side of right-hand spot. The polymer distribution was wider in right hand which could not be identified in conventional method.

Mass spectrometry imaging on mixed conductive/non-conductive substrate using JMS-S3000 SpiralTOF™

Product used: Mass Spectrometry (MS)

Surface analysis methods such as EPMA, AES, or XPS can provide chemical information about element type, bonding states, or functional groups. However, few methods can obtain the molecular-structure information of organic compounds. Matrix-assisted laser desorption/ionization time-of-flight mass spectrometry (MALDI–TOFMS) is a soft ionization technique that can determine elemental composition by accurate mass analysis and can obtain structural information using MS/MS. Recently, MALDI mass spectrometry imaging (MSI), which can map the spatial distribution of organic compounds, has become popular. In MALDI–TOFMS, high voltage is applied to a target plate, accelerating ions into the TOFMS usually set at ground potential. Therefore, conductivity is required for the target plate, and stainless steel is often used for solvent-based analysis. In MALDI–MSI, a tissue section about 10 µm thick is placed on an indium tin oxide (ITO) glass slide to provide conductivity on the sample surface.

In the industrial field, there is interest in measuring organic compounds on non-conductive substrates, such as resins a few millimeters thick. If the mass spectrum is obtained from the non-conductive surface with no pre-treatment, the mass resolution will be lower, and ultimately the ion intensity will decrease significantly due to the charge-up effect. This issue can be solved by providing conductivity to the non-conductive part via the gold deposition method.[1] In this report, MSI is performed using a permanent red marker on a substrate with a conductive part and a non-conductive part. Previously, ions could be observed only from the conductive part. Now, with the gold deposition method, they can be observed from both the conductive and the non-conductive parts, and they can be properly mapped.

Experiment

To create a model substrate, we formed conductive and non-conductive parts using metal patterns (Au 100 nm/Cr 30 nm) on a 1-mm-thick quartz glass substrate, alternating conductive with non-conductive parts at intervals of 400 µm (Figure 1). We used a red permanent marker to ionize the main component without applying a matrix compound. The letters "MS" were written with this marker so that they straddled the conductive and non-conductive parts on the model substrate. We then fixed the model substrate and the stainless-steel target plate with conductive tape (Figure 2). MSI measurement was performed without gold deposition. Thereafter, we used gold deposition on the same sample and performed MSI measurement again. All MSI measurement were performed in SpiralTOF™ positive-ion mode. Pixel size was 50 µm; number of laser shots was 50 per pixel.
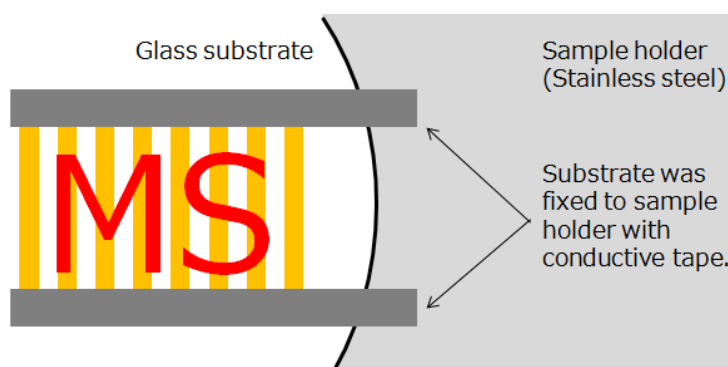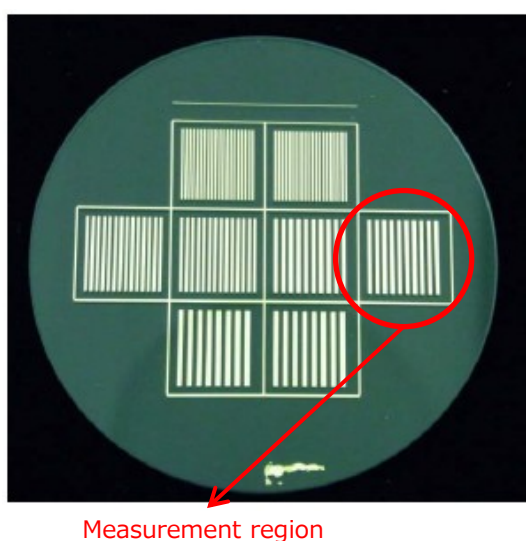

Figure 1. Scheme of the model substrate. The conductive and non-conductive parts were laid out in an alternating pattern on quartz glass.

Figure 2. The model substrate was fixed with conductive tape on a target plate.

Results

Figure 3 shows the results of MSI measurement without gold deposition. At upper left is an optical image with the black parts corresponding to a conductive part. At upper right is a mass image of Rhodamine B ($C_{28}H_{31}N_2O_3^+$), which is the main component of the permanent red marker. At bottom is an image of overlapped optical and mass images. It is difficult to read the letters "MS" on the mass image because the ions were observed only from the conductive part. The region of interest (ROI) mass spectra, which were created in two regions for each of the conductive parts (ROI1, -3) and non-conductive parts (ROI1, -4), are shown in Figure 4. These are monoisotopic peaks of Rhodamine B ions. The ions cannot be observed from the non-conductive regions, ROI2 and ROI4. Even in the conductive regions ROI1 and ROI3, mass resolution was lower than could have been obtained using the gold deposition method described below. Such results pose a problem because if the ion can be detected only from the conductive part, the target compounds will not appear in the non-conductive part, whether they actually exist or not.
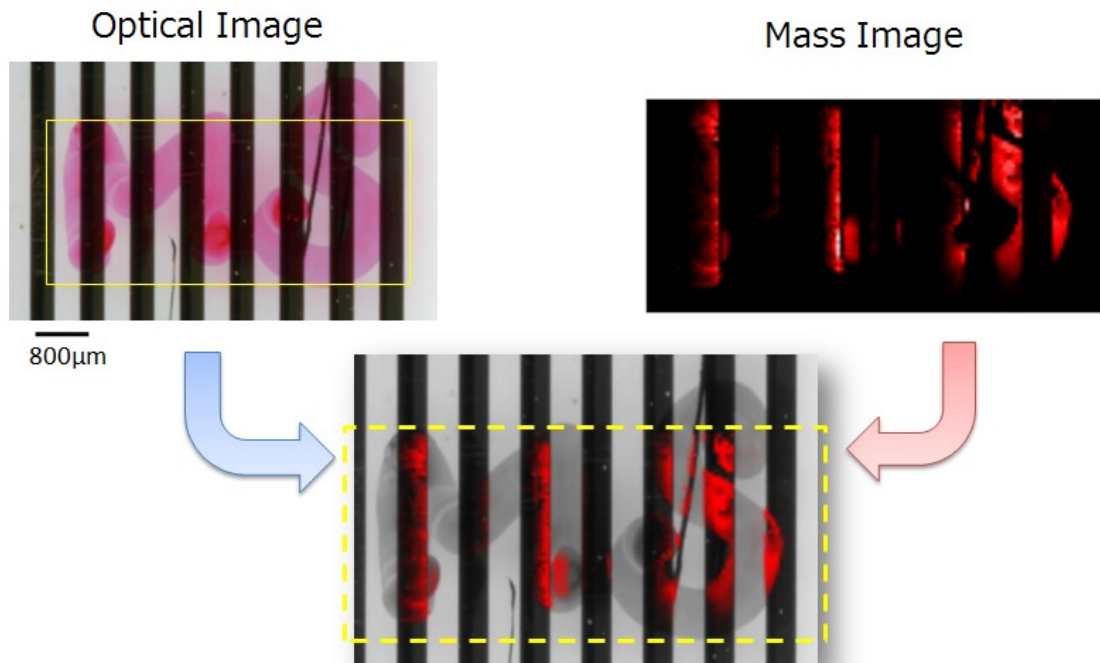
Figure 3. Results of MSI measurement without gold deposition.

The region of interest (ROI) mass spectra, which were created in two regions for each of the conductive parts (ROI1, -3) and non-conductive parts (ROI1, -4), are shown in Figure 4. These are monoisotopic peaks of Rhodamine B ions. The ions cannot be observed from the non-conductive regions, ROI2 and ROI4. Even in the conductive regions ROI1 and ROI3, mass resolution was lower than could have been obtained using the gold deposition method described below. Such results pose a problem because if the ion can be detected only from the conductive part, the target compounds will not appear in the non-conductive part, whether they actually exist or not.
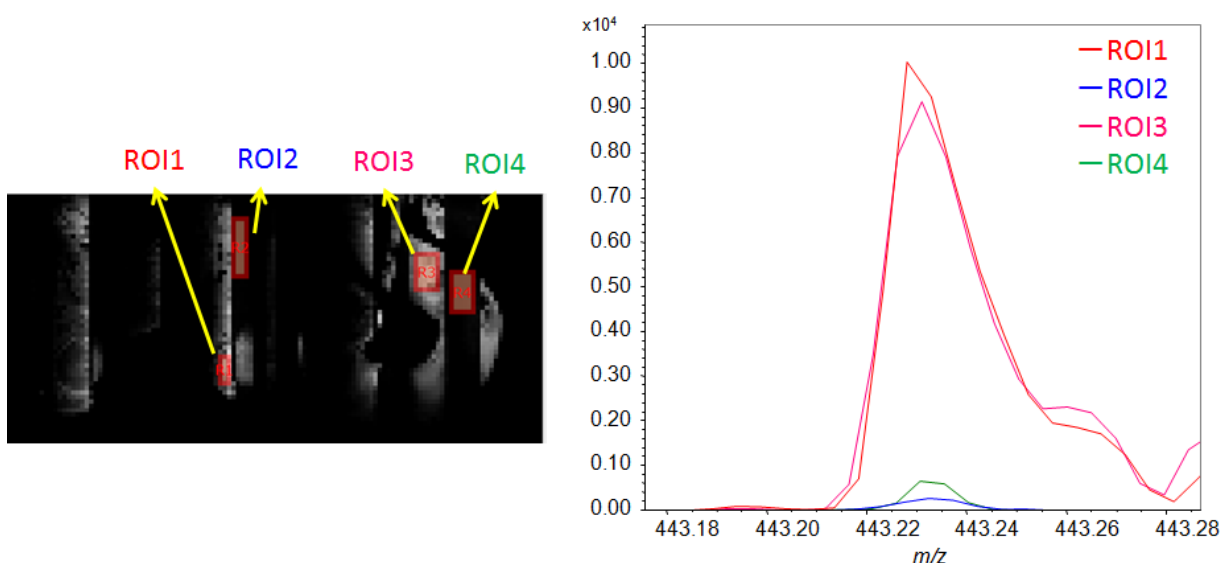

Figure 4. The ROI mass spectra from the conductive parts (ROI1 and -3) and non-conductive parts (ROI2 and -4) on model substrate without gold deposition.

The results of MSI measurement after gold deposition are shown in Figure 5. At upper left is the same optical image as in Figure 3. At upper right is a mass image of the ion ($C_{28}H_{31}N_2O_3^+$) derived from the main component Rhodamine B. At bottom is an image of overlaid optical and mass images. The ions were detected from both the conductive and non-conductive parts, which the letters "MS" can be read . Figure 6 shows the ROI mass spectrum at two places in each of the conductive and non-conductive parts. The observed peak is the monoisotopic ion of Rhodamine B ($C_{28}H_{31}N_2O_3^+$). In contrast to the results without gold deposition, ions can be observed from ROIs 2 and 4 of the non-conductive part, as well as from ROIs 1 and 3 of the conductive part. In addition, high resolution can be realized in all areas, and the influence of charge-up is considered sufficiently small.

Conclusion

If MSI measurements are taken of an organic compound that is placed directly on a conductive/non-conductive mixed substrate, the charge-up effect will influence the results. The ion intensity of the non-conductive part will be too low, and nothing will appear in the non-conductive parts on mass images. The gold deposition method is an easy way to solve this issue by adding conductivity to the sample surface.

Reference

[1] MSTips No. 251, "Analysis of organic compounds on an acrylic plate using JMS-S3000 SpiralTOF™."
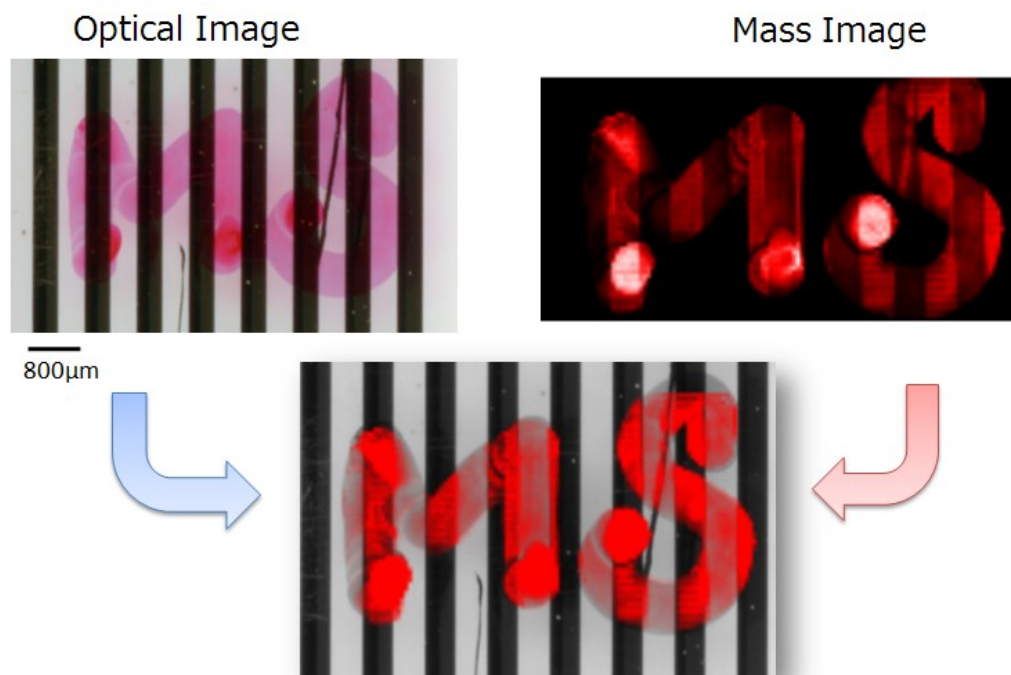
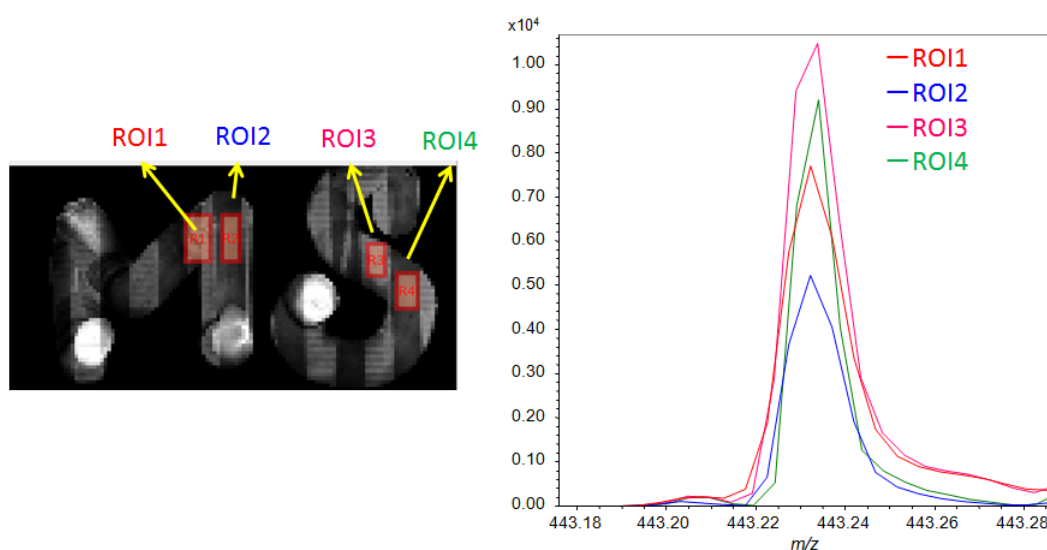Figure 5. The result of MSI measurement with gold deposition.

Figure 6. The ROI mass spectra from the conductive parts (ROI1 and -3) and non-conductive parts (ROI2 and -4) on model substrate with gold deposition.

Analysis of organic compounds on an acrylic plate using JMS-S3000 "SpiralTOF™"

Product used : Mass Spectrometer (MS)

Introduction

Industrial materials are often evaluated by surface analysis instruments that provide information on surface elements, bonding states, and functional groups. However, there are limited options for surface analysis techniques that provide molecular weight and molecular structure information for organic compounds present on surfaces. Matrix Assisted Laser Desorption Ionization - Time of Flight Mass Spectrometry (MALDI-TOFMS) is a soft ionization technique that can be used to analyze surfaces in order to estimate elemental compositions with accurate mass measurements, obtain structural information by using MS/MS, and map surface compounds by using MS imaging. MALDI-TOFMS uses a high voltage on the target plate to accelerate the ions into the TOFMS analyzer. Therefore, the target plates are conductive and are typically made of stainless steel. MALDI imaging mass spectrometry is widely used for analyzing organic substances on frozen tissue sections. In this case, a frozen tissue section with a thickness of about 10 µm is placed on a conductive glass slide coated with an indium tin oxide (ITO) film. However, for the analysis of industrial products, the target organic compounds are on nonconductive substrates such as resins with millimeter thicknesses. MALDI-TOFMS surface measurements using nonconductive substrates lead to a reduction in mass resolution and a significant decrease in ion intensity due to surface charging. This problem can be solved by pretreating the surface with gold vapor deposition in order to change it from nonconductive to conductive. This method was previously shown to work well in MSTips No. 204 in which the gold vapor deposition method was applied to the MALDI-MS imaging analysis of inks on paper. In this report, we used gold vapor deposition to look at samples on the surface of a 1 mm thick acrylic plate.

Experiment

An acrylic plate with a thickness of 1 mm was used as the nonconductive substrate. Polypropylene glycol (PPG, MW 1000) was used for SpiralTOF and TOF-TOF analyses. PPG 1000 was dissolved in water to 1 mg / mL. Matrix compound α-CHCA and cationization agent NaI were dissolved in methanol at concentrations of 10 mg / mL and 1 mg / mL, respectively. Equal amounts of PPG 1000 solution, matrix solution and cationization agent solution were mixed and then 1 µL was spotted on the acrylic plate and air-dried. For the MS imaging measurement, a red permanent ink was used as the sample, and the letters "MS" were written on the acrylic plate. No matrix compound was applied because rhodamine, a major component of the red permanent ink, can be ionized without using a matrix. After the samples were applied, each surface of the acrylic plate was coated with gold by vapor deposition. Afterwards, the acrylic plate was affixed with conductive tape to a special stainless steel plate that was dug down 1 mm from the normal plate surface position. The target plate was then directly introduced into the JMS-S3000 "SpiralTOF™" for MS analysis.
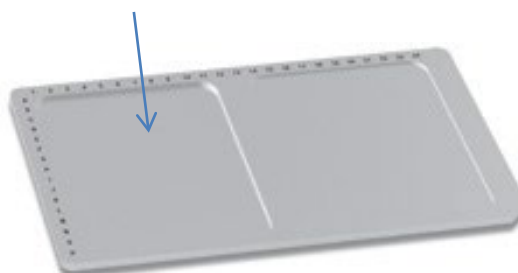

Dug down 1 mm from the target plate surface

Fig1. JMS-S3000 SpiralTOF™ and the plate used for introducing the acrylic plate.

Results

The PPG measurements from the gold vapor deposition acrylic surface showed sodium adduct ions [M + Na]+ for PPG 1000 $HO(C_3H_6O)_nH$ (see Figure 2). A mass resolution of 55000 was obtained for the monoisotopic peak at n = 18 (enlarged in Figure 2). Afterwards the n = 18 product ion spectrum was acquired by using the TOF-TOF option. Figure 3 (a) shows the mass spectra before and after monoisotopic ion selection of n = 18. Figure 3 (b) shows the product ion spectrum for this ion. The results of the SpiralTOF and TOF-TOF modes are equivalent to those measured using a normal stainless steel target plate.
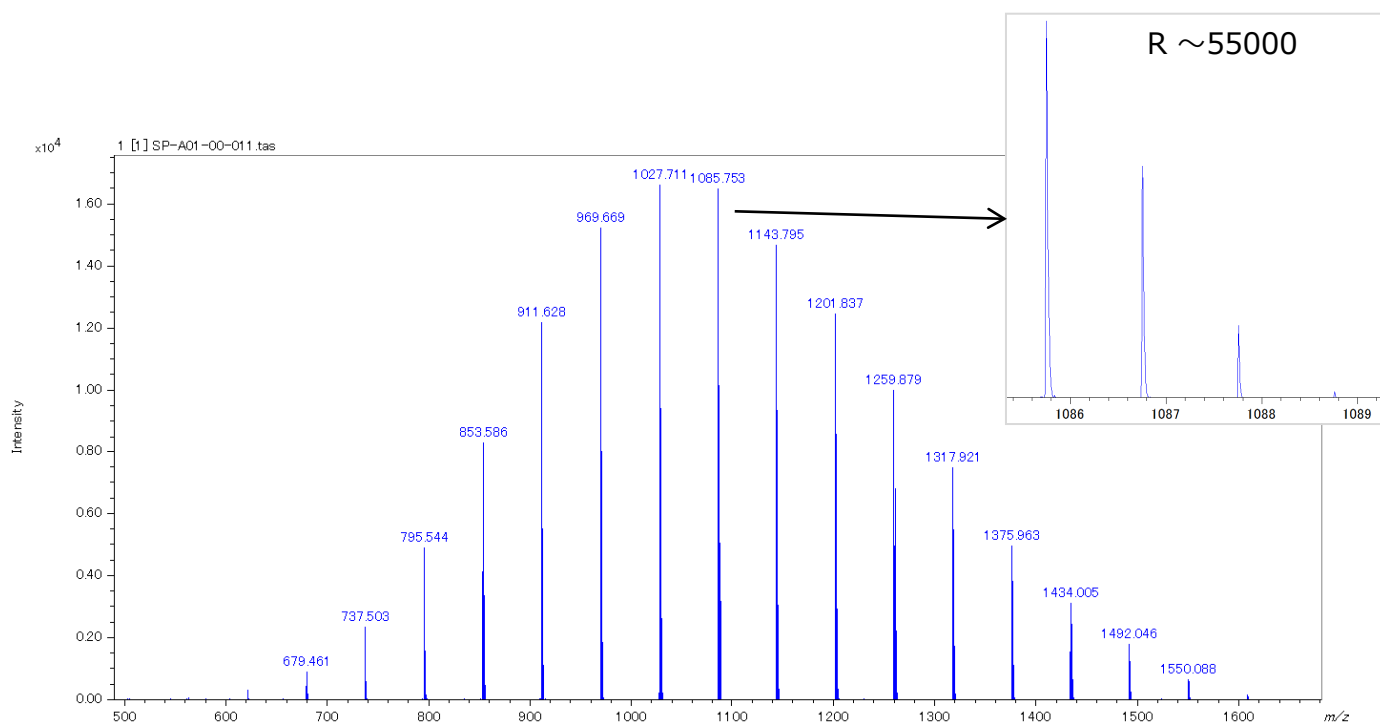
Fig. 2 Mass spectrum of PPG1000
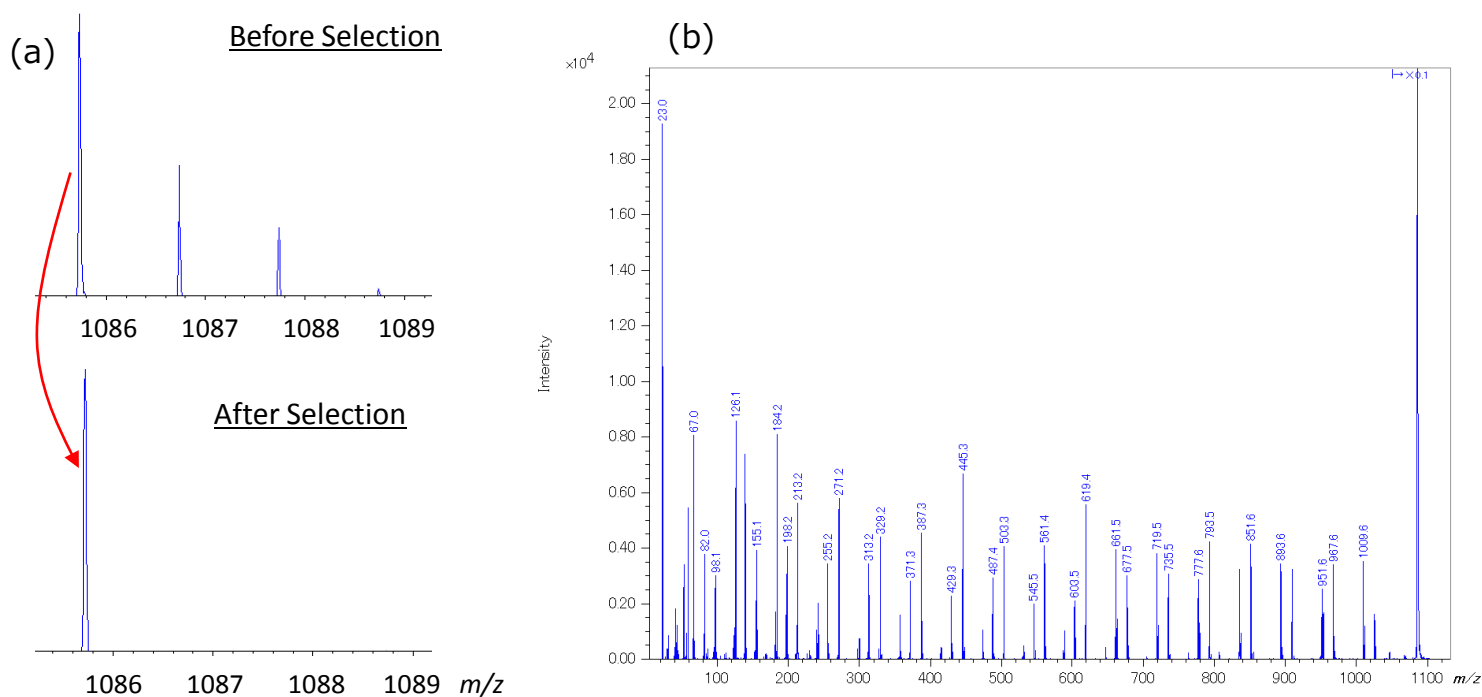
Fig. 3 (a)Precursor ion selectivity and (b) product ion mass spectrum of PPG [M+Na]+(n=18).

The MS imaging results for the red permanent ink "MS" characters on the acrylic plate are shown in Figure 4. The major component in the mass spectrum was ($C_{28}H_{31}N_2O_3^+$) which is related to rhodamine (loss of Cl), a major component in red permanent ink. A mass resolution of 48,000 was observed for this data, thus indicating that this kind of measurement can be done on a pretreated nonconductive substrate without any issues. The *m/z* 443 peak was then used to create a mass image of the surface that clearly showed the "MS" characters in the measurement area. The pixel size for this image was 50 μm, which reflects the laser spot size used during the measurement.

Conclusions

In this report, organic compounds on a 1 mm thick nonconductive acrylic substrate were measured by using MALDI - TOFMS. It was found that high mass resolution mass spectra, MS/MS product ion mass spectra, and MS imaging data can be obtained from a nonconductive substrate if the sample surface is pretreated with gold vapor deposition to make it conductive. Using this method, the range of applications for MALDI-TOFMS can be expanded into areas of surface analysis that involve a variety of substrates, both conductive and nonconductive.
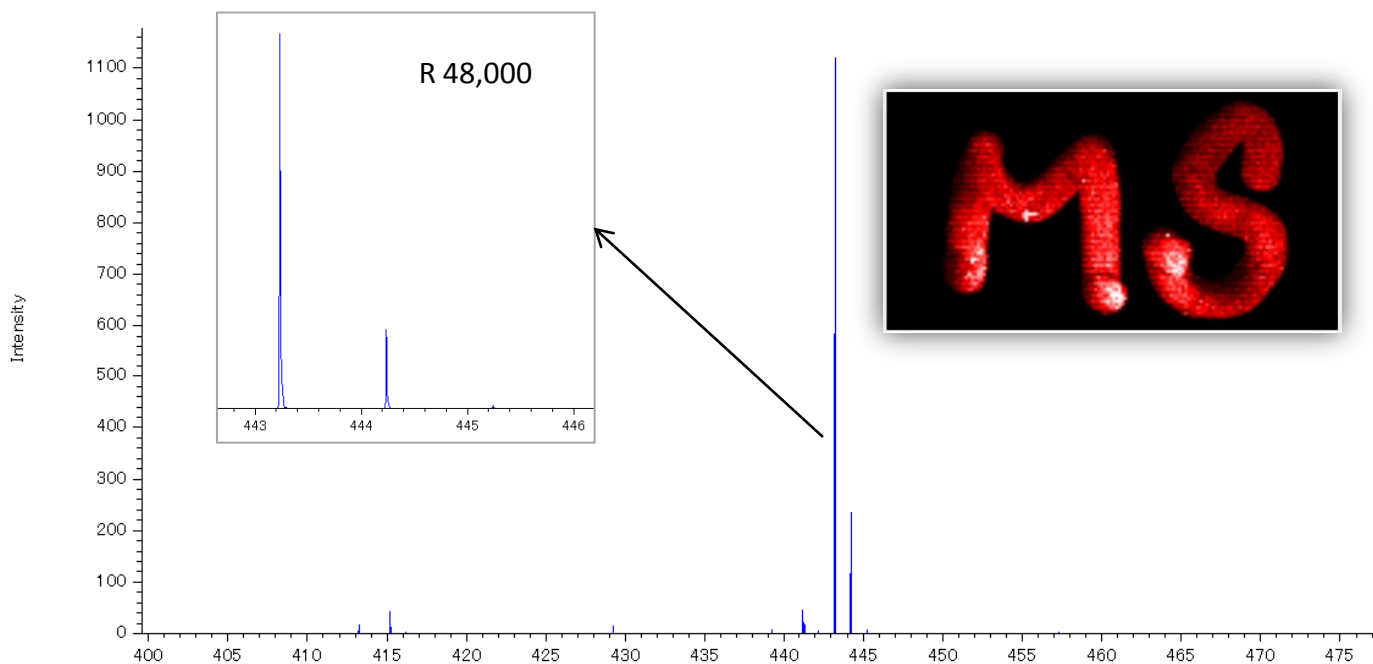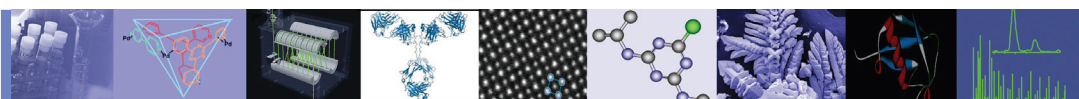

Fig. 4 Mass imaging of "MS" literature written with red permanent ink.

SpiralTOF™

Ballpoint Ink Analyses Using LDI Imaging and SEM/EDS Techniques

Introduction

Recently, matrix assisted laser desorption/ionization (MALDI) imaging techniques have been developed for biological sciences to evaluate and understand the distribution of various chemicals on biological surfaces. In particular, this technique provides useful visual information about the locations of specific chemicals on surfaces. In this work, we explored the use of laser desorption/ionization (LDI) imaging for forensically applicable samples such as a handwriting sample with a ballpoint ink. These measurements were done using a spiral-trajectory ion optics time-of-flight mass spectrometer (SpiralTOF-MS). This TOF system has a 17m flight path that provides high resolution capabilities even down into the lower m/z region. Additionally, we looked at the SEM/EDS imaging using the JEOL JSM-6510LV scanning electron microscope.

Experimental

Sample information and measurement conditions are listed below.

Samples
- A ballpoint pen (black)
- A permanent marker (black)

LDI Imaging measurement
- Measurement mode: SpiralTOF positive mode
- No matrix
- Spatial resolution: 50 or 100 μm
- 5000 laser shots at 1kHz laser repetition rate for each position
- Analytics Software Biomap 3.8
  -Raw data was converted to imzML files

Results and Discussion

First, the ballpoint ink handwriting sample "JEOL" was analyzed using the SpiralTOF LDI imaging technique directly with no other sample preparation. The ink consisted of crystal violet as the main component and was easily detected directly on the surface of the handwriting sample. However, a portion of the letter "J" did not show the presence of this analyte (Figure 1). It was hypothesized that there was likely surface discharging and/or a conductivity problem with the paper. To address this situation, the surface was subjected to a gold vapor deposition in order to improve the conductivity of the paper. Afterwards, the sample was again tested and crystal violet was observed over the entire handwriting sample (Figure 2). These results confirm that the gold vapor deposition enhances the analyte signals from the surface of the paper.
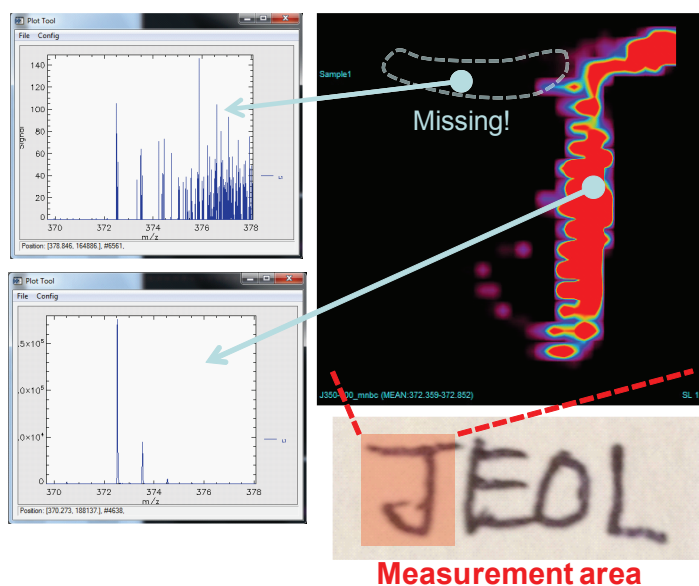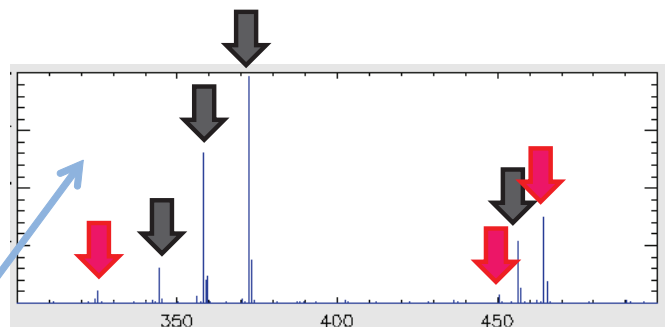

Figure 1. Crystal violet (m/z 372.2) LDI imaging of the handwriting letter "J" on a no-pretreatment paper.

Next, a ballpoint ink sample "Spiral" was covered with black permanent marker and then analyzed using the LDI and a gold vapor desorption technique. The LDI imaging of the handwriting letter "Spiral" covered up with a permanent marker ink is shown in Figure 3. These results clearly show that "Spiral" was easily observed from the LDI imaging data even though it was covered up with another ink.

Afterwards, we then examined the "ral" in the "Spiral" handwriting by using the JEOL JSM-6510LA scanning electron microscope. EDS results showed that the areas containing the ballpoint ink were carbon rich while the areas containing the permanent marker ink were oxygen rich.
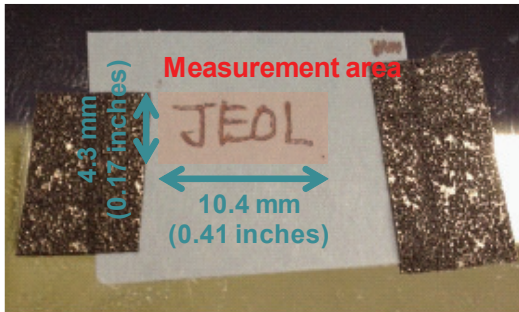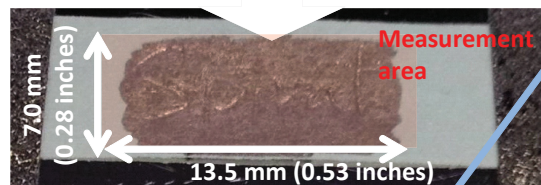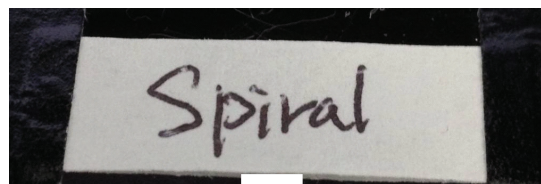

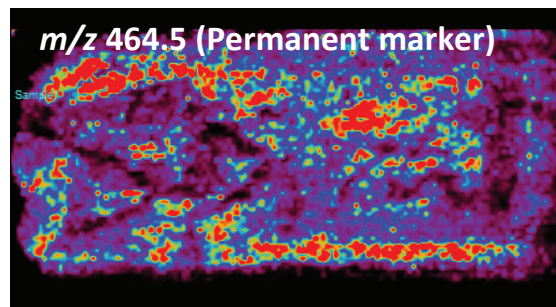Figure 2. Crystal violet (m/z 372.2) LDI imaging of the handwriting letters "JEOL" with a gold vapor deposition.
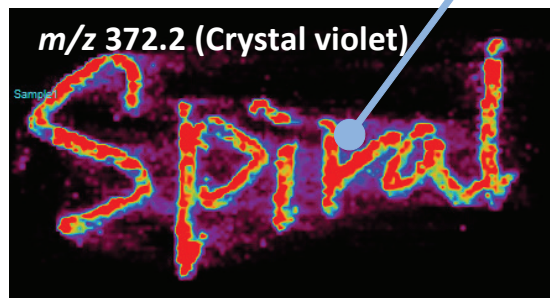
Figure 3. Crystal violet (m/z 372.2) LDI imaging of the handwriting letters "Spiral" covered up with a permanent marker ink.

Applications Note

004 [No letter (permanent marker)]

003 [a (ballpoint ink)]

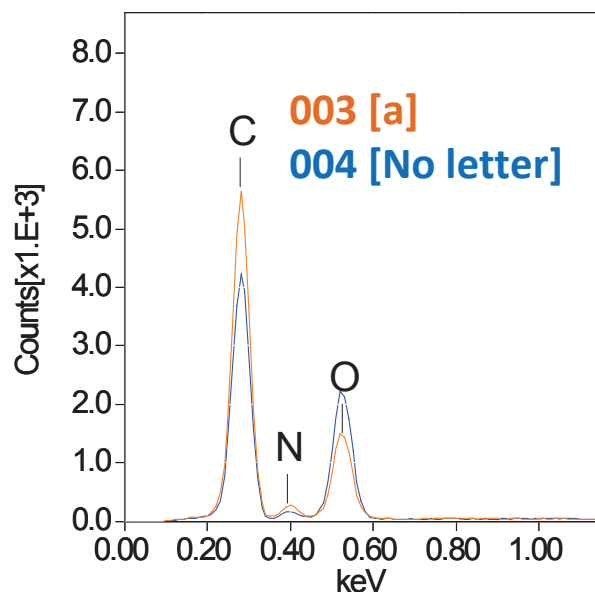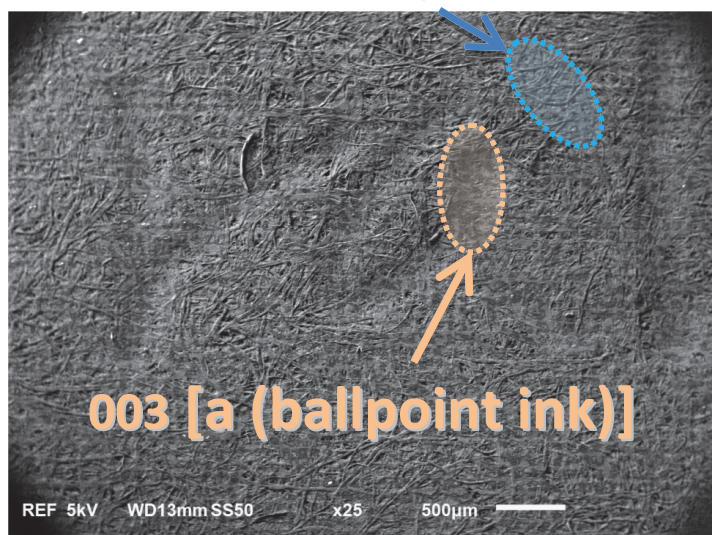REF 5kV   WD13mm SS50   x25   500µm

003 [a]
004 [No letter]

Figure 4. SEM image of the "ral" in "Spiral" handwriting on the paper (x25) and EDS spectrum.

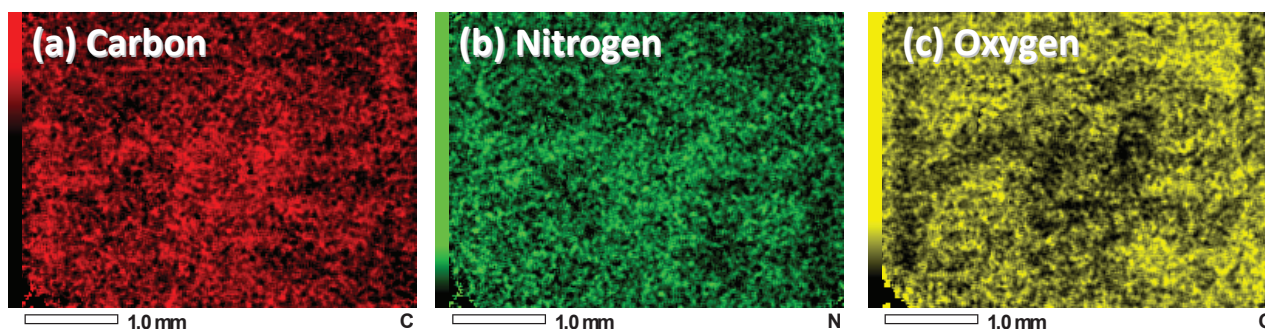**(a) Carbon**   **(b) Nitrogen**   **(c) Oxygen**

1.0 mm   C   1.0 mm   N   1.0 mm   O

Figure 5. EDS images of the "ral" in "Spiral" handwriting on the paper and EDS spectrum,
(a) Carbon, (b) Nitrogen and (c) Oxygen.

MS-030713A

Conclusions

We were able to show LDI images and SEM/EDS images for the ink analysis of handwriting samples that have been obliterated by a marker. The LDI imaging provided the organic compound information and distributions for the ink across the surface. The scanning electron microscope rapidly provided the surface features (indentations and roughness) while also providing elemental differences observed for the two inks. Each instrument, the SpiralTOF and JSM-6510LA, provides complementary information for this kind of sample and could be useful for future forensic applications.
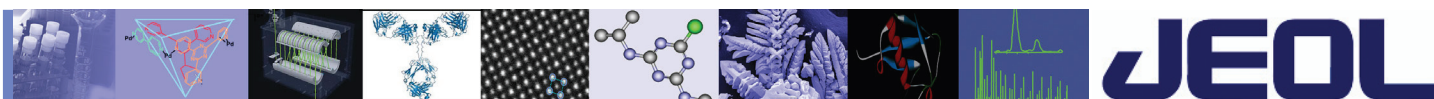
SpiralTOF™

Gunshot Residues (GSR) Analysis by Using MALDI Imaging

Applications Note

Introduction

Recently, matrix assisted laser desorption/ionization mass spectrometry (MALDI-MS) imaging techniques have been developed for biological sciences to evaluate and understand the distribution of various chemicals on biological surfaces. In particular, this technique provides useful visual information about the locations of specific chemicals on surfaces.

In this work, we explored the use of MALDI-MS imaging for the forensically applicable sample of gunshot residues (GSR). These measurements were done using a spiral-trajectory ion optics time-of-flight mass spectrometer (Spiral-TOF-MS) which has a 17m flight path that provides high resolution capabilities, even down into the lower *m/z* region. Additionally, the *m/z* axis remains very stable over the long time period required for MALDI-MS imaging.

Experimental

Sample Preparation and Measurement
The GSR samples were obtained on an electrically conductive adhesive that was adhered to the back of a shooter's

hand while a handgun was discharged. 2, 5-Dihydroxybenzoic acid (DHB) was dissolved in MeOH at a concentration of 30 mg/mL. Two milliliters of this DHB matrix solution was sprayed onto the GSR using an air-brush. Polypropylene glycol (PPG) was used for the external calibration standard. After the samples were dried, they were measured using the JMS-S3000 SpiralTOF MS system.

MALDI-MS Imaging measurement
- Measurement mode: SpiralTOF positive mode
- Matrix: DHB, 2mL spray @ 30mg/mL (MeOH)
- Spatial resolution: 100 mm
- Measurement region: Width 12.7 mm x Length 10.6 mm
- Number of spectra: 13,462
- 5000 laser shots at 1kHz laser repetition rate for each position
- Analytics Software Biomap 3.8 - Raw data was converted to imzML files
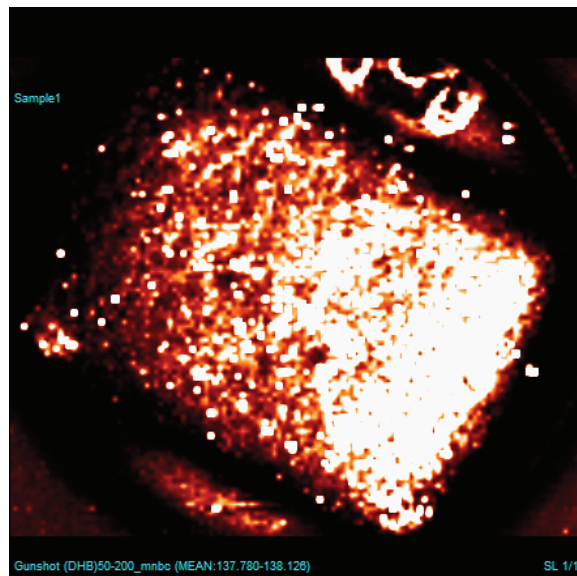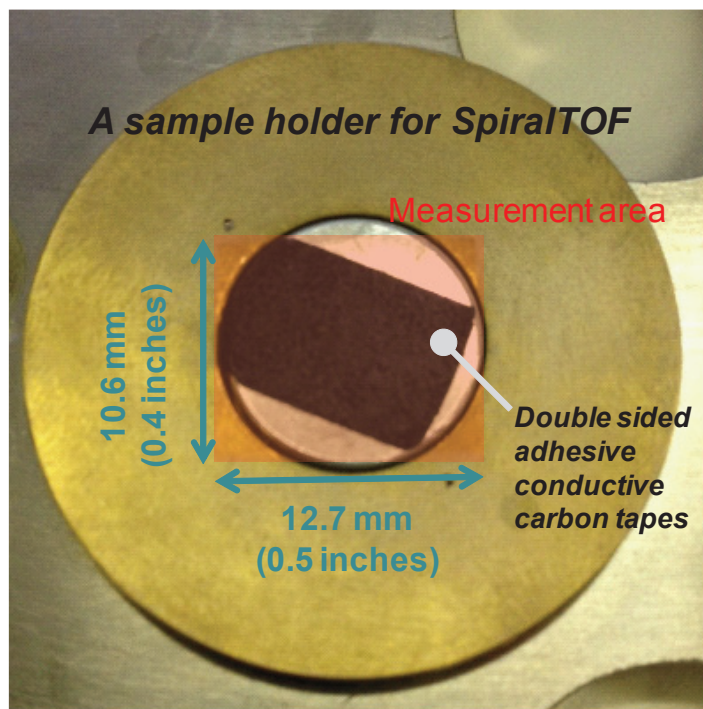
Figure 1. Sample pictures.

Results & Discussion

As a starting point, we evaluated the mass accuracy of the SpiralTOF-MS with external calibration using two different DHB ions, $C_7H_5O_3$ and $C_7H_6O_4Na$, in the measured digest spectrum. Because their monoisotopic ions were saturated, the [M+1] isotope ions were used, and the calculated mass error for each was +6.4 mDa and -5.1 mDa, respectively. As a result, an internal calibration was not required for the qualitative MALDI imaging measurements done on the SpiralTOF-MS.

Next, the GSR sample surface was analyzed for inorganic specie distributions. Figure 2 shows a zoomed in portion of the measured digest mass spectrum and theoretical isotopic distribution for barium. Additionally, this figure shows the MALDI images for the 138Ba m/z 137.9016 and the DHB [M+1]$^+$ isotopic ion m/z 138.02671 ($C_7H_5O_3$).
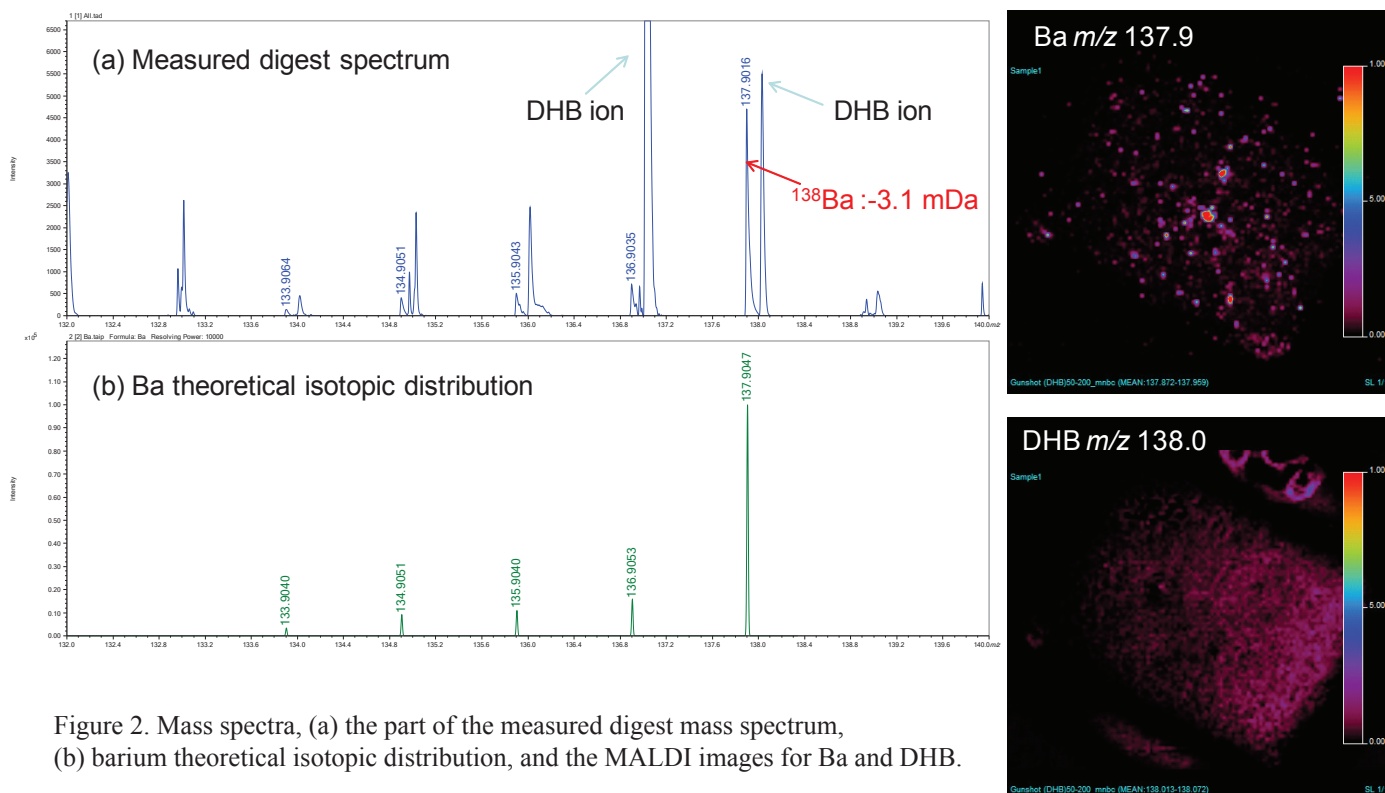

Figure 2. Mass spectra, (a) the part of the measured digest mass spectrum, (b) barium theoretical isotopic distribution, and the MALDI images for Ba and DHB.

Although the difference between each m/z is only 0.125Da, the SpiralTOF-MS provided full separation for both ion peaks which in turn produced strikingly different images for each analyte on the surface. The distribution of the ^{138}Ba m/z 137.9016 was randomly distributed across the surface while the DHB m/z 138.02671 was homogeneously present across the matrix surface.

Figure 3 shows the barium and barium oxide particle distributions while Figure 4 shows the particle distributions for lead (Pb), bismuth (Bi), and calcium oxide (CaO). Each of these images was distinctive for their corresponding metals and metal oxides.

Conclusions

The MALDI-MS images were useful for visualizing the presence of inorganic particle found in the GSR samples. The SpiralTOF MALDI imaging showed:

1. High mass resolving power.
2. High mass accuracy using the external calibration. An internal calibration is not necessary.
3. Good for small molecules.
4. Good spatial resolution.

Therefore, SpiralTOF MALDI imaging is a useful tool for the visualization of forensically significant molecules found in GSR samples.
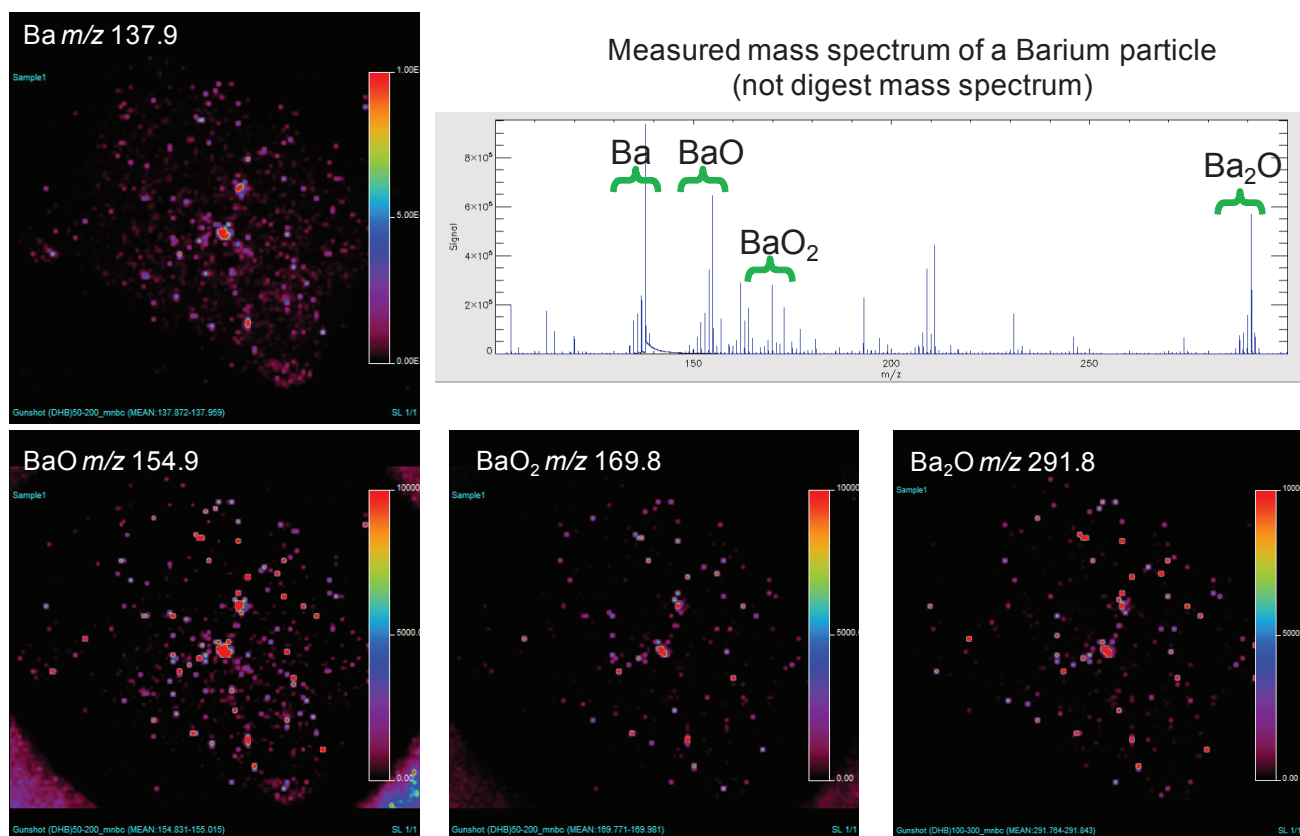
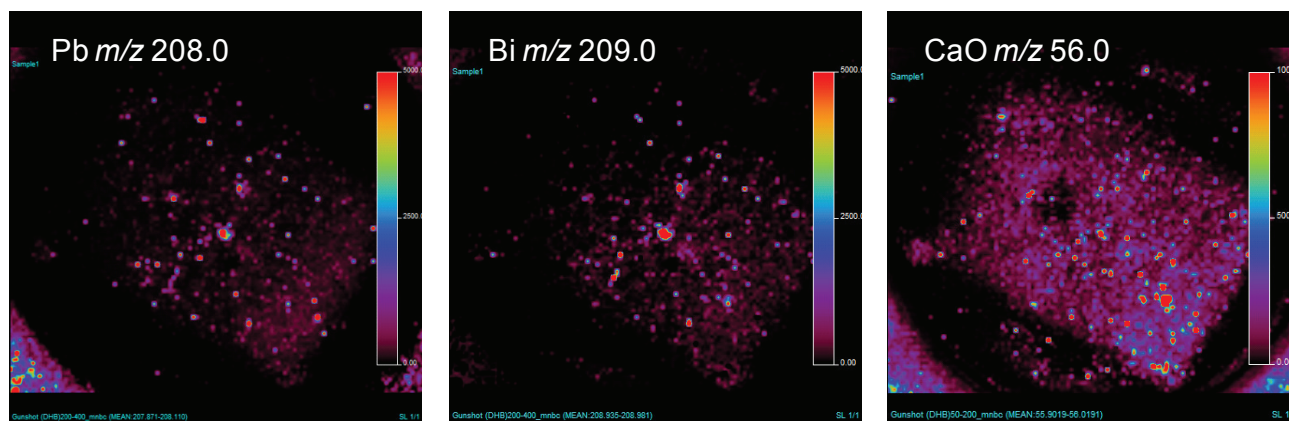Figure 3. Barium and barium oxide particle distributions.

Figure 4. Lead, bismuth and calcium oxide particle distributions.

Analysis of Organic Thin Films by the Laser Desorption/Ionization Method Using the JMS-S3000 "SpiralTOF"

Takaya Satoh

MS Business Unit, JEOL Ltd.

Laser Desorption/Ionization-Time of Flight Mass Spectrometry (LDI-TOFMS) is generally used for analysis of organic compounds because this technique generates little fragmentation of molecular ions at ionization. It makes possible to obtain information on molecular weights and molecular structures in organic compounds. In particular, a technique which uses the matrix compounds for enhancing ionization efficiency is well known as Matrix-Assisted Laser Desorption/Ionization-Time of Flight Mass Spectrometry (MALDI-TOFMS). This technique is widely used in the bio markets owing to its capability of ionizing proteins and peptides with the molecular weights of several thousands to several hundreds of thousands. The MALDI-TOFMS is also utilized for analysis of synthetic polymers. In many cases, LDI-TOFMS and MALDI-TOFMS have been used to estimate the molecular weights of organic compounds in solution. But very recently, techniques of imaging mass spectrometry, which controls the laser irradiation position by two-dimensional scan to acquire mass spectra for visualizing localization of chemical compounds with specific molecular weights, have been improved. The application of this innovative technique is increasingly spreading in the bio markets. The technology of Imaging Mass Spectrometry has been advancing for analyzing biological tissue sections, but in the future, it is expected to develop toward the material science markets. It is noted that various surface analytical techniques are already available in the material science markets. In order to study the advantages of LDI-TOFMS as one of effective surface analysis tools, it is essential to consider the complementary analysis of LDI-TOFMS with the existing surface analytical techniques. In this article, the advantages of using LDI-TOFMS for analyzing organic light-emitting diode material thin films, in accordance with comparison with Time-of-Flight Secondary Ion Mass Spectrometry (TOF-SIMS), X-ray Photoelectron Spectroscopy (XPS) and Scanning Electron Microscopy/Energy-Dispersive X-Ray Spectroscopy (SEM/EDS), have been studied. In addition, since LDI-TOFMS is a destructive analytical technique, the influence on the sample surface caused by LDI-TOFMS was also examined.

Introduction

The surface analytical techniques irradiate an electron beam, an ion beam or X-ray on the surface of the sample for investigation of its morphology and physical characteristics based on the interactions between the beam and substances existing on the sample surface. To observe the sample morphology, an optical microscope and an electron microscope are mainly used. To study the sample characteristics, a wide range of techniques is available depending on the incident particles (beam) and the signals to be detected. They include Electron Probe Microanalysis (EPMA), Auger Electron Spectroscopy (AES), X-ray Photoelectron

Spectroscopy (XPS) and Time-of-Flight Secondary Ion Mass Spectrometry (TOF-SIMS). In recent years, electronic devices are frequently composed of organic compounds such as organic semiconductor, organic light-emitting diode (OLED) and organic film solar cell, and the use of them will be expected to further expand. It is increasingly important to inspect organic-compounds and their degradation mechanism in the products. Among surface analytical techniques, AES and XPS are capable of obtaining chemical bonding states or information on functional groups in chemical compounds, but those techniques have a difficulty in structural analysis of organic compounds. The TOF-SIMS is a mass spectrometry technique well known as a surface analytical technique. By using the dynamic SIMS, fragmentation of the molecular ions is likely to occur at ionization, thus making it difficult to apply SIMS to analyze organic compounds. Recently, techniques which utilize metallic clusters or gas clusters as a

3-1-2 Musashino, Akishima, Tokyo, 196-8558, Japan.

E-mail: taksatoh@jeol.co.jp

primary ion beam attached to TOF-SIMS have been succeeded to ionize more softly. These techniques are expected to expand the TOF-SIMS applications for organic compounds.

This article reports on Laser Desorption/ Ionization-Time of Flight Mass Spectrometry (LDI-TOFMS). As a technique that utilizes the laser desorption mechanism, Matrix-Assisted LDI-TOFMS (MALDI-TOFMS) is in widespread use, which enables ionization of a variety of chemical compounds by properly combining a sample with matrix compounds enhancing ionization. Around 2000 year, the number of installed MALDI-TOFMS has been dramatically increased aiming to analyze proteins and peptides. Moreover in the material analysis fields, MALDI-TOFMS has been utilized for the analysis of synthetic polymers. The use of the matrix is essential for the measurement of these large-molecular weight organic compounds, thus the ionization technique using laser is generally called "MALDI". But, there are many chemical compounds which can be ionized only with laser irradiation. In this case, the used ionization technique is simply called "LDI".

Most of mass spectrometry techniques analyze samples in solution. MALDI-TOFMS also mixes the sample solvent and the matrix solvent to crystallize them by dropping on a target plate. By irradiating the co-crystal of matrix and sample compounds with the ultraviolet, MALDI-TOFMS ionizes various organic compounds contained in the sample and performs mass separation. In recent years, imaging mass spectrometry that adopts MALDI-TOFMS [1,2], which can acquire information about localization on the sample surface, is demonstrating technological improvement and therefore, the use of this unique technique is increasingly spreading. In Imaging Mass Spectrometry, the matrix is sprayed uniformly onto the sample surface and mass spectra are acquired while the laser irradiation position to the sample is two-dimensionally scanned. This process allows acquisition of information on two-dimensional distributions of specific chemical compounds. Imaging Mass Spectrometry has been expanding its applications to the bio markets from its dawn, including proteins, peptides, lipids, drugs and their metabolites. Most of the subjects for this technique are biological tissue section. On the other hand, in accordance with the establishment of biological tissue sectioning techniques, the users gradually start to study the application of Imaging Mass Spectrometry to the material analysis markets and also, this technique is expected to visualize information on localization of organic compounds on a thin film or a solid surface. In order to make Imaging Mass Spectrometry more effective in the material analysis markets, it is very important to carry out complementary analysis with the existing surface analytical techniques. In this article, the fundamental experiments using the JMS-S3000 "SpiralTOF" to examine LDI-TOFMS as one of surface analytical techniques were reported. The comparison with information obtained by XPS and TOF-SIMS and the influence of laser irradiation onto the surface of the organic thin film made of OLED material were examined.

Sample

For complementary analysis among LDI-TOFMS, TOF-SIMS and XPS, N,N'-Di(1-naphthyl)-N,N'-diphenylbenzidine (α-NPD), which is a material for a hole transport layer of an OLED, was deposited onto a Si substrate with 600 nm thick (hereinafter, called "α-NPD/Si"). In addition, in order to examine the influence of LDI on the sample surface, the author prepared a different sample of another Si substrate where a material for a hole transport layer of an organic EL (4,4',4''-Tris[2-naphthyl(phenyl)amino]triphenylamine (2-TNATA) of a thickness of 700 nm) was deposited onto the substrate and furthermore, α-NPD of a thickness of 1300 nm was deposited onto the prepared layer (hereinafter, called "α-NPD/2-TNATA/Si").

Analyses of Organic Thin Film Using LDI-TOFMS, TOF-SIMS and XPS

The JMS-S3000 "SpiralTOF" was used as an LDI-TOFMS. **Figure 1**(a) shows the external view of the SpiralTOF. The biggest feature of the SpiralTOF is adopting a JEOL originally-developed spiral ion trajectory (Fig. 1(b)) and this trajectory is formed by four hierarchical electrostatic sectors. The flight distance of 1 cycle is 2.093 m and the SpiralTOF achieves an effective flight distance of 17 m at 8 cycles. Here, the mass resolution of TOFMS is proportional to the flight distance. The general effective flight distance of the reflectron TOFMS is approximately a few meters, but the SpiralTOF which has an effective flight distance of 17 m can achieve the world-highest mass resolution among MALDI-TOFMSs. Furthermore, the electrostatic sectors which forms the spiral ion trajectory makes it possible to eliminate the fragment ions during their flight, thus a mass spectrum with little noise can be acquired. By attaching the TOF-TOF option [4], it is possible to perform structural analysis with the Tandem Mass Spectrometer (MS/MS). The high energy CID (collision-induced dissociation) could provide much structural information rather than low energy CID used in major MS/MS instruments. The SpiralTOF is equipped with a Newport Nd:YLF (349 nm) as an ionization laser source. The laser irradiation diameter onto the sample surface is approximately 20 µm and the laser intensity is 60 µJ at 100 % laser setting. α-NPD and 2-TNATA are ionized without requiring the matrix, so the experiments were performed by acquiring the mass spectra using LDI-TOFMS. **Figure 2**(a) shows a mass spectrum (*m/z* 10 to 800) acquired by fixing the laser irradiation position on the α-NPD/Si and by accumulations of 250 times. Only molecular ions of α-NPD are observed in the mass spectrum and it is found that ion fragmentation is very little at the ionization. Using the TOF-TOF option, the author acquired a product ion spectrum by selecting the observed molecular ions. Fig. 2(b) shows the observation result of the created fragment ions and the estimated fragmentation position of fragmentation. By the use of the High-Energy

CID technique, sufficiently much information was obtained to estimate the molecular structure.

The Ar gas cluster ion beam source attached to JEOL JMS-T100LP "AccuTOF LC-plus" developed in Matsuo Group at Kyoto University [5] was used for TOF-SIMS experiments. **Figure 3**(a) shows its external view. Fig. 3(b) shows a mass spectrum (*m/z* 0 to 800) which was acquired with the primary ion beam of Ar cluster ions (accelerating voltage: 10 kV) that irradiates on the "α-NPD/Si". The molecular ion peak of α-NPD ($[M]^{+\cdot}$) was observed. However, the fragment ions were also observed with noticeable abundance in low mass range, (*m/z* 100 to 500), compared to LDI-TOFMS. This may be due to two reasons. One is the fragment ions generated from α-NPD at the ionization. It was considered reasonable because the pattern of the product ion spectrum in Fig. 2(b) is relatively similar to the mass spectrum acquired with TOF-SIMS. On the other hand, the measurement region in depth direction by TOF-SIMS is confined to only 10 nm or less from the top surface of the sample, thus many chemical back ground peaks produced from surface contamination. Since Ar cluster ions are used for the primary ion beam, the mass spectrum achieves the littlest fragmentation among TOF-SIMSs. However compared to LDI-TOFMS, it should be taken into consideration the influence of the fragmentation or a remarkable influence of sample-surface contamination on the mass spectrum. TOF-SIMS makes it possible to perform high spatial resolution mapping and depth profiling by monitoring molecular ions or major fragment ions. For example during the mapping, a spatial resolution of 1 μm or less is achieved, indicating that this resolution performance is higher than that obtained by Imaging Mass Spectrometry using the present MALDI-TOFMS (typically a few tens of micrometers). But, when taking account of the fact that many fragment ions and the background originating from the surface contamination are observed, this technique is applicable only to the ions of major components. The chemical compounds deriving from the major components in degradations expected to be minor components; therefore, distinction with fragment ions or with surface contamination may become difficult.

The JEOL JPS-9010 was used for XPS experiments. **Figure 4**(a) shows its external view of the JPS-9010. The analysis area was set to be 1 mm diameter. Fig. 4(b) and (c) show the measurement result of α-NPD/Si. A spectrum shown in Fig. 4(b) is a wide spectrum (energy resolution: 1.7 eV equivalent to Ag3d$_{5/2}$) and the peaks of C and N which are constituent elements of α-NPD are clearly observed. In the spectrum obtained by XPS, which is a top-surface analysis instrument like TOF-SIMS, a Si peak originating from a substrate is not observed. Furthermore, a narrow spectrum (energy resolution: 0.5 eV equivalent to Ag3d$_{5/2}$) was acquired from the vicinity of the C peak. It was able to understand the peaks including the information on C-C
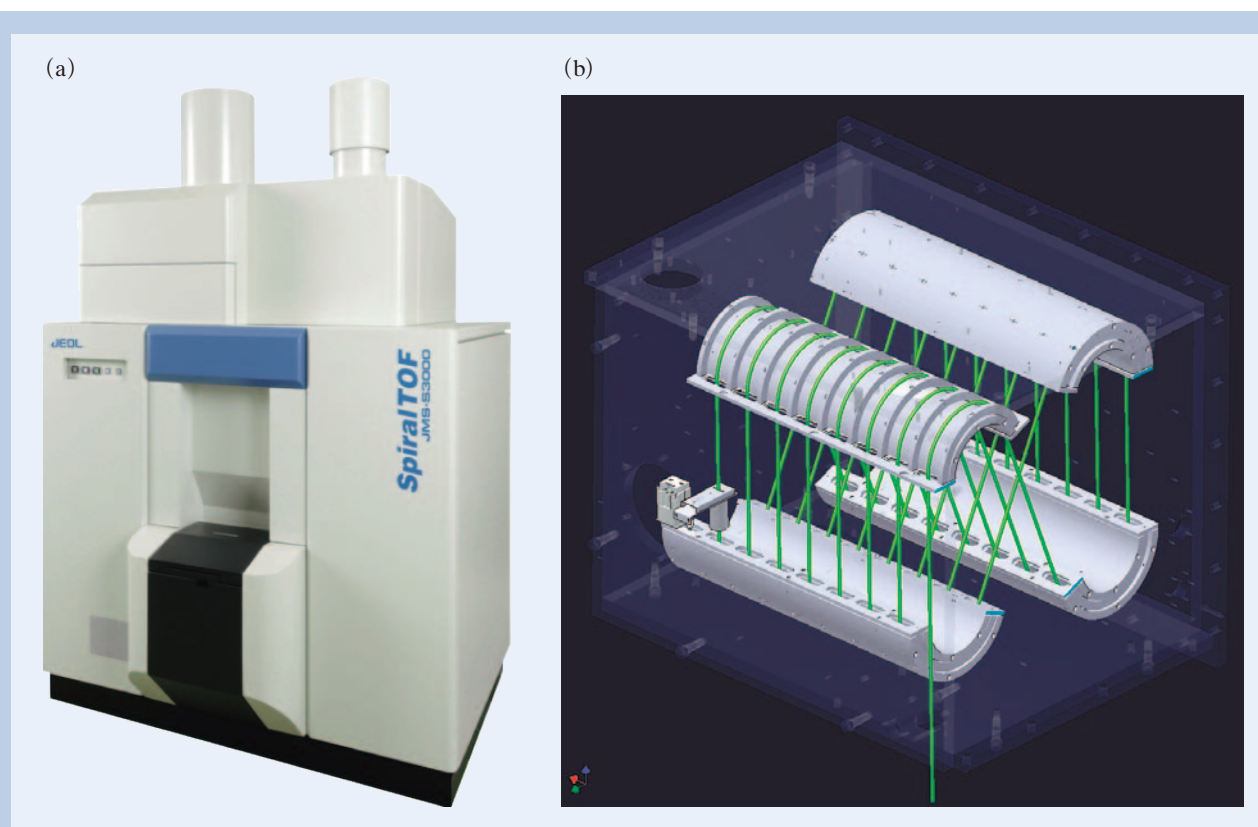
(a)

(b)

Fig. 1 (a) External view of the JMS-S3000 (when the Linear TOF option and the TOF-TOF option are attached), and (b) the schematic of the spiral ion trajectory in the JMS-S3000.

bonding and the C-N bonding. As compared to mass spectrometry techniques (LDI-TOFMS, TOF-SIMS, etc.), XPS provides non-destructive analysis and also can perform quantitative analysis which is difficult in mass spectrometry caused by ionization uncertainty. However, when the sample is an organic compound formed by a combination of limited elements, it is not easy to quantitatively analyze mixtures in the compounds with an XPS instrument. In particular, it is estimated that, when the limited elements are mixed as minor components where the composition of a degradation product does not change largely, the separation of their spectral peaks becomes more difficult.

As described above, the chemical information from LDI-TOFMS with both TOF-SIMS and XPS, which are the existing surface analytical techniques, are compared. The advantages of LDI-TOFMS in the analysis of organic compounds are the followings. LDI-TOFMS enables one to confirm mainly molecular ions from the mass spectrum and also, makes it possible to perform structural analysis through MS/MS analysis. These powerful features play a significant role especially in the analysis of
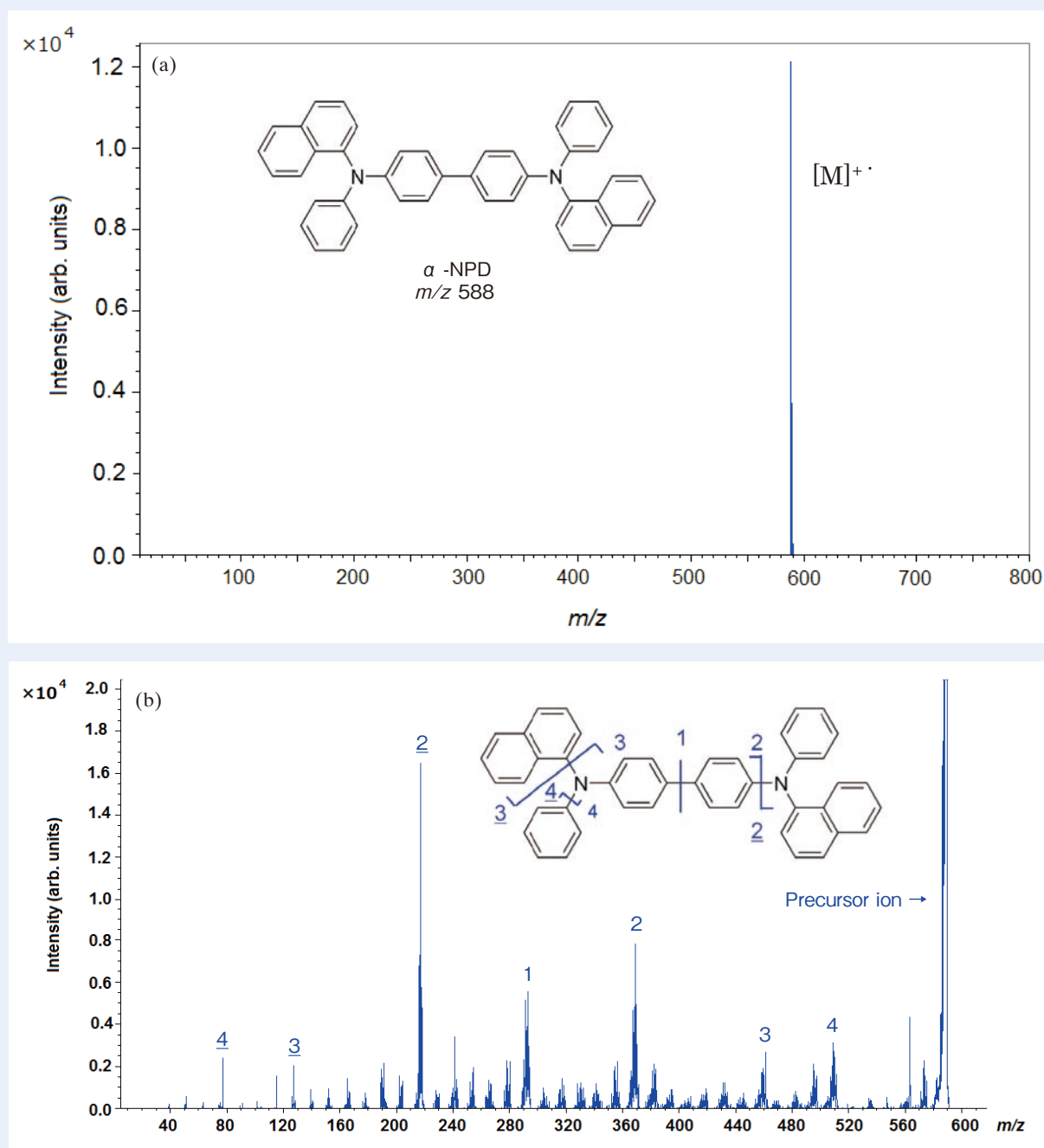
Fig. 2 (a) Mass spectrum of α -NPD acquired by LDI-TOFMS. Peaks indicating the molecular information on α -NPD are clearly observed. (b) MS/MS spectrum of α -NPD. Peaks well reflecting the structures of α -NPD are observed.

organic mixtures which exist on the sample surface. Also in degradation analysis, this technique is expected to allow the analysis of a minor component which is a degradation product created from the major component.

Influence of Laser Irradiation on the Sample Surface

The influence of laser irradiation on the sample surface by using the Scanning Electron Microscope/ Energy-Dispersive X-ray Spectrometer (SEM/EDS)

was confirmed. **Figure 5**(a) shows the external view of the instrument used for this experiment, JEOL SEM JSM-7001FTTLLV equipped with the OXFORD Instruments AZtec Energy Standard X-Max50. Fig. 5(b) shows an SEM image of an irradiation scar after the sample surface was irradiated with a laser beam under the conditions of laser intensity 40% and the number of laser shot of 250. From this SEM image, the ablation of organic thin-film layers was observed at a diameter of 35 µm in the scar after the laser irradiation. In addition, Fig. 5(c) and (d) respectively show the analysis result of EDS spectra acquired from the irradiation scar
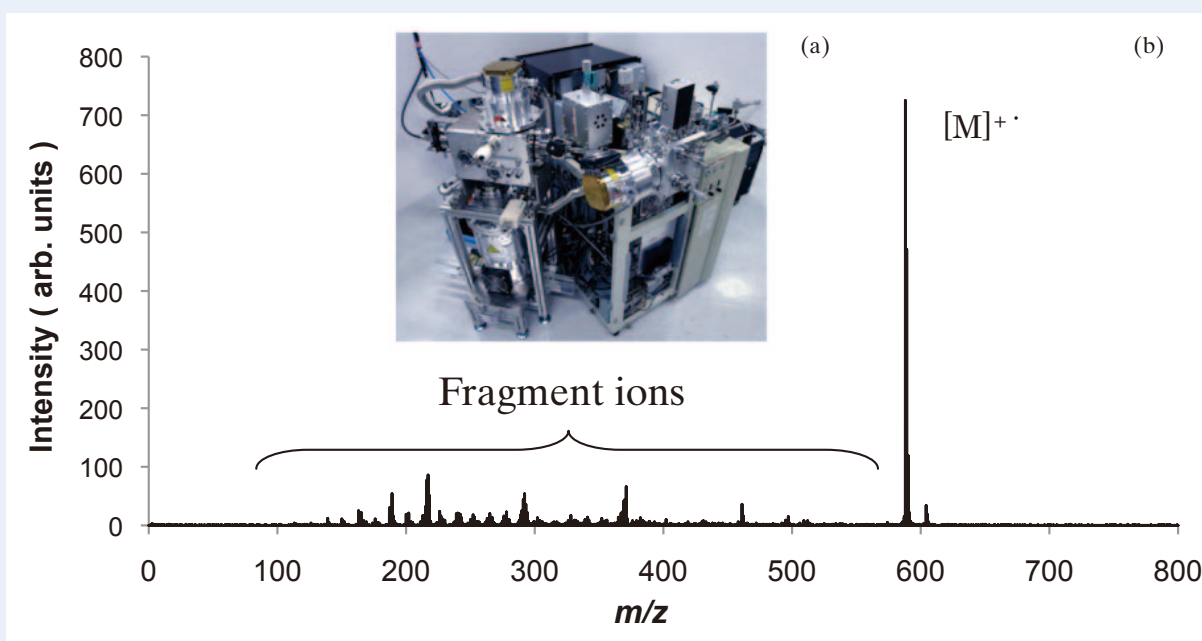
Fig. 3 (a) TOF-SIMS possessed by Matsuo Group, and (b) a mass spectrum of α-NPD mass spectrum acquired with TOF-SIMS. In addition to peaks indicating the molecular information on α-NPD, many peaks are observed, which are considered to originate from the fragment ions of α-NPD and the surface contamination.
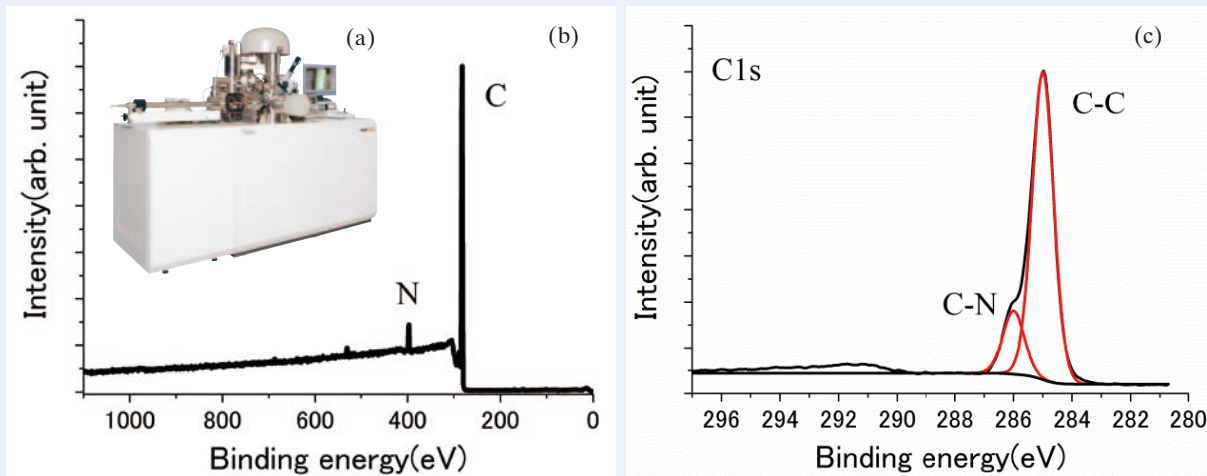
Fig. 4 (a) External view of the JPS-9010, and (b) A wide spectrum of α-NPD/Si. C and N which are constituent elements of α-NPD are clearly observed. (c) A narrow spectrum of α-NPD/Si and a narrow spectrum in the vicinity of C allows observation of peaks indicating the C-C bonding and C-N bonding.
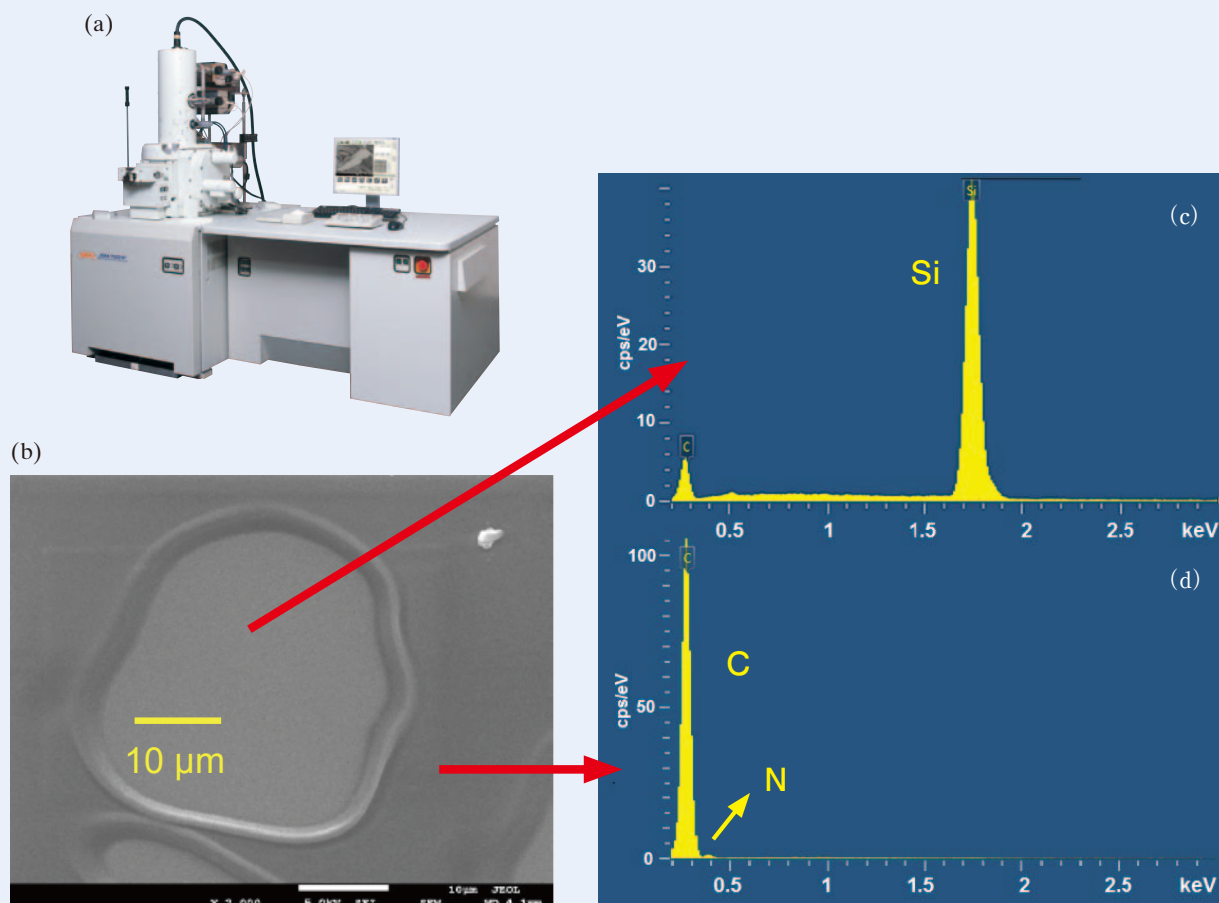
Fig. 5 (a) External view of the JSM-7001FTTLLV. (b) SEM image of an irradiation scar acquired after laser irradiation of the sample surface with laser intensity 40 % and the number of laser spot of 250. (c) EDS analysis result obtained from an area of a laser irradiation scar and an area in the vicinity of a laser irradiation scar. The result indicates that organic thin-film layers penetrate into the scar, confirmed by observation of Si from the laser irradiation scar and of C from the vicinity of the irradiation scar.
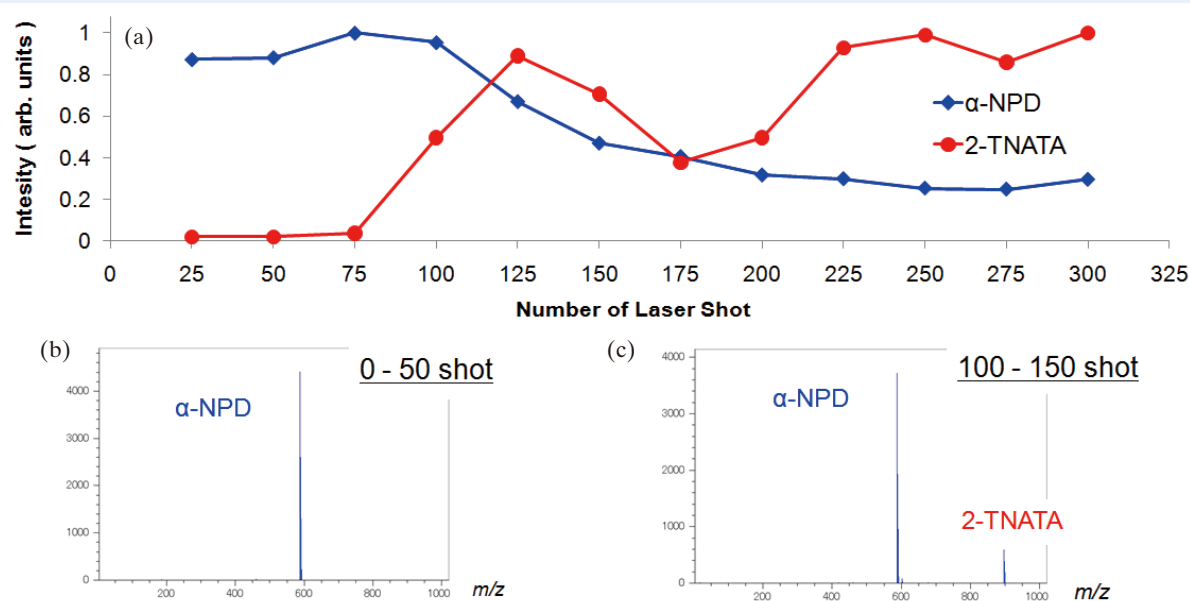

Fig. 6 (a) Ion intensity transitions of α-NPD and 2-TNATA when α-NPD/2-TNATA/Si is fixed and measured. Mass spectra acquired with the number of laser shot of 0 to 50 (b) and 100 to 150 (c) are also shown, respectively.

and from an area on which organic thin-film layers exist near the irradiation scar. The peaks of Si and C were observed from the former and latter spectrum, respectively, indicating that the laser irradiation allows penetration of the organic layers into the scar to be confirmed.

Mass spectra of α-NPD/2-TNATA/Si were acquired under the conditions of laser irradiation position fixed and laser intensity 40%. **Figure 6**(a) shows the plot diagram of ion intensity variations of molecular ions of α-NPD and 2-TNATA with respect to the number of laser shot. The ion intensity of α-NPD on the upper layers decreased as the number of laser shot increases. On the other hand, 2-TNATA on the lower layers started to be observed in the mass spectrum when the number of laser shot reached 100. Fig. 6(b) and (c) respectively show the accumulation mass spectrum acquired with the number of laser shot of 0 to 50 and 100 to 150 are shown in Fig. 6(b) and (c), respectively. The fragment ions are hardly observed in both spectrum and the 2-TNATA is clearly appeared in only Fig. 6(c). However, α-NPD on the upper layers was still observed even after 2-TNATA on the lower layers started to be observed. , It is expected that as the number of laser shot increases, the ionization region spreads in the plane direction as well as in the depth direction. The variation of the number of laser shot for the appearance of 2-TNATA in the mass spectrum according to the laser intensity is shown in **Fig. 7**. It is found that, as the laser intensity increases, 2-TNATA appears even when the number of laser shot is decreased. This result indicates that

the influence of depth is affected by the number of laser shot and the laser intensity.

From these results, the author found that the influence of laser irradiation on the sample surface changes greatly depending on the laser irradiation conditions (laser intensity and the number of laser shot). For the depth direction, the present experiments indicate that the comprehensive information on regions between 100 nm and 1 μm is obtained. Compared to the measurement results obtained by top-surface analytical techniques such as XPS and TOF-SIMS, the present depth regions are considerably large. When increasing the number of laser shot and the laser intensity, the ionization region increases for not only in the depth direction but also in the plane direction, thus care is required for mapping.

Summary

This article reported on comparison and examination of organic thin-film analysis for LDI-TOFMS, TOF-SIMS and XPS. The XPS and TOF-SIMS have a difficulty in applying the techniques to multi-component samples. This is because XPS can obtain information only on elements and chemical bonding states, and TOF-SIMS makes a mass spectrum complicated caused by fragment ions. To the contrary, LDI-TOFMS can mainly observe molecular ions, thus it is suitable for the analysis of multi-components. In degradation analysis of organic chemical compounds in electronic parts, it
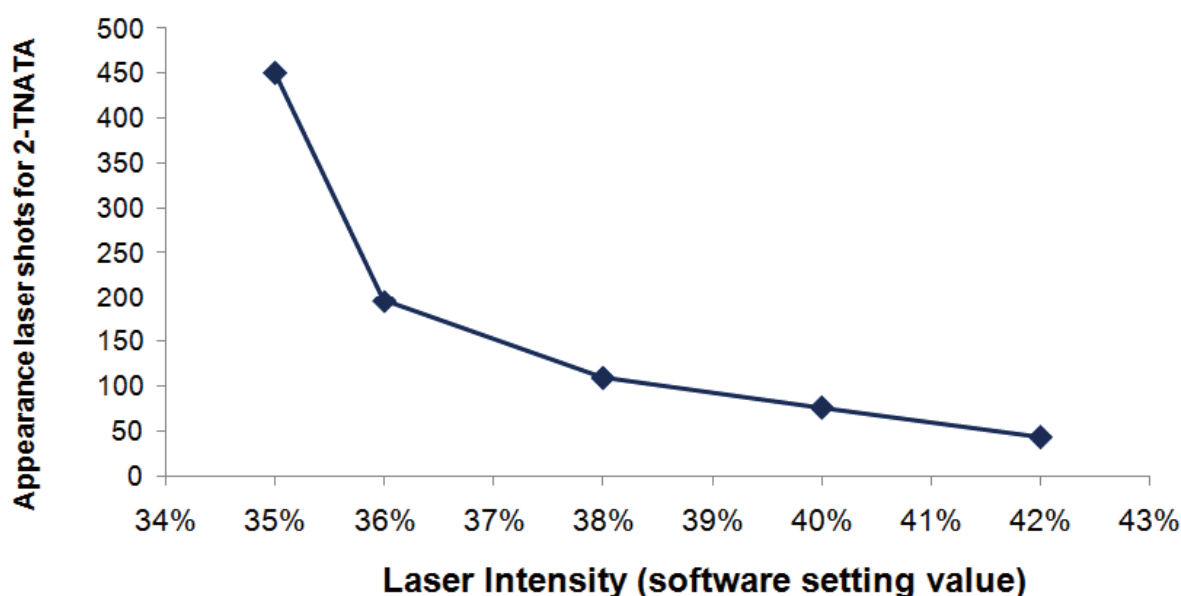
Fig. 7 The number of laser shot at which 2-TNATA starts to be observed when the laser intensity is changed. As the laser intensity increases, the influence of laser irradiation on the sample surface becomes large.

is expected that the total element composition ratio does not change largely, thus LDI-TOFMS can be used as an important tool for identifying degradation components because this technique enables one to confirm molecular ions and to perform structural analysis by MS/MS. In addition, it may be considered that the amount of the degradation product is not so large compared to original compound; therefore, the use of LDI-TOFMS allows one to expect clear analysis because LDI-TOFMS produces almost no fragment ions at the ionization.

Furthermore, the SEM observation result which revealed the sample-surface states after laser irradiation clarified that the comprehensive information of 100 nm or more was obtained in the depth direction of a thin film in an organic EL material. Influence of laser irradiation on the depth direction depends on the laser intensity and the number of laser shot. When LDI-TOFMS is used, the information of depth direction is considerably larger than that obtained by XPS and TOF-SIMS, in which the typical analysis depth is 10 nm or less. In the analysis of thin films having structures in the depth direction using XPS or TOF-SIMS, it is often combined with ion etching because they are top-surface analytical technique. In this case, it is possible to perform depth profiling with high resolution to depth direction. On the other hand, when LDI-TOFMS is used, clear acquisition of the information in the depth direction is rather difficult compared to XPS and TOF-SIMS, but it may be considered that LDI-TOFMS can classify chemical compounds contained in the same thin-film layer.

Now, the use of the (MA) LDI-TOFMS is making it possible to acquire two-dimensional distributions of chemical compounds on the specimen surface in accordance with the progress of Mass Imaging technologies. In the future, by accumulating the knowledge about ionization of samples of thin films and the influence of laser irradiation on the sample surface, LDI-TOFMS will widely be applied as one of powerful surface analytical techniques.

Acknowledgments

References

[1] Caprioli, R.M., Farmer, T.B., Gile, J.: Molecular imaging of biological samples: localization of peptides and proteins using MALDI-TOF MS. *Anal. Chem*. **69**, 4751–4760 (1997).

[2] Jungmann, J.H., Heeren, R.M.A.: Emerging technologies in mass spectrometry imaging. *J. Proteomics* **75**, 5077–5092 (2012).

[3] T. Satoh, T. Sato, J. Tamura, "Development of a high-Performance MALDI-TOF mass spectrometer utilizing a spiral ion trajectory": *J. Am. Soc. Mass Spectrom*., **18**, 1318 –1323, (2007).

[4] T. Satoh, T Sato, A. Kubo, J. Tamura, "Tandem Time-of-Flight Mass Spectrometer with High Precursor Ion Selectivity Employing Spiral Ion Trajectory and Improved Offset Parabolic Reflectron": *J. Am. Soc. Mass Spectrom*., **22**, 797-803, (2011).

[5] K. Ichiki, J. Tamura, T. Seki, T. Aoki, J. Matsuo, "Development of gas cluster ion beam irradiation system with an orthogonal acceleration TOF instrument" *Surface and Interface Analysis,* **45**(1), 522-524 (2013).

Table 1 Comparison of LDI-TOFMS with the other surface analytical techniques.

	Probe	Detected signal	Spatial resolution	Depth direction	Chemical information
Energy-Dispersive X-ray Spectroscopy (EDS)	Electron	X-ray	1 µm	< 1 µm	Element
Auger Electron Spectroscopy (AES)	Electron	Auger electron	10 nm	< 10 nm	Element, Chemical bonding states
X-ray Photoelectron Spectroscopy (XPS)	X-ray	Electron	10 µm	< 10 nm	Element, Chemical bonding states, Functional group
Time-of-Flight Secondary Ion Mass Spectrometry (TOF-SIMS)	Ion	Ion	100 nm	< 10 nm	Element,Partial molecular structure
Laser Desorption/ Ionization-Time of Flight Mass Spectrometry(LDI-TOFMS)	UV light	Ion	10 µm	a few 100 nm	Molecular structure

JEOL Ltd. 3-1-2 Musashino Akishima Tokyo 196-8558 Japan   Sales Division Tel. +81-3-6262-3560   Fax. +81-3-6262-3577

www.jeol.com   ISO 9001 • ISO 14001 Certified